

The development of bioabsorbable hydrogels on the basis of polyester grafted poly(vinyl alcohol)

Von der Fakultät für Mathematik, Informatik und Naturwissenschaften
der Rheinisch-Westfälischen Technischen Hochschule Aachen zur
Erlangung des akademischen Grades einer Doktorin der
Naturwissenschaften genehmigte Dissertation

vorgelegt von

Master of Science
Elvira Vidović
aus Mostar, Bosnien und Herzegowina

Berichter: Universitätsprofessor Dr. rer. nat. H. Höcker
Universitätsprofessorin Dr. D. Klee

Tag der mündlichen Prüfung: 04. September 2006

Diese Dissertation ist auf den Internetseiten der Hochschulbibliothek online verfügbar.

Acknowledgments

I would like to acknowledge my gratitude to Professor Dr. H. Höcker for his supervision and constructive criticism for the successful completion of my PhD work, carried out at the Department of Textile Chemistry and Macromolecular Chemistry, RWTH Aachen, from January 2002 to January 2005.

I would like to extend my gratitude to Professor Dr. D. Klee, who allowed me to carry out the PhD work, for her suggestions and help.

I owe a lot of thanks to Professor Dr. Z. Janović, whose motivation, constant encouragement and support, helped me to make this effort and complete the PhD work.

A very special thanks goes to Dr. A. Jukić who helped me out lots of times in different stages of this work.

I am greatly indebted to Dr. P. Dalton for his assistance and encouragement.

Many hearty thanks to all my colleagues working at the German Wool Research Institute and at the Department of Textile Chemistry and Macromolecular Chemistry, RWTH Aachen, for their cooperation and friendly discussions. In particular, I am grateful to my colleague, Dr. Carla Terenzi for her backing and understanding during the entire PhD work.

Contents

Abbreviations and symbols	IV
1. Introduction	1
1.1 Biomaterials	1
1.1.1 The influence of different parameters on properties	3
1.1.2 Biodegradable materials	4
1.2 Hydrogels	6
1.2.1 The diverse application of hydrogels	6
1.2.2 The degree of swelling	8
2. Aim and concept of the thesis	9
3. Synthesis of networks based on poly(<i>rac</i>-lactide) or poly(<i>rac</i>-lactide-<i>co</i>-glycolide) with poly(vinyl alcohol)	12
3.1 Ring-opening polymerization (ROP) of cyclic esters	12
3.2 Ring-opening polymerization of lactide and glycolide	15
3.3 Transformation reaction of end groups	15
3.4 The reaction of grafting of poly(lactide) or poly(lactide- <i>co</i> -glycolide) oligomers onto poly(vinyl alcohol) and crosslinking	16
4. Characterization of networks	18
4.1 Synthesis of networks	18
4.2 IR analysis of networks	26
4.3 Thermal properties of networks	30
4.3.1 Thermogravimetry (TGA)	30
4.3.2 Differential scanning calorimetry (DSC)	33
4.3.2.1 Influence of the length of polyester chains on the thermal properties of networks	33
4.3.2.2 Influence of glycolide content on the thermal properties of networks	36
4.3.2.3 Influence of the degree of grafting on the thermal properties of networks	36
4.4 Mechanical properties of hydrogels	37
4.5 Surface properties of hydrogels	41
4.6 Biocompatibility	42

5. Controlled degradation of hydrogels	45
5.1 Mass loss of degraded hydrogels	45
5.1.1 Influence of the length of the polyester chains	45
5.1.2 Influence of the composition of the polyester chains	48
5.1.3 Influence of the degree of grafting	49
5.1.4 Influence of degradation conditions	50
5.2 Swelling of degraded hydrogels	53
5.2.1 Influence of the length of the polyester chains	53
5.2.2 Influence of the composition of the polyester chains	56
5.2.3 Influence of the degree of grafting	58
5.2.4 Influence of degradation conditions	60
5.3 Topography of degraded networks	61
5.3.1 Influence of the length of the polyester chains	71
5.3.2 Influence of the composition of the polyester chains	71
5.3.3 Influence of the degree of grafting	72
5.3.4 Influence of degradation conditions	73
5.4 Mechanical properties of degraded hydrogels	75
5.4.1 Influence of the length of polyester grafts on the mechanical properties of degraded hydrogels	75
5.4.2 Influence of the composition of polyester chains	77
5.4.3 Influence of the degree of grafting	82
5.5 Surface properties of degraded hydrogels	86
5.6 IR analysis of degraded networks	90
5.7 Thermal properties of degraded networks	97
5.7.1 Thermogravimetry (TGA)	97
5.7.2 Differential scanning calorimetry (DSC)	102
6. Summary	104
7. Experimental Part	108
7.1 Materials	108
7.2 Synthesis	108
7.2.1 Ring opening polymerization	108
7.2.2 Transformation of hydroxy into carboxylic end groups	109
7.2.3 Grafting of poly(<i>rac</i> -lactide) or poly(<i>rac</i> -lactide- <i>co</i> -glycolide) chains onto the poly(vinyl alcohol) backbone	110

7.2.4	Crosslinking of hydrogels	111
7.3	Characterization methods	112
7.3.1	Nuclear magnetic resonance (NMR)	112
7.3.2	Infrared spectroscopy (IR)	112
7.3.3	Thermogravimetry (TGA)	113
7.3.4	Differential scanning calorimetry (DSC)	113
7.3.5	Tensile strength measurements	113
7.3.6	Contact angle measurements	113
7.3.7	Biocompatibility test	114
7.3.8	Hydrolytical degradation experiment	115
7.3.9	Weight loss of hydrogels during degradation	115
7.3.10	Gravimetrical determination of the degree of swelling	115
7.3.11	Scanning electron microscopy (SEM)	116
8.	Literature	117
9.	Appendix	121

Abbreviations and symbols

A_0	surface area in m^2
A	area of the particular stretching band in relative units
AIBN	2,2'-azobis(2-methylpropionitrile)
DA	degree of acetate groups in %
DCC	dicyclohexyl carbodiimide
DEE	diethyl ether
DG_{exp}	experimental degree of grafting in %
DG_{the}	theoretical degree of grafting in %
DH	theoretical degree of hydrolysis in %
DMAP	4-(<i>N,N</i> -dimethylamino)pyridine
DMEM	Dulbecco's modified Eagle's medium
DMSO	dimethyl sulfoxide
DSC	Differential Scanning Calorimetry
DTGA	Differentiated ThermoGravimetry Analysis
E	E -modulus / Young's modulus in MPa
<i>e.g.</i>	<i>exempli gratia</i>
Eq.	equation
F	force in N
FCS	fetal calf serum
Fig.	figure
FTIR	Fourier Transform Infrared
FTIR-PAS	Fourier Transform Infrared-PhotoAcoustic Spectroscopy
GA	glycolide
HEMA	2-hydroxyethyl methacrylate
hF	primary human dermal fibroblasts
HQ	hydroquinone
<i>i.e.</i>	<i>it is (id est)</i>
IOL	intraocular lenses
IUPAC	International Union of Pure and Applied Chemistry
LA	lactide
m_0	weight of hydrogel sample before degradation in g
MAG	magnification
m_d	weight of dry hydrogel sample after degradation in g
m_{rel}	relative weight of sample in g
m_s	weight of swollen hydrogel sample in g
M_w	weight average molecular weight
N	number of repeating units in the graft
NMR	Nuclear Magnetic Resonance
<i>p.a.</i>	<i>pro analysi</i>
PA	polyamide
PBS	phosphate buffer solution

PC	polycarbonate
PDMS	poly(dimethyl siloxane)
PE	polyethylene
PEG	poly(ethylene glycol)
PEO	poly(ethylene oxide)
PES	polyester
PGA	poly(glycolide)
PLA	poly(D,L-lactide) / poly(<i>rac</i> -lactide)
PLGA	poly(lactide- <i>co</i> -glycolide)
PMMA	poly(methyl methacrylate)
PP	polypropylene
<i>ppm</i>	<i>parts per million</i>
PTFE	polytetrafluoroethylene
PVA	poly(vinyl alcohol)
PVC	poly(vinyl chloride)
ROP	ring-opening polymerization
RT	room temperature in °C
<i>S</i>	weight related degree of swelling in %
SEM	Scanning Electron Microscopy
$T_{10\%}$	temperature of 10% loss of weight in °C
Tab.	table
T_g	glass transition temperature in °C
TGA	ThermoGravimetry Analysis
T_{\max}	temperature of maximum rate of weight loss in °C
$Y_{600\text{ °C}}$	residuum at $T = 600\text{ °C}$ in %
δ	chemical shift in <i>ppm</i>
ΔC_p	change of specific heat capacity during glass transition in $\text{J g}^{-1} \text{K}^{-1}$
ΔW	weight loss at T_{\max} in %
ε	strain in %
σ	stress in MPa

1 Introduction

1.1 Biomaterials

In 1986 the Consensus Conference of the European Society for Biomaterials defined a biomaterial as "a nonviable material used in a medical device intended to interact with biological systems" ^[1].

Another definition of a biomaterial is "any substance (other than a drug) or combination of substances synthetic or natural in origin which can be used for any period of time as whole or as a part of a system which treats, augments, or replaces any tissue, organ, or function of the body" ^[2].

The application of biomaterials is diverse: surgical instruments, prostheses, implants, scaffolds, bone regeneration, artificial hips, artificial organs: kidney, liver, heart auxiliary devices, vascular stents, catheters, intraocular lenses, plastic and reconstructive surgery and drug delivery vehicles ^[3]. They are made of different materials and each has specific requirements. The requirements for the mechanical and surface properties of materials are many. The first and most important requirement is that biomaterials must be compatible with the organism.

Biomaterials can be natural (biopolymers such as collagen, gelatin, cellulose, chitosan, starch) or synthetic in origin (metallic, ceramic, polymer, and other) ^[4,5]. Cellulose and its various modifications are the most frequently used biopolymers on natural basis. Biomaterials used as implants were synthetic, at first. Later came a whole range of different synthetic, natural and modified materials with a broad application ^[6-9]. They were mostly well tolerated by the body ^[8,10-17]. Materials now the subject of researchers' focus are hybrid materials that associate inert and living materials created by tissue engineering ^[18-27]. Polymers are a group of materials gaining interest in medicine. One of the most common and longest recognized homopolymers used as a biomaterial is poly(methyl methacrylate) (PMMA). Since Wichterle and Lim (1960) ^[28] discovered its application in intraocular lenses (IOL) it has been widely used. In addition, it is used for different orthopedic purposes. PMMA is a tough, stable material used for different applications. Soft contact lenses are obtained from polyhydroxy(ethyl methacrylate), poly(HEMA), which is a hydrophilic gel. Many other polymers are also used as biomaterials for different purposes as shown in Tab. 1-1.

Tab. 1-1 Examples of biomedical application of different polymers ^[3].

Polymer	Application
Polyethylene (PE)	catheters, hips (high molecular mass)
Polypropylene (PP)	catheters, hips (high molecular mass)
Polytetrafluoroethylene (PTFE)	vascular grafts
Poly(vinyl chloride) (PVC)	various medical tubing
Poly(dimethyl siloxane) (PDMS)	catheters, parts of pacemakers
Polycarbonate (PC)	lenses, heart-lung bypass machine
Polyamide (PA)	surgical sutures

Copolymers are synthesized in order to obtain materials with improved properties by combining different monomers in which each of them contributes to the final properties of the material. The most recent search for materials with well defined properties for specific medical applications has drawn attention to creating high-performance biomaterials, such as biodegradable materials or materials with other specific properties, through varying structure, chemical/physical modifications and the development of hybrid materials ^[29].

Among biomaterials biodegradable materials have a special place ^[6,7,30-34]. These materials are attracting more and more interest not only in the field of biomaterials, but also in the field of packaging, food containers, coating materials, etc. ^[35]

Until recently, the main interest in the polymer industry has been devoted to materials with stable properties. In contrast, biodegradable polymers, particularly aliphatic polyesters of the poly(hydroxy acid) type and copolymers have attracted interest, especially for their hydrolytical instability. Synthetic poly(hydroxy acids) derived from lactic acid, glycolic acid, ϵ -caprolactone and their various copolymers, are among the few synthetic polymers that have been used to obtain temporary scaffolds for the tissue engineering of tendons, skin, liver, bones, cartilage, heart valves and targeted drug delivering systems ^[31].

The degradation products that are formed upon hydrolysis, lactic acid and its oligomers or glycolic acid, have a very low physiological and environmental toxicity. For this reason the polymers are being extensively used and studied for various biomedical and pharmaceutical applications ^[36,37].

When these materials are used as drug release systems their biodegradable nature presents a great advantage compared to non-degradable materials. It enables the adjustment of the delivery rate by tuning their degradation and consequently improves efficacy. Also, when they are used as temporary scaffolds, their biodegradable nature presents an advantage because a second surgical procedure to remove the implant can be avoided ^[38].

Commercial interest in the poly(hydroxy acid) type copolymers started in 1970 with the introduction of synthetic resorbable sutures of PGA under the trade name Dexon™^[40] and is still growing^[38,41-51]. They are successfully used as bioerodible materials since they degrade into naturally occurring metabolites. Ester bonds in the homo- and copolymers are hydrolytically unstable, the degradation mechanism follows random hydrolytical chain scission through ester bonds with possible enzymatic effects^[52]. Carboxylic acid end groups appear as a result of ester hydrolysis reactions which can further catalyze the hydrolysis reaction. The resulting lactic and glycolic acids enter the tricarboxylic acid cycle and are metabolized and subsequently eliminated from the body as carbon dioxide and water^[52,53].

1.1.1 The influence of different parameters on properties

Molecular weight as well as structure plays an important role in physical properties such as thermal and mechanical properties, crystallinity and degradation behavior of the poly(hydroxy acid)s. Polymeric material has to have a high molecular weight in order to provide the desired mechanical properties^[39]. Various biomaterials are prepared from polyesters based on lactic and glycolic acid. Apart from their wide use in drug delivery systems, they can be easily processed to fibers and films with high tensile strength, or they can be fashioned into highly porous structures, suitable for invasion by proliferating cells^[54].

High molecular weight linear poly(L-lactide) is required for orthopedic applications, but its high melt viscosity results in degradation during the melt processing. As a possible solution, star-shaped polymers are suggested, which for the same molecular weight exhibit significantly lower melt viscosity^[55]. Also, in the very important field of their application as drug delivery systems, linear aliphatic polyesters display significant problems regarding the tuning of their release properties. A branched molecular structure offers the possibility of manipulating the degradation and release properties^[42,55,57-62]. In order to obtain diverse copolymers of α -hydroxy esters, different alcohols were used such as sorbitol, mannitol, pentaerythritol, glycerol, poly(vinyl alcohol), as well as the widely used poly(ethylene glycol), because of its hydrophilic nature, which presents an additional possibility of varying properties^[37,42,63,64]. This is important when copolymers are used as drug delivery systems or when cell growth is eligible. Following that concept, biodegradable comb-shaped polyesters of poly(lactide), poly(glycolide) and poly(lactide-*co*-glycolide) grafted onto poly(vinyl alcohol) were synthesized in order to study the influence of the structure and the increase of the hydrophilicity on degradation, solubility, and mechanical properties^[42,58,60,61].

Further modification of the physical properties of poly(α -hydroxy acid)s led to the synthesis of networks. These networks are obtained by reacting poly(α -hydroxy acid)s with different homopolymers such as PEG, dextran, PVA, or HEMA, bearing a double bond, in order to obtain scaffolds for various applications ^[65,66] or as drug delivery systems. Cross-links introduced in polylactides affect the physical properties such as crystallinity, melting point and glass transition temperature. The degradation characteristics will in turn also be influenced. Some mechanical properties, like high temperature dimensional stability, are in general improved upon cross-linking. These properties are very important in biomedical applications. Furthermore, directly or indirectly, the modulus, tensile strength and impact strength will be altered when the polymers are cross-linked ^[67].

1.1.2 Biodegradable materials

Degradability is an important property of a biomaterial that depends on the physical and chemical nature of the material. Biodegradable materials must have bonds which are susceptible to cleavage under physiological conditions, hydrolytically or enzymatically. One important and well established group present in poly(hydroxy acid ester)s such as poly(lactide), poly(glycolide), poly(trimethylene carbonate), polycaprolactone, poly(dioxanone), polydepsipeptides, is the ester group ^[30,68-71,167].

Materials having higher M_w degrade more slowly. The influence of the chemical structure is evident. Linear poly(lactide), poly(glycolide) and their copolymers show a slower rate of degradation than branched polymers of the same molecular weight ^[42,57]. Branched and star-shaped macromolecules have a different entanglement structure and possess a higher density of chain-ends than linear chains of comparable molecular weight. Furthermore, branched and star-shaped polymeric structures possess lower melt viscosity than linear polymers due to a smaller hydrodynamic volume of the polymer chains in the melt at comparable molecular weight ^[57]. This could affect the mechanical properties, the degradation behavior and physical aging. Furthermore, branched structures offer the additional possibility of modulating the hydrophilic/hydrophobic properties through the introduction of a more or less hydrophilic backbone ^[42,57,58]. By varying the composition, e.g. the ratio of lactide to glycolide in copolymers or the ratio of poly(hydroxy acid ester)s to the backbone polymer, e.g. (poly(ethylene glycole), ^[64,72] PVA, ^[42,49,58,60] dextrane, charged dextrane ^[57]) in linear, brush- and star-shaped copolymers, the degradation rate as well as other properties such as thermal and mechanical properties can be modulated in order to obtain materials with the desired properties. Additionally, the nature of the backbone polymer influences the degradation

mechanism. It means that not only the length and composition of grafted chains but also the length and functionality of the backbone significantly influence the properties and the degradation of graft copolymers^[49,57,61,62]. Ester groups in linear PLA hydrolyze randomly. In the case of linear PLA-PEO-PLA block copolymers the hydrolysis of ester bonds occurs at comparable rate along the PLA blocks, even in the vicinity of the PEO blocks excluding the general influence of the presence of the hydrophilic PEO^[73]. Linear PLGA degrades in a heterogeneous way, i.e. via an «inside-out» mechanism. Poly(lactide) or poly(lactide-co-glycolide) grafted onto different backbones degrades either following the «inside-out» mechanism or by erosion from the surface, depending on the nature of the backbone^[47]. Poly(lactide) possesses a slow biodegradation rate even in the non-crystalline form of poly(D,L-lactide), as well as in enantiomeric, semicrystalline forms of poly(D-lactide) and poly(L-lactide)^[74]. Poly(lactide) stereocopolymers are amorphous except for a percentage of L-lactide units higher than 90%^[75]. Crystalline residues remain much longer in the body as a result of slower degradation and cause necrosis^[76]. Thus the degradation rate of poly(lactide) based materials may be too slow for certain biomedical applications.

The thermochemical properties of a polymer are important for its degradation. In general, a polymer having higher T_g and higher crystallinity is less prone to degradation. Poly(lactide) degrades more slowly than poly(glycolide). This results from its higher hydrophobicity on the one hand, and from higher crystallinity in case of semicrystalline forms of poly(D-lactide) or poly(L-lactide) on the other. The crystallinity varies with molecular mass. The semicrystalline morphology of these materials leads to heterogeneous degradation rates whereby the amorphous regions degrade faster than the crystalline regions^[77,78]. In semicrystalline poly(lactide)s a distinction should be made between the mode of degradation of the crystalline and of the amorphous regions. In the first stage of degradation, water will diffuse into the amorphous regions of the polymer hydrolyzing the amorphous polymer. Cleaved chains become more mobile and will tend to crystallize. Poly(lactide) crystallizes in a helical form, where the hydrophobic methyl groups are at the outside of the helix and the hydrolysable ester bonds are directed more toward the inside of the helix. It appears that the helical structure is an important factor in the hydrolysis of the polymer. Modification of poly(lactide)s can strongly influence the degradation characteristics. For instance, the degradation of amorphous poly(D,L-lactide) can be slowed down by using the comonomers trimethylene carbonate^[79], ϵ -caprolactone^[69,80], or enhanced by incorporation of structurally similar but faster degrading glycolide^[26,69,81]. Copolymers of L-lactide and glycolide are amorphous in the range of 25% to 70% glycolide, whereas copolymers of D,L-lactide and glycolide are amorphous up to 70%

glycolide ^[31,68,76]. Not only the degradation mechanism but also the degradation location depends on the structure and the composition of the copolymer. Even though there are controversial data in the literature on degradation mechanisms, it is generally accepted, as Vert et al. ^[76] have shown, that large-sized PLGA devices degrade faster inside than at the surface and that cleavage proceeds non-randomly. In vitro degradation of poly(D,L-lactide-co-glycolide) films have shown that thick films degrade faster than thin films with the same composition ^[82].

1.2 Hydrogels

Hydrogels are water swollen, cross-linked two- or multicomponent systems consisting of a three-dimensional network of polymer chains and water that fills the space between the macromolecular chains. Depending on the properties of the polymer(s) used, as well as on the nature and density of the network joints, such structures in equilibrium can contain various amounts of water. Typically, in the swollen state the mass fraction of water in a hydrogel is much higher than the mass fraction of the polymer. Two general classes of hydrogels can be defined

- **physical gels (pseudogels)**, where the chains are connected by electrostatic forces, hydrogen bonds, hydrophobic interactions or chain entanglement (such gels are non-permanent and usually they can be converted to polymer solutions by heating) and
- **chemical (true or permanent) hydrogels** with covalent bonds linking the chains.

Since according to the definition hydrogels must be able to hold, in equilibrium, a certain amount of water, this implies that polymers must have at least a moderate hydrophilic character. In practice, to achieve high degrees of swelling, it is common to use synthetic polymers that are water-soluble when in the non-crosslinked state. Typical simple materials used as hydrogels are poly(ethylene oxide), poly(vinyl alcohol), poly(vinyl pyrrolidone), poly(ethylene glycol), and poly(hydroxyethyl methacrylate).

1.2.1 The diverse application of hydrogels

Hydrogels have a number of applications; in the cosmetic industry, as industrial absorbents, spill dams, sealers, and in agriculture such as water retention and herbicide/pesticide applications, but their use in medicine and pharmacy is the most successful and promising ^[83-85]. Most commonly, after over 40 years of research in this field, they are used for soft contact lenses, drug-delivery systems, superabsorbents, wound dressings etc. Hydrogels possess many

characteristics that make them highly attractive for tissue engineering applications. Hydrogel materials' properties, such as permeability, mechanical strength and biocompatibility can be easily engineered for particular applications. Their high water content allows easy exchange of nutrients and wastes with the surrounding environment. The molecules of the extracellular matrix, such as proteins and polysaccharides, are generally hydrophilic molecules and from a material point of view are essentially hydrogels. Due to their similarity with the extracellular matrix, synthetic hydrogels have been investigated for uses in biology and medicine since Wichterle and Lim discovered the use of poly(HEMA) in the early 1960s ^[28]. Since then it has become the most widely used hydrogel with a water content similar to that of living tissue and exhibits a surface energy similar to that of body tissue; other advantages are that it is permeable for metabolites, inert to biological processes, not absorbed by the body, resistant to degradation, withstands sterilization with heat and can be prepared in various shapes and forms.

The majority of hydrogels for biomedical purposes is made of synthetic polymers, but there are also examples where cross-linked natural polymers, mainly polysaccharides, are applied. Widely used natural polymers are cellulose derivatives, alginates, collagen, gelatin and agarose ^[86]. The wide and successful application of hydrogels can be partially related to the fact that some of their important properties, such as the ability to absorb aqueous solutions without losing their shape and mechanical strength, are commonly met by many natural constituents of the human body, like muscles, tendons, cartilage etc. Besides that, hydrogels usually exhibit good biocompatibility in contact with blood, body fluids and tissues ^[87].

Recently, biodegradable hybrid material of synthetic or natural polymers with natural materials, e.g. proteins, is gaining importance ^[87]. A new category of advanced or smart hydrogels which change their molecular arrangement when exposed to a specific stimulus, such as light, pH change, temperature, solute concentration, ionic strength, electric field, sound or mechanical stress, has been developed ^[87].

Hydrogels are classified according to

- the method of preparation
- the structure (amorphous, semi-crystalline, hydrogen bonded)
- crosslinks between chains.

There are several methods of introducing crosslinks into a hydrogel, such as

- radiation cross-linking
- cross-linking through chemical reactions
- a combination of both.

Radiation cross-linking is performed by means of electrons, γ -rays, and X-rays or UV rays. For chemical cross-linking at least one bifunctional reagent has to be used, further a small amount of a multifunctional reagent can be used. Hydrogels may be synthesized in a number of chemical ways. These include one-step procedures like polymerization and parallel cross-linking of multifunctional monomers, as well as the multiple step procedures involving synthesis of polymer molecules having reactive groups and subsequent cross-linking by reacting the polymers with suitable cross-linking agents ^[88-91]. Nowadays, chemically cross-linked or physically associated hydrogel molecules can be generated in situ, injected, or implanted. In this way, proteins, peptides, oligonucleotides and small-molecule drugs can be incorporated ^[92-94].

Swollen, cross-linked poly(vinyl alcohol) hydrogels have been developed and tested as potential biomaterials for the replacement of diseased or damaged articular cartilage ^[95,96]. Hydrogels can be prepared by electron-beam irradiations of aqueous poly(vinyl alcohol) solution at various temperatures and doses of irradiation ^[97] or by repeated freeze-thawing ^[98-100]. The lack of sufficient mechanical properties presents a critical obstacle to their use as tissue replacement, but the compressive and tensile properties of poly(vinyl alcohol) hydrogels have been reported to be similar to those of articular cartilage ^[96].

1.2.2 The degree of swelling

The degree of swelling is an important property of a hydrogel. It influences the diffusion coefficient through the hydrogel, surface properties and surface mobility, mechanical properties and optical properties, particularly for contact lens application. The degree of swelling can be quantified and expresses the ratio between the weight of the sample in its swollen state and the weight of the sample in its dry state, or the ratio of the sample volume in the swollen state and the volume in the dry state.

2 Aim and concept of the thesis

The aim of this thesis is the synthesis and characterization of biodegradable hydrogels which are biocompatible and good swelling at the same time, which will allow cell growth and transport of nutrients and metabolites.

Considering the possible applications of these materials in medicine, different materials already widely used as biomaterials will be combined in order to achieve the desired properties.

An extensive investigation into the dependence between structure and properties will be conducted. Therefore the chemical composition, structure and theoretical cross-linking density in hydrogels will be varied and their influence on the surface properties, thermal and mechanical properties will be examined.

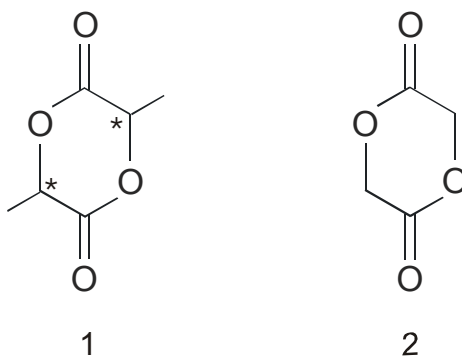
The examination will also encompass the degradation process and the influence of chemical composition, structure and cross-linking on the degradation pathway as well as on the mechanical and thermal properties of degraded materials.

The synthesis of polymer networks based on oligo(*rac*-lactide) or oligo(*rac*-lactide-co-glycolide) grafted onto a poly(vinyl alcohol) backbone is performed stepwise which allows good control of composition and length of grafts.

This procedure, when compared to the others resulting in similar (grafted) copolymers, displays the advantage of facilitating the variation of the degree of substitution on poly(vinyl alcohol).

In the first step, the ring-opening polymerization of lactide (**1**) or glycolide (**2**) will be carried out. This reaction is well known considering the above mentioned diesters as well as ϵ -caprolactone and *p*-dioxanone^[101].

The lactide comes in three stereoisomeric forms: L,L-dilactide, D,D-dilactide and D,L-dilactide^{*)}, which is used in this work.



^{*)} IUPAC name: (3*S*,6*R*)-3,6-dimethyl-1,4-dioxane-2,5-dione.

The number of repeating ester units in the oligomers is controlled by the ratio diester to the initiator 2-hydroxyethyl methacrylate (HEMA). The double bonds will allow cross-linking and in a later stage, the formation of a hydrogel.

The different length of polyester grafts is expected to influence the thermal properties of networks, the hydrophilicity/hydrophobicity and the surface properties of hydrogels as well as their mechanical properties (polyesters display a much higher elastic modulus than poly(vinyl alcohol))^[31,38,95,148].

Glycolide, introduced into the system, should influence the properties of the copolymer system and offers the additional possibility of modifying the hydrophobicity of the system due to its hydrophilicity.

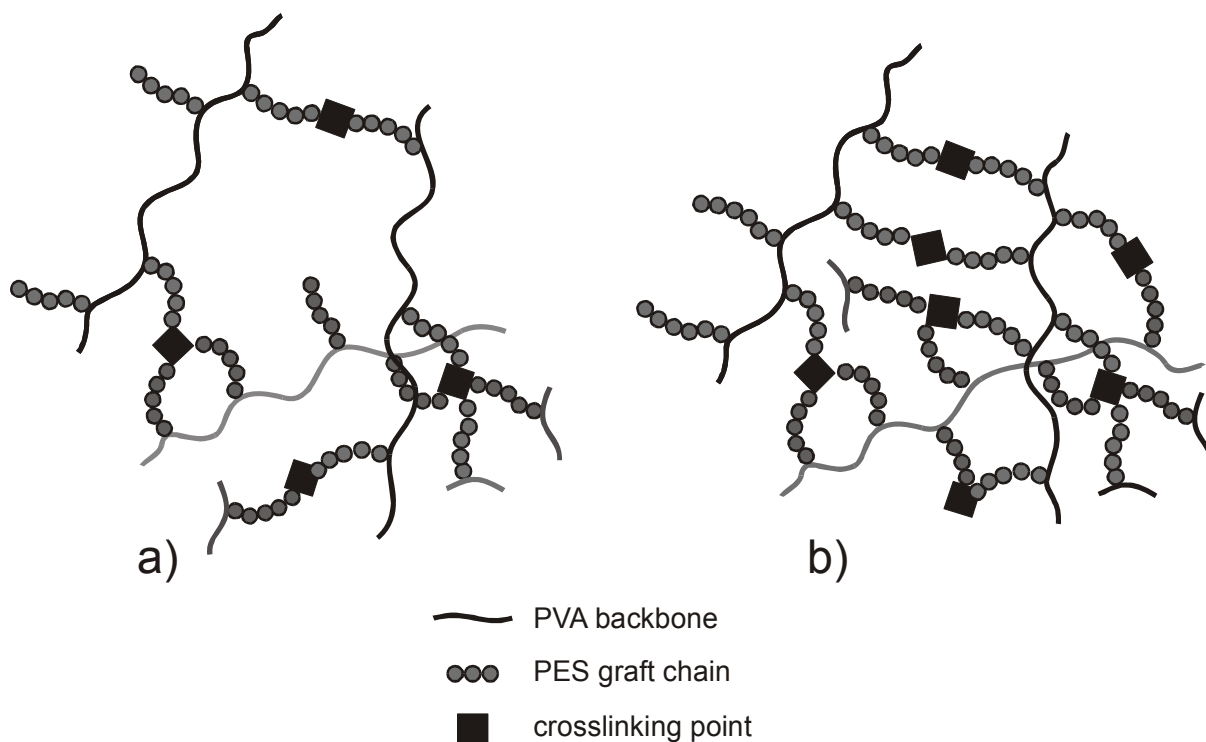
In order to enable grafting of polyester chains onto the poly(vinyl alcohol) (PVA) backbone, the polyester hydroxyl end groups will be transformed into carboxylic groups using succinic anhydride. The final step will be the free radical cross-linking reaction.

Different network architectures are expected to be achieved by varying different molecular parameters (Scheme 2-1). The networks will have fewer crosslinks due to a smaller number of long polyester grafts on the PVA backbone (Scheme 2-1a) or more crosslinks due to the higher number of short polyester grafts on the PVA backbone (Scheme 2-1b).

After synthesis the resulting networks/hydrogels^{**)} will be examined considering their thermal, mechanical as well as surface properties. An attempt to correlate the chemical characteristics such as composition, length and structure of networks with the former properties will be made. The degradation behavior of hydrogels with time will be investigated, as well.

The hydrolytical degradation behavior of hydrogels should differ depending on the ratio polyester grafts/PVA and the structure of both. Regarding the degradation behavior of the single components, it is well documented in the literature that the degradation of poly(lactide) depends on stereoregularity, crystallinity, molecular weight, structure, sample geometry and the time of degradation lasts from several months to several years^[30,38].

^{**)} In the dry state they are called “networks”, in the water-swollen state “hydrogels”.



Scheme 2-1 Schematic description of a) looser and b) denser form of resulting networks depending on their structure.

Thus semi-crystalline poly(lactide)s have excellent mechanical properties, but exhibit long degradation periods, depending on their molecular weight, of between 1 and 8 years and may induce long-term complications *in vivo*, while amorphous D,L-lactide stereo-copolymers fully degrade in about 20 weeks, but suffer from poor mechanical properties. Poly(glycolide) shows a shorter degradation period from 4 to 12 weeks and displays lower mechanical strength than poly(lactide) ^[30]. In the case of poly(vinyl alcohol) there are several findings on its hydrolytical stability and solubility where is reported that if the molecular weight does not exceed 15 000, it is water soluble and leaves the body without degradation ^[7,58,67].

The properties of the materials can be tuned and above all the degradation, in a fairly wide range. Thus, a material that will exhibit biocompatibility in order to enable cell attachment and proliferation, retain shape and some mechanical strength for ca. 8 weeks in order to enable cell attachment and proliferation is sought for in the present case.

3 Synthesis of networks based on poly(*rac*-lactide) or poly(*rac*-lactide-co-glycolide) with poly(vinyl alcohol)

Synthesis was performed in three steps starting with the ring opening reaction of lactide and glycolide. The next synthesis step was the transformation reaction of hydroxyl end groups into carboxylic groups. The third step was the grafting reaction of polyester chains on the PVA backbone and finally a hydrogel was obtained upon free radical reaction of the double bonds.

3.1 Ring-opening polymerization (ROP) of cyclic esters

Aliphatic polyesters, *generally*, and polylactides in particular, can be synthesized via one of two pathways: either the step-polycondensation of α -hydroxyacids, or the ring-opening polymerization (ROP) of cyclic esters, lactones or lactides. By the step-polycondensation method polycondensates of low molecular weight and with poor mechanical properties are obtained ^[39]. This procedure usually requires a long reaction time, a high temperature and the continuous removal of by-products such as water and careful adjustment of the reagents' stoichiometry. All these disadvantages are overcome by ring-opening polymerization, which provides direct, simple access to the related polyesters and a high degree of polymerization is typically achieved ^[43,46,51,102-107].

Polymerization occurs either in bulk or solution, however, bulk polymerization is desirable when the end product is intended for medical applications. Bulk polymerization avoids the use and potential residual presence of organic solvents.

Nontoxic, resorbable initiators or catalysts for the copolymerization of cyclic esters may be based on cations such as Na, K, Mg, Ca, Zn and Fe which play a role in human metabolism. However, Na, Ca, Mg and K salts are very basic and in that way they catalyze side reactions such as deprotonation of glycolide and lactide in α -position. As a result, low molecular weight and racemization of the copolyesters typically occur. A couple of resorbable Zn salts such as ZnCl₂, ZnI₂, Zn(stearate) and ZnLac₂, as the most suitable catalysts of this kind were studied ^[108]. Strong Lewis acids like tin (IV) halides, tin tetraphenyl, Zr salts Zr(acetylacetonate) were also studied as catalysts ^[107,109].

The ring-opening polymerization of lactides is promoted by various inorganic and organic compounds that have been classified in two categories depending on their activation

mechanism. Lewis acid type catalysts such as metals, metal halogenides, oxides, aryls, and carboxylates, in combination with protic compounds, activate the lactide ROP.

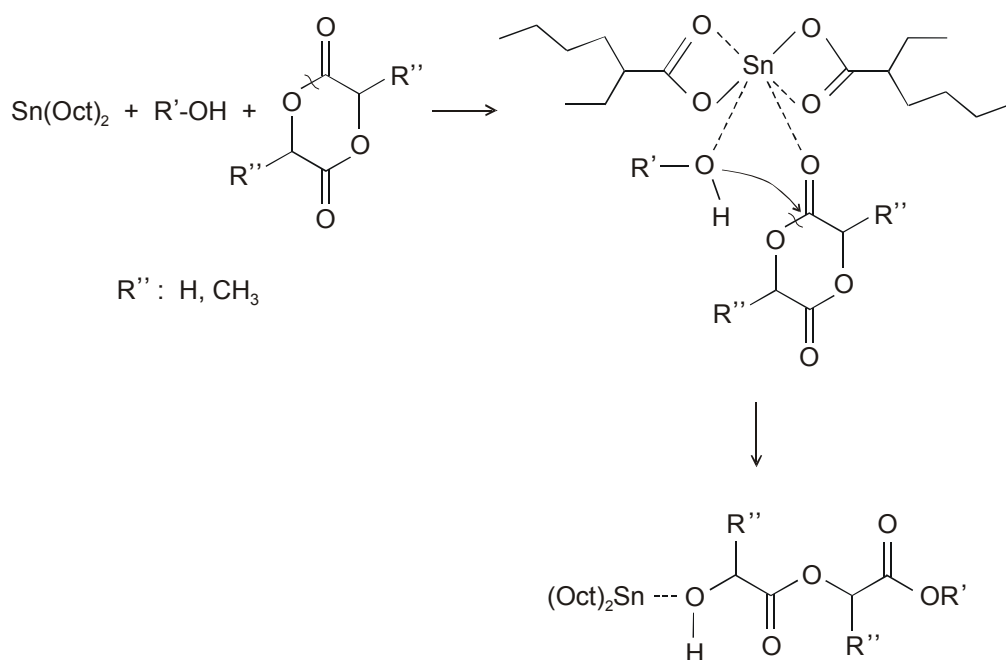
When the ring-opening polymerization of lactide is initiated by antimony ^[110], lead ^[111], zinc ^[106,112], diethyl zinc ^[113], or preferably tin catalysts, such as tin(IV) halides ^[114,115], tin oxide ^[116], tin octoate ^[38,46,51,55,63,103,117-122], and tin tetraphenyl ^[123], but also various metallic alkoxides ^[124-126], high molecular weights are obtained. Alkoxides of metals containing free p, d and f orbitals of a favorable energy, e.g., Sn, Ti, Zn, Zr, Y, Nd, Sm, and Al, have been considered as initiators for the ROP of lactides.

Copolymerization of glycolide with lactide and glycolide with ϵ -caprolactone was performed in the presence of zirconium (IV) acetylacetonate ^[109] and calcium acetylacetonate ^[44] which are efficient initiators.

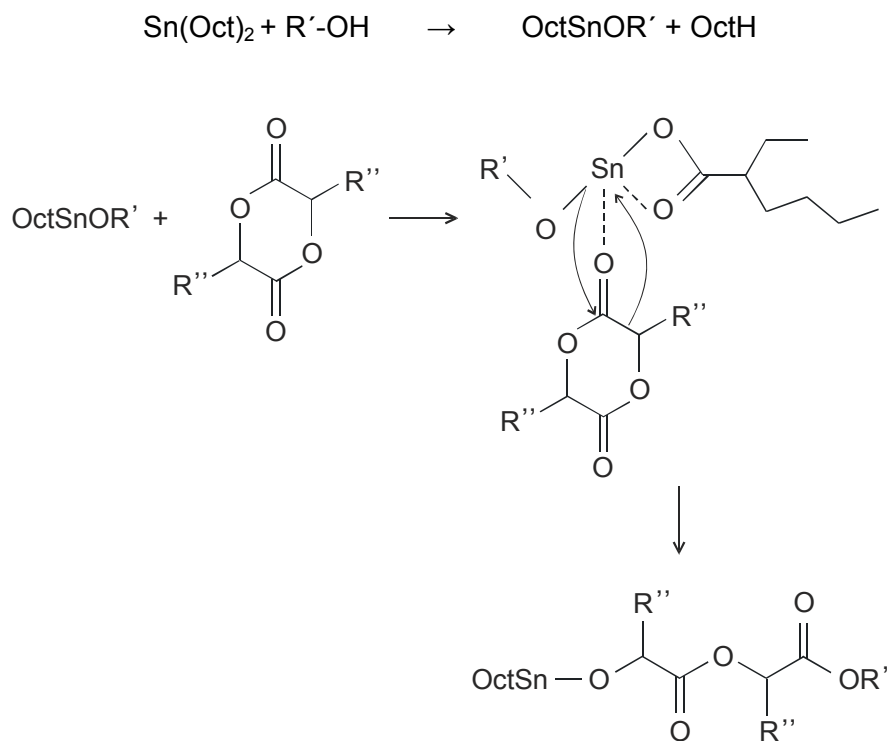
For the solution polymerization of lactide potassium methoxide CH_3OK ^[124,125] and aluminium trisopropoxide, $\text{Al}(\text{OiPr})_3$, which is efficient both in bulk ^[127] and solution ^[107], were used.

The ring-opening polymerization of lactides was studied parallel using aluminium trisopropoxide, $\text{Al}(\text{OiPr})_3$ and tin(II) bis (2-ethylhexanoate), $\text{Sn}(\text{Oct})_2$, as the initiator ^[127]. The activating mechanism for both is «coordination-insertion». The polymerization rate for both increases when equimolar amounts of a Lewis base are added ^[43].

Tin(II) bis (2-ethylhexanoate) ($\text{Sn}(\text{Oct})_2$) has been extensively used as a Lewis acid catalyst in combination with protic compounds such as water, alcohols, primary and secondary amines and thiols ^[38,43,46,51,55,63,103,104,106,120,121]. Tin octoate was accepted by the FDA as a food additive which means that its toxicity is very low; it is a highly efficient and commercially available catalyst ^[128]. The mechanism of the $\text{Sn}(\text{Oct})_2$ catalyzed polymerization has been widely investigated and several proposals have been made ^[104,128-130]. Two slightly different reaction pathways are presented in Scheme 3-1, where the alcohol functionality and the monomer both are coordinated to the tin-complex during propagation ^[128,130] and in Scheme 3-2, where the tin-complex is converted into tin-alkoxide before complexing and ring-opening of the monomer ^[129].



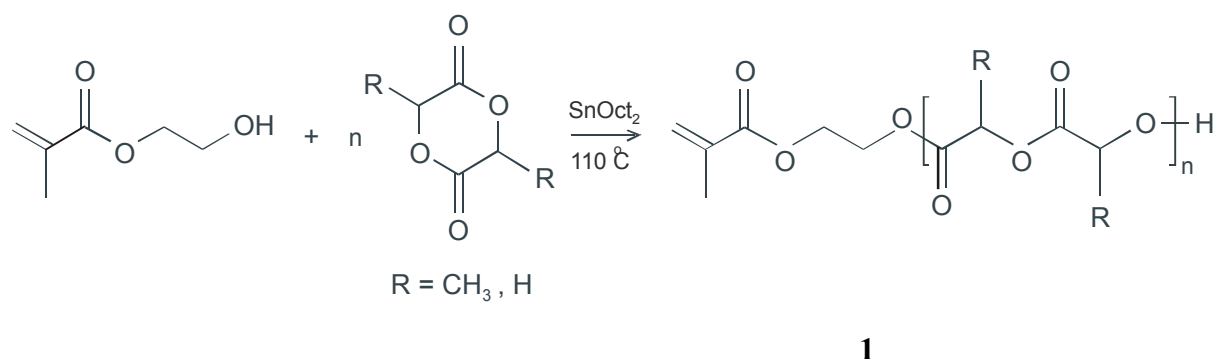
Scheme 3-1 $\text{Sn}(\text{Oct})_2$ catalyzed ring-opening polymerization (ROP): complexation of monomer and alcohol functionality precedes ROP.



Scheme 3-2 $\text{Sn}(\text{Oct})_2$ catalyzed ring-opening polymerization (ROP): formation of tin-alkoxide before ROP.

3.2 Ring-opening polymerization of lactide and glycolide

Poly(lactide) or poly(lactide-*co*-glycolide) oligomers were obtained according to Scheme 3-3.

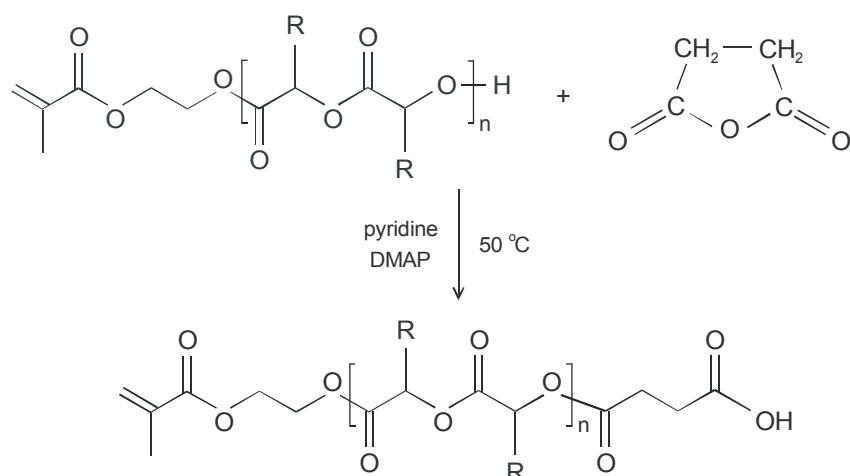


Scheme 3-3 Reaction scheme for the synthesis of poly(lactide) or poly(lactide-*co*-glycolide) oligomers.

The oligomer **1** was obtained by ring-opening polymerization of *rac*(lactide) and glycolide using hydroxyethyl methacrylate (HEMA) as an initiator and tin octoate as a catalyst. The number of repeating units was kept low by the molar ratio of the monomer to the initiator. More detailed conditions are given in Tab. 7-1 (Chapter 7.2.1).

3.3 Transformation reaction of end groups

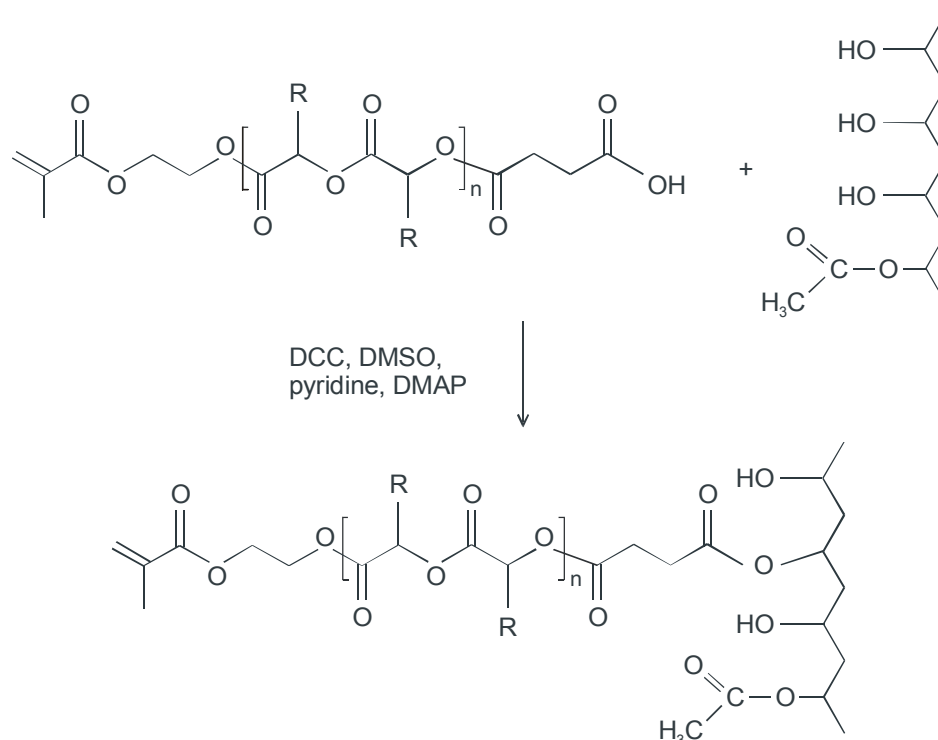
Oligomers **1**, having methacrylate double bonds at one end and hydroxy groups at the other end, were further reacted with succinic anhydride according to Scheme 3-4. The aim was the transformation of hydroxy end groups into carboxylic end groups in order to enable grafting onto the poly(vinyl alcohol) chain. More detailed reaction conditions are given in Tab. 7-2 in Chapter 7.2.2.



Scheme 3-4 Transformation of hydroxy into carboxylic end groups.

3.4 The reaction of grafting of poly(lactide) or poly(lactide-*co*-glycolide) oligomers onto poly(vinyl alcohol) backbone and crosslinking

The grafting reaction of poly(lactide) or poly(lactide-*co*-glycolide) chains onto PVA backbone was performed as shown by Scheme 3-5, with the assistance of dicyclohexyl carbodiimide (DCC), a common coupling reagent. More detailed reaction conditions are given in Tab. 7-3 (Chapter 7.2.3).



Scheme 3-5 Grafting reaction of poly(lactide) or poly(lactide-*co*-glycolide) oligomers onto the poly(vinyl alcohol) backbone.

In order to obtain networks, the crosslinking reaction was performed through reacting of methacrylate double bonds. The radical initiator 2,2'-azobis(2-methylpropionitrile) (AIBN) was used. A more detailed description of the cross-linking reaction is given in Chapter 7.2.4.

In Tab. 3-1 the theoretical compositions of synthesized hydrogels are given.

Tab. 3-1 Theoretical compositions of copolymer networks; N presents the number of polyester unit in grafts, DG_{the} theoretical degree of grafting on PVA backbone.

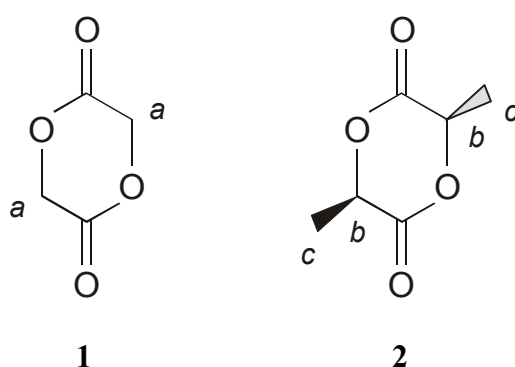
Sample	LA : GA	N	DG_{the} , %
A	100 : 0	16	15
B	100 : 0	8	15
C	100 : 0	4	20
D	100 : 0	4	15
E	100 : 0	4	10
F	75 : 25	16	20
G	75 : 25	16	15
H	75 : 25	16	10
I	75 : 25	8	20
J	75 : 25	8	15
K	75 : 25	8	10
L	75 : 25	4	20
M	75 : 25	4	15
N	75 : 25	4	10
O	50 : 50	16	15
P	50 : 50	8	15
Q	50 : 50	4	20
R	50 : 50	4	15
S	50 : 50	4	10

4 Characterization of networks

Different methods of analysis were applied in order to characterize the properties of networks and NMR analysis was used to follow their synthesis.

4.1 Synthesis of networks

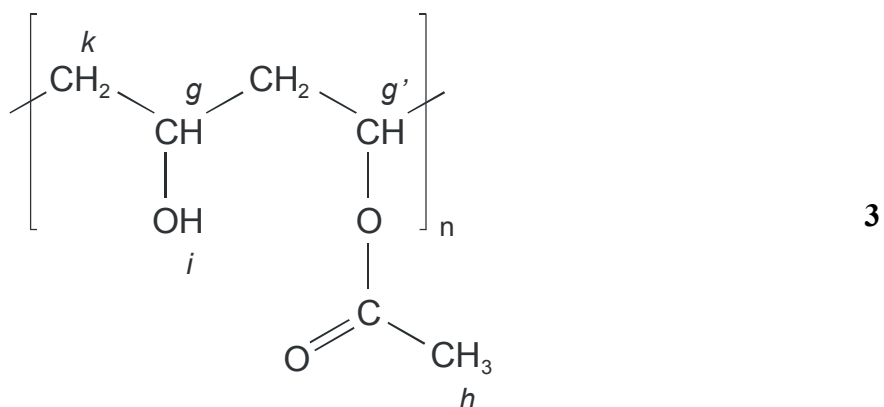
The efficacy of each synthetic step was followed by means of ^1H -NMR analysis. The ^1H -NMR data of the glycolide (1) and the *rac*-lactide (2) dimers are given in Tab. 4-1.



Tab. 4-1 ^1H -NMR data of glycolide (1) and lactide (2) dimers.

Proton	Multiplicity	δ / ppm
a	s	4.95
b	q	5.06
c	d	1.67

Data of PVA (3) are given in Tab. 4-2 and the spectrum is shown in Fig. 4-1.



Tab. 4-2 ^1H -NMR data of the PVA (3) ($M_w = 6\ 000$; 80% hydrolyzed).

Proton	Multiplicity	δ / ppm
i	m	4.73-4.13
g	m	3.98-3.71
h	m	2.05-1.87
k	m	1.66-0.97

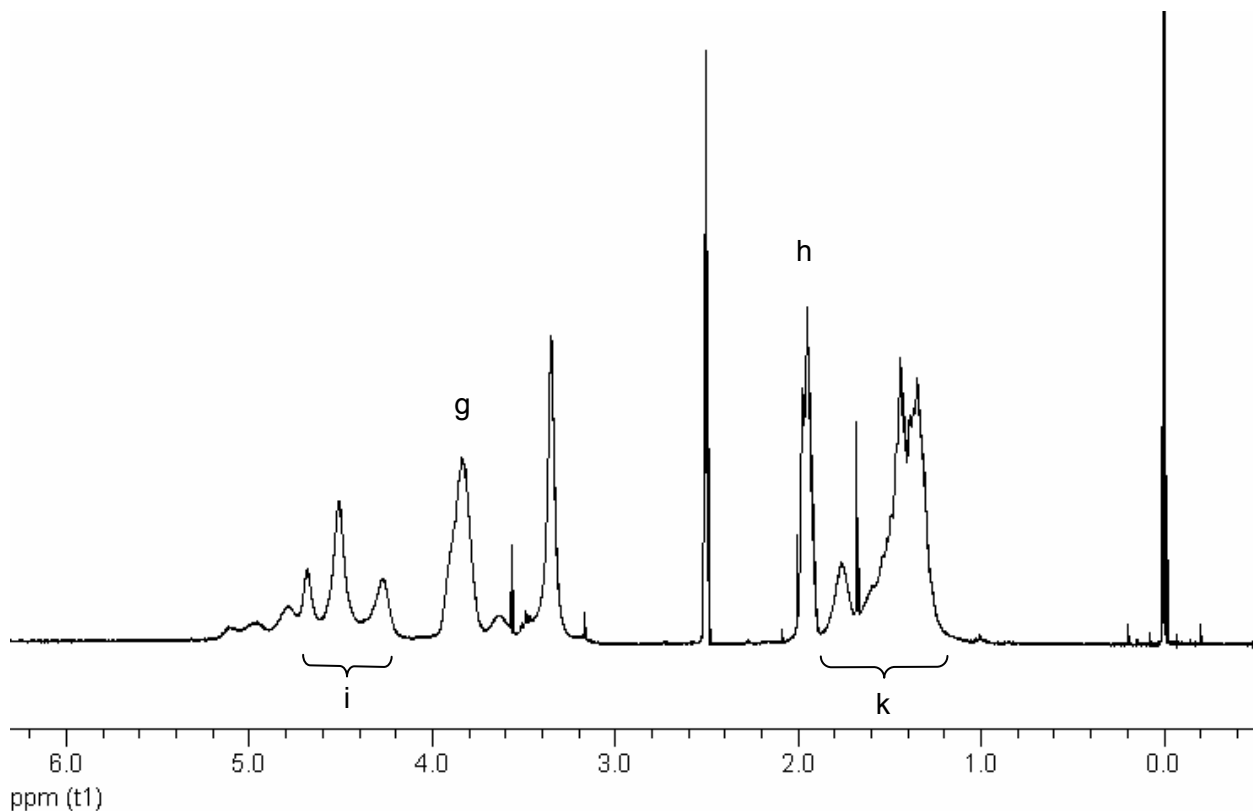
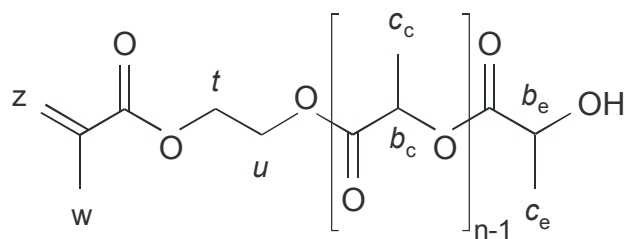


Fig. 4-1 ^1H -NMR spectrum of PVA (3) ($M_w = 6\ 000$; 80% hydrolyzed) in $\text{DMSO-}d_6$.

The data of intermediates and the final grafted copolymer are given in Tab. 4-3 to Tab. 4-6 and the spectra in Fig. 4-2 to Fig. 4-5.

The ratio of resonance integrals of the methyl protons of lactic units $I(c_c + c_e)$ at 1.4-1.6 ppm and of vinyl protons of the methacrylate end groups, $I(z)$ at 5.6 or 6.1 ppm (Fig. 4-2, Tab. 4-3), gives the number of repeating ester units in the poly(*rac*-lactide) initiated with HEMA (4) (Eq. 4-1):

$$N(LA) = \frac{I(c_c + c_e)/3}{I(z)} \quad (4-1)$$



4

Tab. 4-3 ^1H -NMR data of poly(*rac*-lactide) (4) initiated with HEMA.

Proton	Multiplicity	δ / ppm
z (<i>trans</i>)	s	6.12
z (<i>cis</i>)	s	5.60
b_c	m	5.29-5.09
t + u + b_e	m	4.50-4.27
w	s	1.95
c_c + c_e	m	1.64-1.42

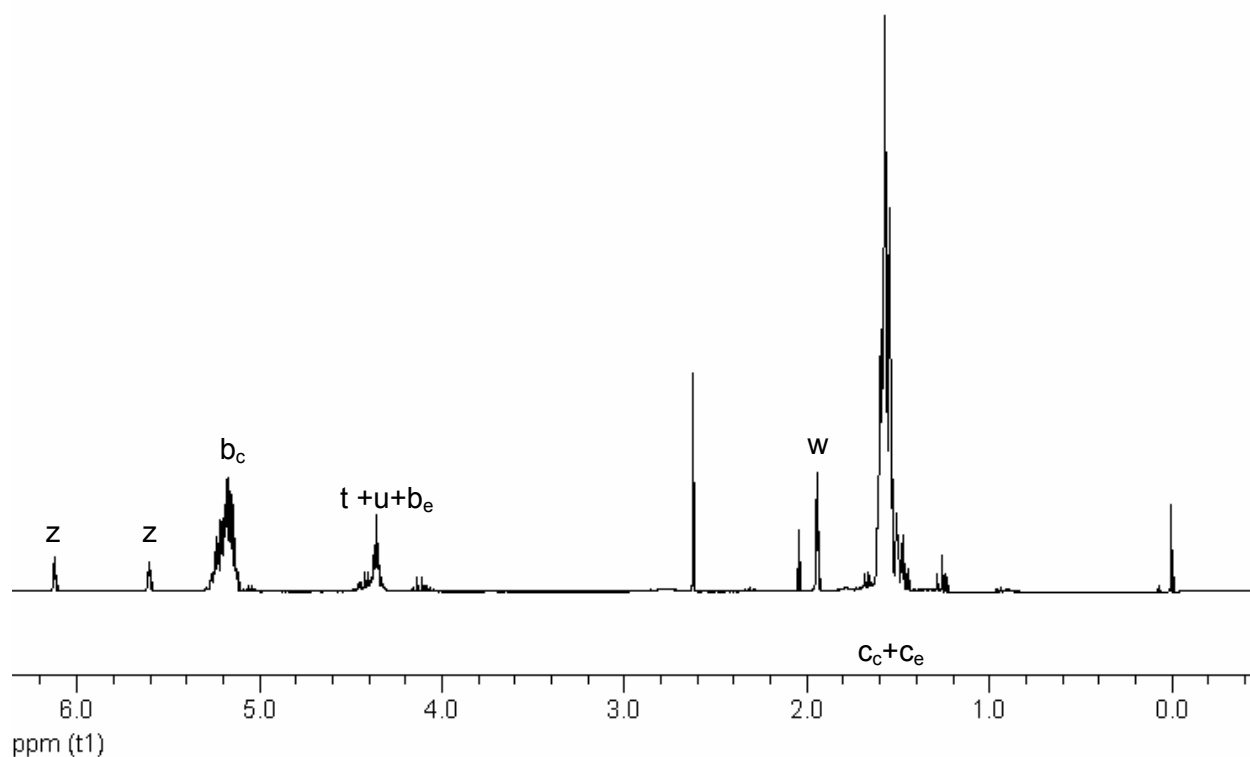
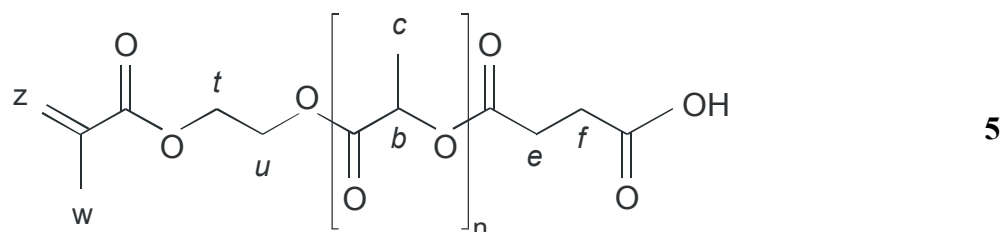


Fig. 4-2 ^1H -NMR spectrum of poly(*rac*-lactide) (4) initiated with HEMA in CDCl_3 .

The number of ester repeating units was calculated to be 16 in the poly(*rac*-lactide) grafts of copolymer A and 8 in grafts of copolymer B. Samples C, D and E also showed agreement between the calculated number of repeating ester units and the theoretical ones given in Tab. 3-1.

The conversion of the hydroxy end groups into acid groups in the following synthesis step was verified by comparing the resonance integrals of the methylene protons $I(e + f)$ at 2.8-2.6 ppm of the succinic ester end group to the methylene $I(t + u)$ protons at 4.5-4.3 ppm of the HEMA end group (Fig. 4-3, Tab. 4-4). The ratio was found to be close to 1 which corresponds to a conversion of 100% for all products.



Tab. 4-4 ^1H -NMR data of poly(*rac*-lactide) (5) initiated with HEMA after reacting with succinic anhydride.

Proton	Multiplicity	δ / ppm
z (<i>trans</i>)	s	6.12
z (<i>cis</i>)	s	5.60
b	m	5.31-4.99
t + u	m	4.51-4.26
e + f	m	2.83-2.57
w	s	1.95
c	m	1.74-1.46

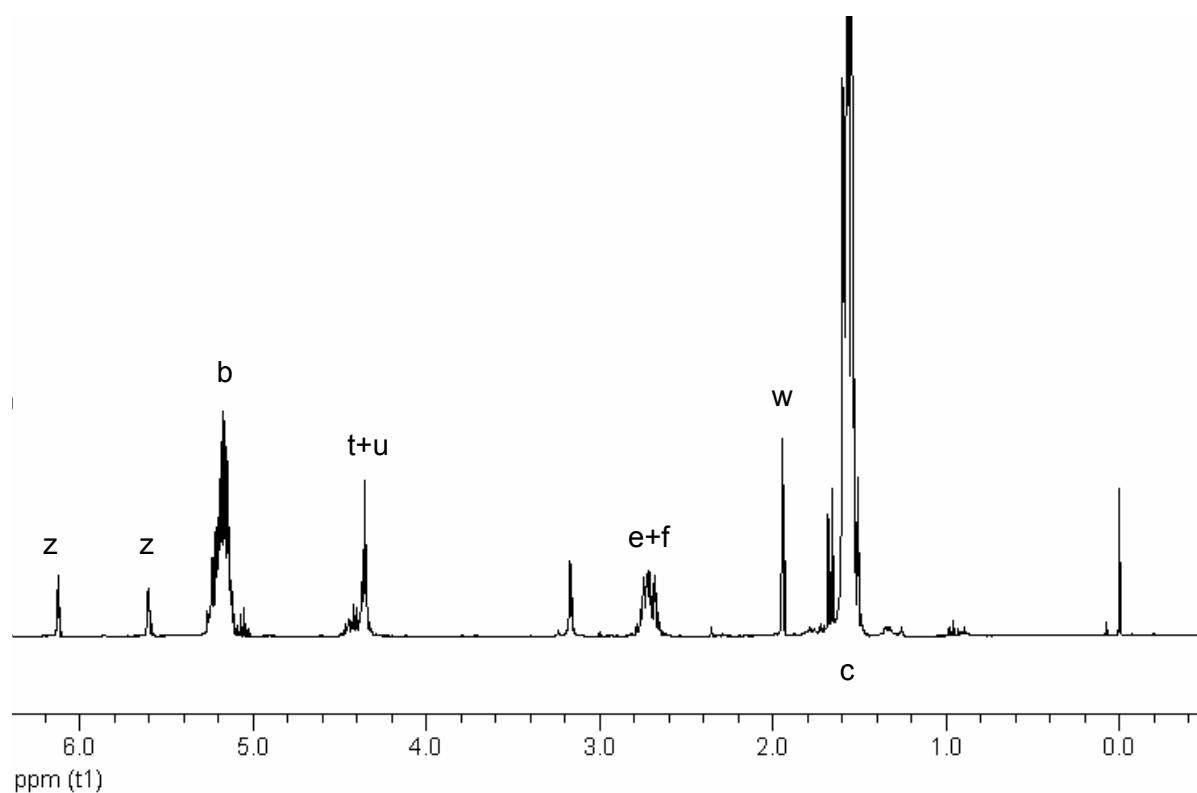


Fig. 4-3 ^1H -NMR spectrum of poly(*rac*-lactide) initiated with HEMA after reacting with succinic anhydride (5) in CDCl_3 .

Copolymers containing lactide and glycolide were submitted to NMR analysis after reacting with succinic anhydride. The number of repeating ester units in poly(lactide-*co*-glycolide) $N(LA+GL)$ was calculated from the ratio of resonance integrals of the methyl protons of lactic acid ester $I(c_c + c_e)$ at 1.4-1.6 ppm and of methylene protons of glycolic acid ester $I(a)$ at 4.5-5.0 ppm (Tab. 4-5, Fig. 4-4) to methacrylate protons, $I(z)$ at 5.6 or 6.1 ppm (Eq. 4-2):

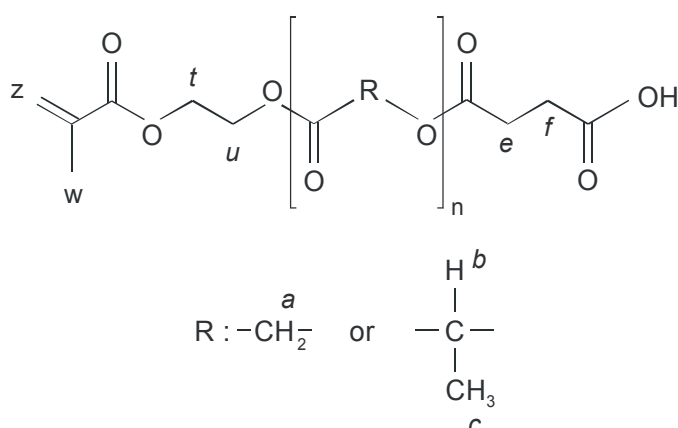
$$N(LA + GL) = \frac{I(c_c + c_e)/3 + I(a)/2}{I(z)} \quad (4-2)$$

All copolymers that contain lactide and glycolide had a number of calculated repeating units equal to the theoretical ones (Tab. 3-1) except for those in network P, which had 9 repeating units according to NMR analysis compared to the theoretical number of 8, and the copolymer in network O with 18 repeating ester units as compared with the theoretical number of 16.

The ratio between lactide and glycolide moieties was calculated as the ratio of resonance integrals of the methine $I(b)$ at 5.3-5.0 ppm and methylene $I(a)$ at 5.0-4.5 ppm protons (Eq. 4-3).

$$\frac{x(LA)}{x(GL)} = \frac{I(b)}{I(a)/2} \quad (4-3)$$

The calculated molar ratios matched the theoretical ones (Tab. 3-1) in all copolymers.



6

Tab. 4-5 ^1H -NMR data of poly(*rac*-lactide-*co*-glycolide) (6) initiated with HEMA after reacting with succinic anhydride.

Proton	Multiplicity	δ / ppm
z (trans)	s	6.12
z (cis)	s	5.60
b	m	5.34-5.04
a	m	5.00-4.52
t + u	m	4.52-4.17
e + f	m	2.87-2.56
w	s	1.97
c	m	1.80-1.45

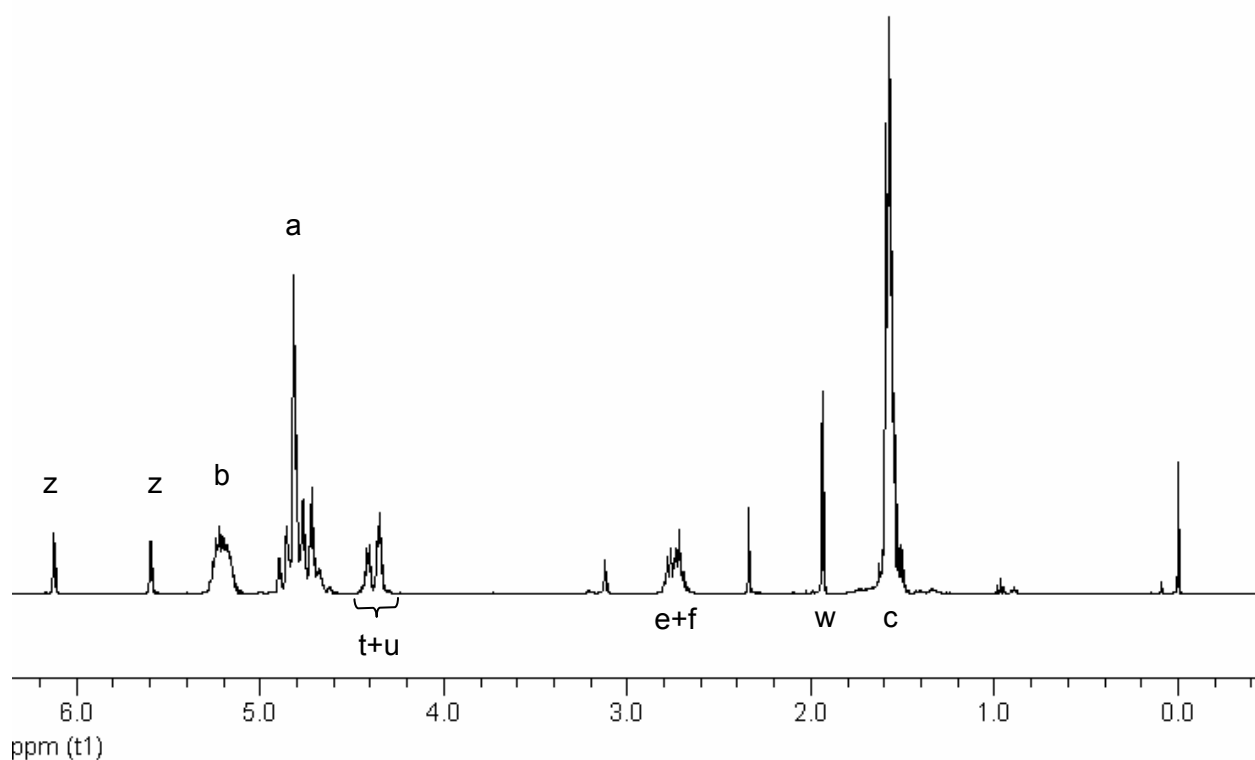


Fig. 4-4 ^1H -NMR spectrum of poly(*rac*-lactide-*co*-glycolide) (6) initiated with HEMA after reacting with succinic anhydride in CDCl_3 .

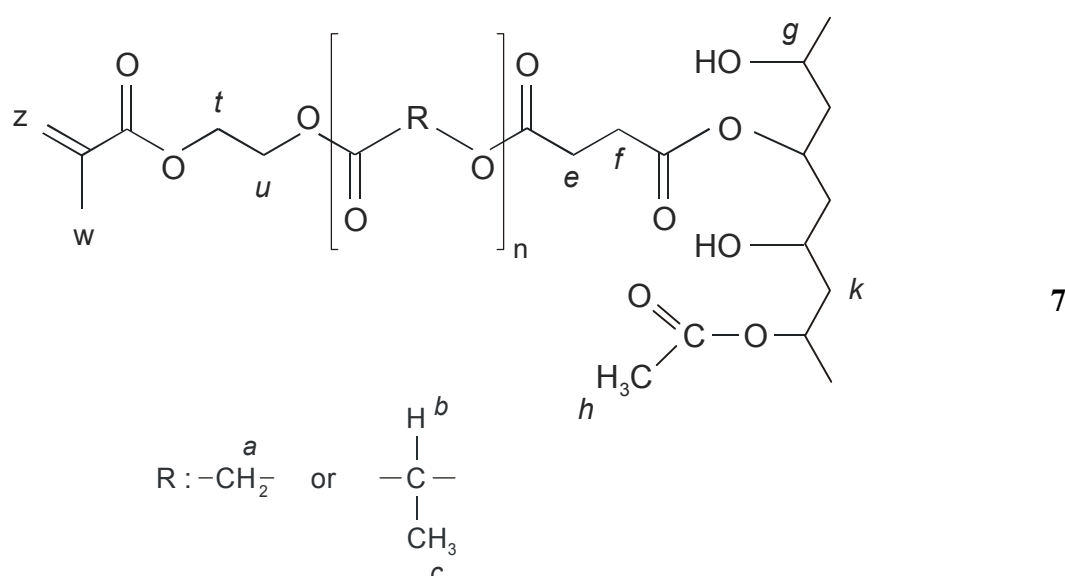
The number of polyester grafts per vinyl alcohol units is defined as degree of grafting, DG . Theoretical degree of hydrolysis (DH) of PVA is declared to be 80% which means that 20% of acetate groups (DA) are still present on the backbone. The degree of hydrolysis of PVA was also calculated from NMR spectra (Fig. 4-1, Tab. 4-2) examining percentage of acetate groups on the backbone based on the Eq. 4-4:

$$DA = \frac{I(h)/3}{I(g)} \times 100 \quad (4-4)$$

where $I(h)$ at 1.95 ppm is the resonance integral of the acetate methyl protons and $I(g)$ at 4.00-3.70 ppm the resonance integral of methine proton. DA is found to have value of 24% and consequently DH value of 76%.

The degree of grafting (DG_{exp}) of the polyester oligomers on the PVA backbone was calculated from the ratio of the resonance integrals of the methacrylate methyl protons $I(w)$ at 1.85 ppm and the acetate methyl protons $I(h)$ at 2.00 ppm (Fig. 4-5, Tab. 4-6) knowing that percentage of acetate groups (DA) on the PVA is 24%:

$$DG_{\text{exp}} = \frac{I(w)}{I(h)} \times 24\% \quad (4-5)$$



Tab. 4-6 ^1H -NMR data of poly(*rac*-lactide-*co*-glycolide) (7) grafted onto PVA backbone.

Proton	Multiplicity	δ / ppm
z (trans)	s	6.04
z (cis)	s	5.70
b	m	5.35-5.00
a	m	5.00-4.70
t + u + i	m	4.70-4.00
g	m	4.00-3.70
h	m	2.00
w	s	1.85
c + k	m	1.82-1.20

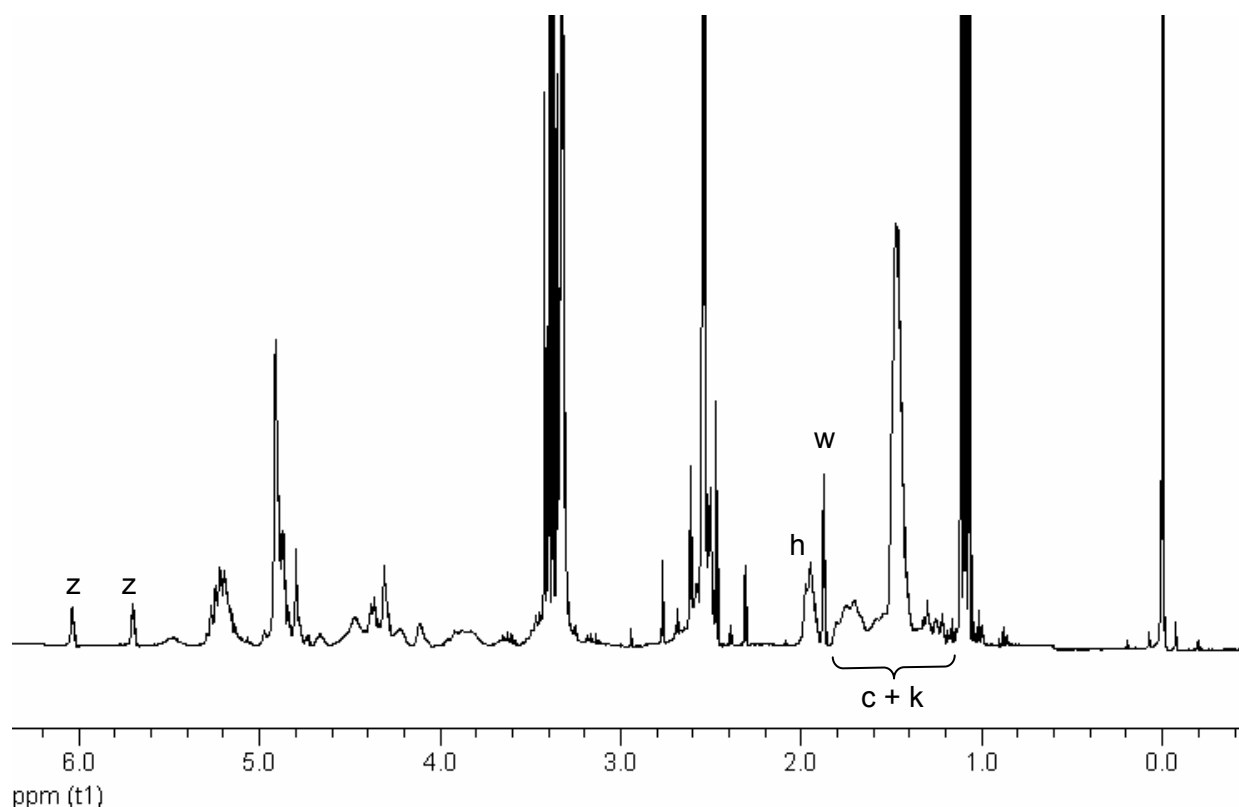


Fig. 4-5 ^1H -NMR spectrum of poly(*rac*-lactide-*co*-glycolide) (7) grafted onto PVA backbone, in $\text{DMSO-}d_6$.

In some cases physical cross-linking made ^1H -NMR analysis of the grafted samples impossible because they became non-soluble ^[65]. In Tab. 4-7 the DG_{exp} and DG_{the} of copolymers where it was possible to apply ^1H -NMR analysis are given.

Tab. 4-7 Theoretical and experimental values of the degree of grafting (DG).

Sample	DG_{the} , %	DG_{exp} , %
B	15	8
D	15	7
F	20	15
G	15	11
I	20	14
M	15	11
O	15	11
P	15	13
Q	20	11
R	15	8

The experimentally determined degree of grafting on the PVA backbone revealed lower than theoretical values. Grafted copolymer Q showed a major deviation; the experimental degree of grafting DG_{exp} of 11% compared to the theoretical DG_{the} of 20% and the best match showed sample P; DG_{exp} of 13% compared to the theoretical DG_{the} of 15%.

4.2 IR analysis of networks

In order to follow the different composition of the networks, the IR spectra of *rac*-lactide and glycolide, of their homopolymers, of a copolymer, and of poly(vinyl alcohols) were recorded. The obtained spectra are shown in Fig. 9-1 to Fig. 9-7. Tab. 9-1 gives the characteristic group frequencies.

The analysis was performed on the networks A, B, D (100 mol% poly(lactide), number of repeating ester units: 16, 8, 4; theoretical degree of grafting on PVA backbone, DG_{the} , 15%), O and P (50 mol% poly(lactide), number of repeating ester units: 18 and 9; DG_{the} 15%) and their spectra are shown in Fig. 4-6.

Tab. 4-8 Group frequencies in the IR spectra of networks A, B, D, O and P ^[131].

Bond	Type of compound	Frequency range, cm^{-1}	Intensity
O-H	Alcohols	3200-3600	variable, sometimes broad
C-H	Alkanes	2850-2970	strong
		1340-1470	
	CH ₃ , CH ₂ , CH	1470	medium
	CH ₃	1380	strong
	CH ₂ scissor	~1300	variable
C = O	Aldehydes, ketones, carboxylic acids, esters	1690-1760	strong
C-O	Alcohols, ethers, carboxylic acids, esters	1050-1300	strong
C-O		~1250, ~ 1100	
CH ₃ -CO-OR		1240	
R-CO-OR		1190	
>C(CH ₃)-COO		1140	
sec. alcohol		1100	
>CH-COO		1050	

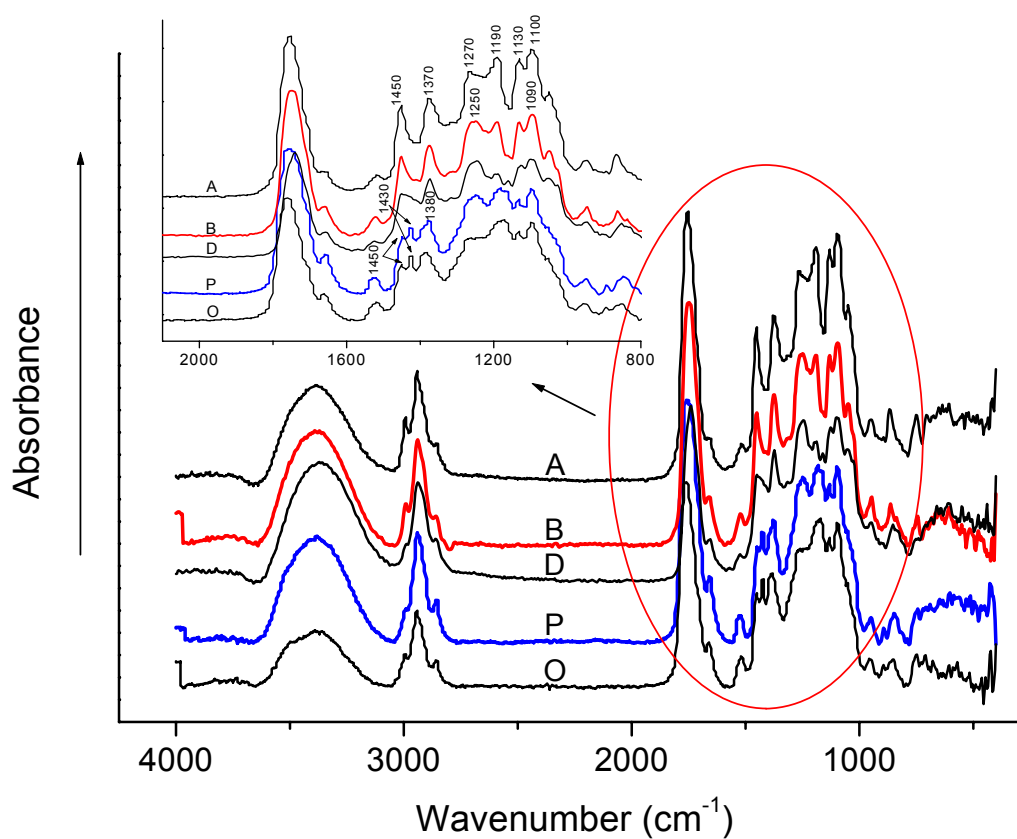


Fig. 4-6 IR spectra of networks A, B, D, O and P.

Characteristic absorption bands are observed around 3380 cm^{-1} (OH), 2940 cm^{-1} (C-H) and 1750 cm^{-1} (C=O), their intensities and intensity ratios are given in Tab. 4-9.

Tab. 4-9 Characteristic absorption bands, the bands area and their ratios of networks A, B, D, O and P.

Characteristic signals							Area ratio	
Sample	O-H _{str} cm ⁻¹	A _{O-H}	C-H _{str} cm ⁻¹	A _{C-H}	C=O _{str} cm ⁻¹	A _{C=O}	A _{O-H} /S _{C-H}	A _{O-H} /A _{C=O}
A	3390	3176	2943	1029	1754	2451	3.085	1.295
B	3390	3846	2939	958	1747	2285	4.015	1.683
D	3383	3981	2939	914	1739	1537	4.356	2.590
O	3390	1836	2940	782	1760	2095	2.348	0.876
P	3380	3825	2940	1160	1750	2671	3.297	1.432

The IR spectra do not show the absorption bands of the methacrylate double bond at 1637 cm⁻¹ which indicates that cross-linking has occurred to a large extent.

Comparing the C=O band in networks A, B and D, with increasing length of polyester grafts, there is a shift of the band toward higher wave numbers, as mentioned in the literature [64]. Similar dependence exhibit network P (1750 cm⁻¹) with 9 ester units in poly(lactide-*co*-glycolide) and network O (1760 cm⁻¹) with 18 units. Comparing networks A (1754 cm⁻¹) and O (1760 cm⁻¹), and especially B (1747 cm⁻¹) and P (1750 cm⁻¹), it is evident that different composition causes less shifting than different number of repeating ester units in grafts. The influence of the composition depends on the length of grafts; it is less significant in networks with shorter grafts. The band around 3380 cm⁻¹ is very broad and is assigned mainly to residual OH groups of PVA. The band at 2940 cm⁻¹ is the most stable one and has a value of around 2939±4 cm⁻¹ for all networks.

Higher polyester content results in lower OH/C-H and OH/C=O band intensity ratios. Thus network A with 16 ester repeating units has an OH/C-H band ratio of 3.09 and an OH/C=O band ratio of 1.29 while network D with only 4 ester repeating units has an OH/C-H band ratio of 4.36 and an OH/C=O band ratio of 2.59.

A small difference in the structure and constitution of a molecule results in significant changes in the distribution of absorption bands in the region between 1200 and 700 cm⁻¹. Exact interpretation of spectra in this region is hardly possible [131].

The spectra of poly(vinyl alcohol) PVA 6 ($M_w = 6000$, 80% hydrolyzed) (Fig. 9-6) and PVA 16 ($M_w = 16\ 000$, ≈98% hydrolyzed) (Fig. 9-7), show that in this region there are two absorption bands, at approximately 1465 cm⁻¹ (δCH of methylene and methyl) and at 1380 cm⁻¹ (δCH of methyl). PVA 16 shows a very weak band at 1380 cm⁻¹, which indicates the

presence of only a few acetate groups, as opposed to PVA 6, which shows quite an intense band as a consequence of several acetate groups along the chain. The methylene group exhibits bands at approximately 1300 cm^{-1} . Further in this region, bands at 1250 cm^{-1} and 1100 cm^{-1} give evidence of the presence of C-O. Since the $\text{CH}_3\text{-CO-OR}$ group shows a stretching vibration (νCH) at 1240 cm^{-1} while the *sec* alcohol stretching vibration ($\nu\text{C-O}$) appears at 1100 cm^{-1} , it is obvious that in the case of PVA 6 both are present, while in the case of PVA 16 only the band at 1100 cm^{-1} is present from *sec* alcohol C-O vibrations.

Absorptions that appear in the fingerprint region of the spectra of *rac*-lactide or glycolide and are characteristic of alkanes are around 1445 cm^{-1} ($\delta\text{C-H}$ of methylene and methyl) and 1386 cm^{-1} ($\delta\text{C-H}$ of methyl). Characteristic C-O bands (1240 and 1100 cm^{-1}) appear in the lactide spectrum, Fig. 9-1, while the spectrum of glycolide, Fig. 9-2, shows a more pronounced band at 1307 cm^{-1} , characteristic of CH_2 wagging and twisting vibrations, and a band at 1052 cm^{-1} characteristic of $>\text{CH-COO}$ groups. After homopolymerization, in the spectrum of poly(lactide) (PLA) there is a band characteristic of R-CO-OR appearing at 1192 cm^{-1} , Fig. 9-3, while in the spectrum of poly(glycolide) (PGA) this band is merged with the C-O band at 1240 cm^{-1} , Fig. 9-4. A spectrum of poly(lactide-co-glycolide) is given in Fig. 9-5 where all characteristic bands appear.

In the region $1500\text{-}1000\text{ cm}^{-1}$, networks A, B, D, O, P show significant differences of absorption bands as a consequence of different composition (Fig. 4-6).

Samples with poly(lactide) grafts (A, B and D) show one band around 1450 cm^{-1} while samples with 50 mol% of glycolide in the polyester chain (O and P) show split bands at 1450 and 1425 cm^{-1} , as a consequence of the glycolide-lactide interactions^[51,165] (Fig. 9-8 and Fig. 9-9). These samples also show a much stronger band around 1180 cm^{-1} , sample O and especially sample P, relative to the band around 1250 cm^{-1} . This is also a consequence of the glycolide present in the polyester chain because the polyester groups give bands of R-CO-OR around 1190 cm^{-1} and $\text{C}(\text{CH}_3)\text{-COO}$ around 1130 cm^{-1} in networks with pure lactide (i.e. A and B) while in networks containing glycolide (i.e. O and P) there is one strong band of R-CO-OR appearing around 1190 cm^{-1} .

In networks A, B, and D (Fig. 4-6) the difference of intensity between the bands at 1450 cm^{-1} and 1375 cm^{-1} increases with decreasing length of polyester chain. Thus, network A has a slightly weaker band at 1450 cm^{-1} than at 1375 cm^{-1} , while the band at 1450 cm^{-1} of network B and especially network D are significantly weaker than the band at 1375 cm^{-1} . This indicates the lower contribution of the polyester share in networks B and D than in A, which is in agreement with the fact that in the poly(D,L-lactide) spectrum (Fig. 9-5) the band at 1455

cm^{-1} is stronger than the band at 1383 cm^{-1} while in the PVA spectrum (Fig. 9-6) the band at 1430 cm^{-1} is weaker than the band at 1370 cm^{-1} . With an increasing polyester content in networks D, B and A, the band at 1100 cm^{-1} becomes stronger than the band at 1250 cm^{-1} , as it is the case in poly(D,L-lactide), which emphasizes an increasing amount of polyesters relative to the PVA in networks because in the spectrum of PVA (Fig. 9-6) the band at 1100 cm^{-1} is weaker than the band at 1250 cm^{-1} . Thus, sample D with the lowest amount of polyester, has a weak band at 1189 cm^{-1} compared to the band at 1245 cm^{-1} , while in network B the band at 1190 cm^{-1} is equal, or stronger in network A, than the band at 1245 cm^{-1} .

This confirms that IR analysis is useful for the qualitative analysis of networks based on polyester grafted PVA chains.

4.3 Thermal properties of networks

In order to investigate the thermal properties of networks TGA and DSC analysis were performed. The hydrogels were freeze dried before analysis.

4.3.1 The thermogravimetry (TGA)

The TGA and DTGA curves of PVA and networks A, B, D, G and P are shown in Fig. 4-7. The thermal degradation process can be divided into three stages. In the first stage (the total weight loss is up to 10%), a small loss in weight occurs due to water evaporation, followed by the second and third stage with a rather sharp decrease of the weight indicating the onset of a decomposition process.

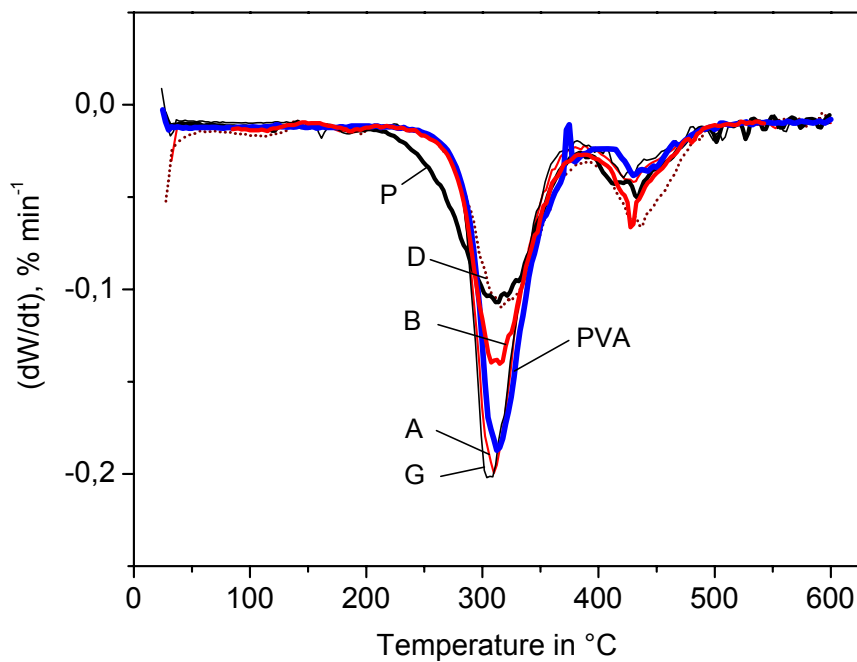
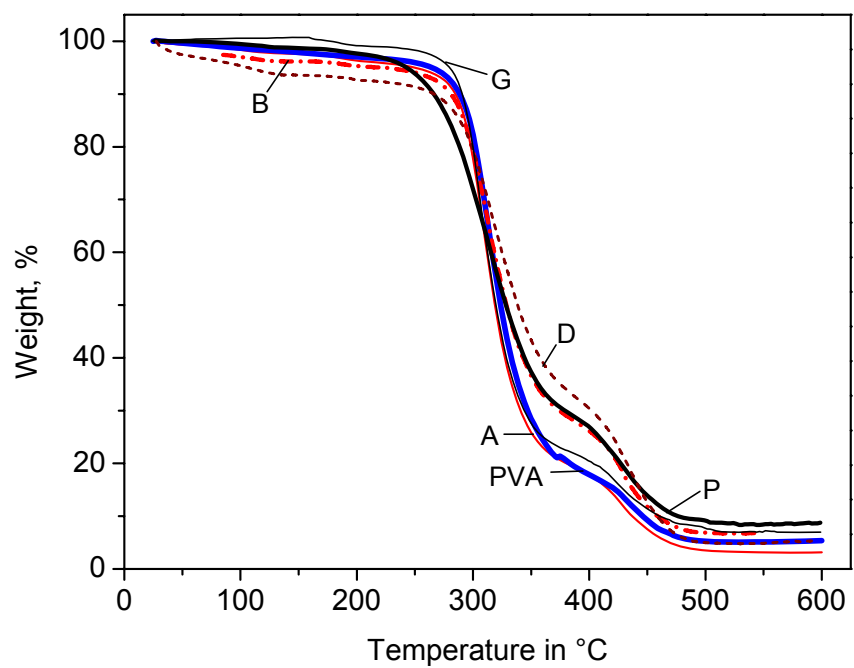


Fig. 4-7 TGA and DTGA plots of networks A, B, D, G, P and of the PVA sample ($M_w = 6000$, 80% hydrolyzed) measured at a rate of $10\text{ }^{\circ}\text{C min}^{-1}$.

In the case of PVA there is a three-stages decomposition process, as has been well documented in the literature ^[67,133,134]. The first process is below 270 °C due to water evaporation, the second one between 270–360 °C indicating the onset of a decomposition process involving a rapid loss of weight, and the third one, 360–500 °C, might be due to the formation and evaporation of volatile products ^[68,135,136]. Polylactide shows a small mass loss below 350 °C. Afterwards complete degradation takes place fairly rapidly in one step ^[55]. The thermograms of poly(lactide-co-glycolide) copolymers display a similar shape. There is a slightly higher starting weight loss; the main decomposition starts at a lower temperature and proceeds at an insignificantly slower rate than decomposition of polylactide ^[68].

Related with the structure, the weight loss in the second stage might be caused by oxidation and cleavage of ester bonds. In the third stage, methylene groups might be oxidized. The main thermal degradation in the examined networks starts above 250 °C and ends around 490 °C, Fig. 4-7. T_{max1} values within the main decomposition temperature range are around 311 °C for networks A, B and P and the PVA sample while network D exhibits a higher T_{max1} value of 318 °C and G a lower T_{max1} value of 301 °C relative to the former (Tab. 4-10). In the third stage the behavior between PVA and networks A and B is similar, while networks P and D show a higher and network G a lower T_{max2} value. The weight loss (ΔW_1) within the second stage decreases with decreasing length of the polyester grafts in the networks. The presence of glycolide in the network leads to an increase in weight loss in the second stage (comparison between networks B and P). The weight loss (ΔW_2) in the third stage increases with decreasing length of the polyester grafts in the networks. $Y_{600\text{ °C}}$ shows that the total amount of the residue at 600 °C has values between 4% and 11%.

Tab. 4-10 Thermal characterization of networks A, B, D, G and P and of poly(vinyl alcohol) (PVA), obtained by means of TGA at a heating rate of 10 °C min⁻¹;
 $T_{10\%}$, 10% loss of weight temperature; T_{max1} and T_{max2} , temperatures of maximum rate of weight loss; ΔW_1 and ΔW_2 , weight loss at T_{max1} and T_{max2} ;
 $Y_{600\text{ °C}}$, residue at $T = 600\text{ °C}$ in %.

	PVA	A	B	D	G	P
$T_{10\%}/^{\circ}\text{C}$	288	285	281	266	285	266
$T_{max1}/^{\circ}\text{C}$	311	310	312	318	301	312
$\Delta W_1/\%$	69	76	64	62	75	68
$T_{max2}/^{\circ}\text{C}$	430	429	429	436	424	433
$\Delta W_2/\%$	13	16	23	27	12	21
$Y_{600\text{ °C}}$	5	4	7	5	11	8

4.3.2 Differential scanning calorimetry

Differential scanning calorimetry has become the most widely used one of all thermal methods. The transparent network samples were measured in the temperature range from 20 °C to 150 °C (Chapter 7.3.4). The first heating run was performed in order to erase the thermal history.

4.3.2.1 Influence of the length of polyester chain on the thermal properties of the networks

The second run DSC thermograms of the networks: A, B, C, D, E, O, P, Q, R and S, are given in Fig. 4-8. All samples show only one glass transition temperature which means that there is no evidence for a phase separation. Since neither crystallization nor melting is observed in any of the networks, they can be considered as being amorphous.

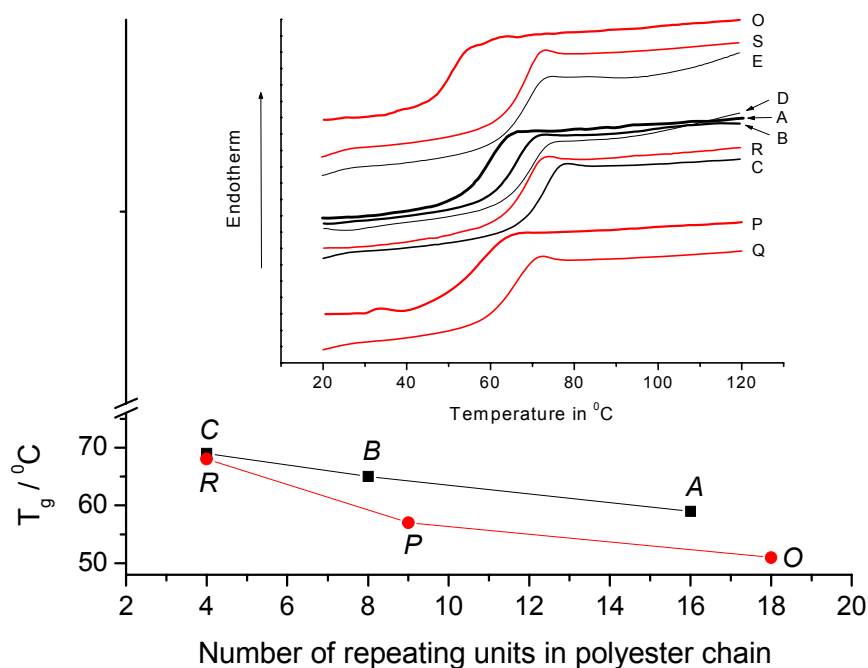


Fig. 4-8 DSC second run curves of different networks. T_g s belong to the two sets of networks with the same composition but different number of repeating units in the polyester branches.

A: 100 mol% LA;	$N = 16$;	$DG_{the} 15\%$	O: 50 mol% LA;	$N = 18$;	$DG_{the} 15\%$
B: 100 mol% LA;	$N = 8$;	$DG_{the} 15\%$	P: 50 mol% LA;	$N = 9$;	$DG_{the} 15\%$
C: 100 mol% LA;	$N = 4$;	$DG_{the} 20\%$	Q: 50 mol% LA;	$N = 4$;	$DG_{the} 20\%$
D: 100 mol% LA;	$N = 4$;	$DG_{the} 15\%$	R: 50 mol% LA;	$N = 4$;	$DG_{the} 15\%$
E: 100 mol% LA;	$N = 4$;	$DG_{the} 10\%$	S: 50 mol% LA;	$N = 4$;	$DG_{the} 10\%$

■ poly(*rac*-lactide)

● poly(*rac*-lactide-*co*-glycolide)

The glass transition temperatures of the examined networks are in the range between 51 °C and 71 °C (Tab. 4-11).

Tab. 4-11 Thermal properties of PVA and different networks.

Sample	$T_g / ^\circ\text{C}$	$\Delta C_p / \text{J g}^{-1} \text{K}^{-1}$
PVA	88	0.358
A	59	0.551
B	65	0.596
C	71	0.576
D	69	0.581
E	67	0.630
O	51	0.549
P	57	0.612
Q	69	0.606
R	68	0.618
S	67	0.668

The values of T_g of the networks are between the glass transition temperature of poly(vinyl alcohol) and of polylactide and polyglycolide (Tab. 4-12). All networks show similar values of ΔC_p . Only ΔC_p of the PVA sample is significantly lower due to its linear structure in comparison with the crosslinked structures of networks A-S.

Tab. 4-12 Comparison of thermal properties of the networks in this work with data available in the literature.

Polymers	T_g / °C	Comments	Literature
PVA	71	$M_w = 125\ 000$; 88% hydrolyzed	[137]
PVA	83	$M_w = 59\ 500$	[138]
PVA	58-85	87-99% hydrolyzed	[139]
L-LA	57	$M_w = 101\ 000$	[59,42]
L-LA	59	$M_w = 150\ 000$	[140]
L-LA	54	$M_w = 50\ 000$	[30]
L-LA	58	$M_w = 100\ 000$	
L-LA	59	$M_w = 300\ 000$	
L-LA	73.5		[141]
D,L-LA	53	$M_w = 134\ 000$	[59,42]
D,L-LA	50-60	$M_w = 200\ 000$ -250 000	[106]
D,L-LA	50	$M_w = 21\ 000$	[30]
D,L-LA	51	$M_w = 107\ 000$	
D,L-LA	53	$M_w = 550\ 000$	
PGA	34		[44]
PGA	35	$M_w = 50\ 000$	[30]
PLGA	45	$M_w = 40\ 00$ (LA:GA = 75:25)	[49]
PLGA	34	$M_w = 48\ 000$ (LA:GA = 75:25)	[142]
PVA-g-PLGA	34-41	brush like	[49]
PVA-g-PLGA	35-44	comb like	[59]
	51-71	Networks: A-S	Tab. 4-11

Thermal properties are found to be a function of the polyester chain length. In case of branched or comb-shaped copolymers there is a decrease of T_g with increasing length of side chains [58]. The polyester chains in the networks within the scope of this work are rather short ($M_w \leq 2000$). Oligomers of poly(*rac*-lactide) or poly(*rac*-lactide-co-glycolide) of different composition and having $M_n < 2000$ show low values of glass transition temperature (15-20°C) and a significant dependence of T_g on the initiating system used [143]. Oligomers initiated with triols or tetrols ($M_n \approx 10\ 000$) show much higher glass transition temperature: oligo(*rac*-lactide)tetrol (T_g , 46 °C) and oligo(glycolide)tetrols (T_g , 35 °C) [143]. Polyester segments within the networks in this work are comparable regarding their architecture and the molecular weight. The grafted architecture of polyester segments on the poly(vinyl alcohol) chain contributes additionally to the increase of the glass transition temperature. In networks A, B and D there is an increase of T_g from 59 °C for the network with 16 ester repeating units in grafts to 65 °C for the network with 8 ester repeating units and to 69 °C for the network

with 4 repeating units (Tab. 4-11). A similar behavior is observed for networks O, P, and R which contain glycolide in the polyester chain. Network O with 18 ester repeating units has a T_g of 51 °C, network P with 9 repeating units has a T_g of 57 °C and network R with 4 repeating units has a T_g of 68 °C.

4.3.2.2 Influence of glycolide content on the thermal properties of networks

DSC thermograms of the networks containing glycolide show lower glass transition temperature than networks with pure lactide grafts. The glycolide present causes the glass transition decrease as was documented ^[38]. The influence of the glycolide amount in poly(*rac*-lactide-*co*-glycolide) on the glass transition decreases with decreasing chain length. Thus, network A with a number of repeating ester units of 16 has a T_g of 59 °C and network O with a number of repeating *rac*-lactic-*co*-glycolic ester units of 18 has a T_g of 51 °C. The same difference of the T_g value of 8 °C is displayed by networks B and P with 8 and 9 repeating ester units, while for networks D and R, with only 4 repeating units, the difference in the glass transition temperature is 4 °C.

4.3.2.3 Influence of the degree of grafting on the thermal properties of networks

The influence of the degree of grafting on the thermal properties of the networks was difficult to quantify while experimental values of the degree of grafting were not available for all networks. Comparing the influence of the degree of grafting, regarding theoretical values, on thermal properties, network C, with the highest DG_{the} of 20%, which means the highest amount of lactide, and similar networks D and E, which have DG_{the} values of 15% and 10%, respectively, show the highest T_g (Fig. 4-9).

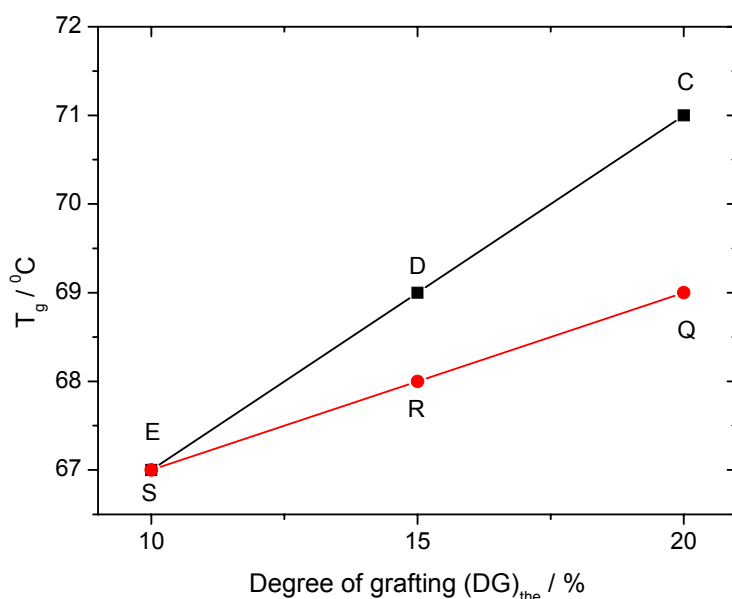


Fig. 4-9 The dependence of T_g on the theoretical degree of grafting for networks with only 4 repeating units in the polyester chain.

■ poly(*rac*-lactide) ● poly(*rac*-lactide-co-glycolide)

This seems to be surprising since the higher amount of lactide should result in a lower glass transition temperature; the high degree of grafting, however, results in an increased stiffness of the whole network C which yields a high T_g . Networks Q, R and S, which contain glycolide in the grafts showed a similar influence of the degree of grafting. By comparing the DG_{the} values, the influence of the degree of grafting (DG_{the} 20%, 15% or 10%) on T_g is evident but not significant. The difference is 1-2 °C for a theoretical difference of substitution on the poly(vinyl alcohol) chain of 5%. The increase of T_g is a consequence of lower segmental mobility due to higher crosslinking density.

4.4 Mechanical properties of hydrogels

The dependence of the mechanical properties of the hydrogels on composition and length of grafts, as well as on the degree of grafting was determined using a *MiniMat2000* apparatus. The hydrogel films were cut into stripes of similar shape having a width of 8 mm and a length of 50 mm. The samples were placed between two metal clamps, fixed and exposed to the force at given rate.

The strain on a material can be defined as any force acting on a material producing a stress and any change in the dimension of the material. With tensile materials, strain (ε) is the same as stretch, and is simply the ratio of the change in size to the original size, often given as a percentage (Eq. 4-6).

$$\varepsilon = \frac{l - l_0}{l_0} = \frac{\Delta l}{l_0} \quad (4-6)$$

The unit for stress (σ) is the force per unit area (Eq. 4-7).

$$\sigma = \frac{F}{A_0} \quad (4-7)$$

The relationship between stress and strain that a material displays is known as a stress-strain curve (Eq. 4-8) ^[144].

$$\sigma = E \cdot \varepsilon \quad (4-8)$$

It is characteristic for each material and is found by recording the amount of deformation (strain) at distinct intervals of tensile or compressive loading. This curve reveals many of the properties of a material. Young's modulus (E), also known as the elastic modulus, is the ratio between stress and strain and has the same units as stress (Eq. 4-8a).

$$E = \sigma / \varepsilon \quad (4-8a)$$

The E modulus presents the slope of the linear section of a stress-strain graph: the steeper the slope, the stiffer the material. For polymers, the maximum height of the stress-strain curve is called the tensile strength, since the stress resistance of the material decreases after the peak of the curve, this is also known as the yield point, which is a measure of the amount of stress a material can take before tearing apart. The point of rupture, or breaking strain, is the furthest horizontal extent of the stress-strain curve, and like strain is dimensionless.

The E modulus of water-swollen samples at the beginning of hydrolytical degradation is given in Fig. 4-10. Tab. 9-2 gives the values of Young's modulus as an average of five measurements for each sample with standard deviation.

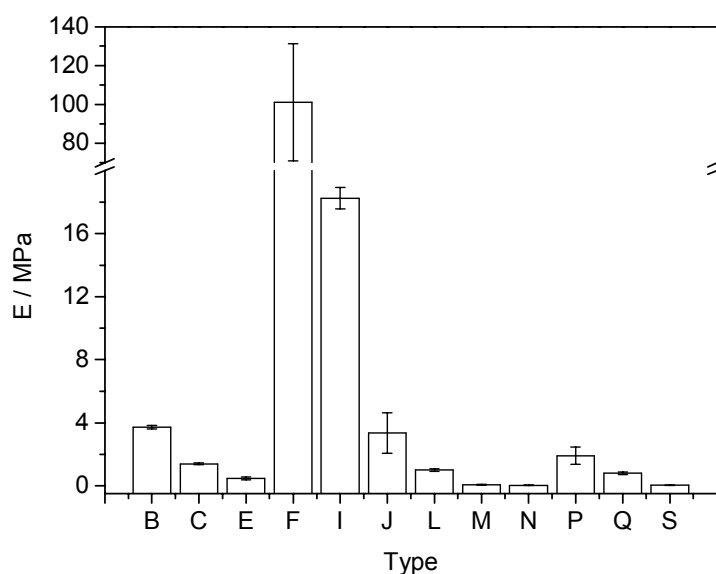


Fig. 4-10 E moduli of hydrogels, measured at room temperature at the onset of the hydrolytical degradation experiment (pH 7.4, room temperature).

B: 100 mol% LA; $N=8$; DG_{the} 15%	C: 100 mol% LA; $N=4$; DG_{the} 20%
E: 100 mol% LA; $N=4$; DG_{the} 10%	F: 75 mol% LA; $N=16$; DG_{the} 20%
I: 75 mol% LA; $N=8$; DG_{the} 20%	J: 75 mol% LA; $N=8$; DG_{the} 15%
L: 75 mol% LA; $N=4$; DG_{the} 20%	M: 75 mol% LA; $N=4$; DG_{the} 15%
N: 75 mol% LA; $N=4$; DG_{the} 10%	P: 50 mol% LA; $N=9$; DG_{the} 15%
Q: 50 mol% LA; $N=4$; DG_{the} 20%	S: 50 mol% LA; $N=4$; DG_{the} 10%

The E modulus of the hydrogels show significant differences having values between 0.01 and 100 MPa, depending on the composition and number of polyester repeating units and especially on the degree of substitution of PVA. Higher values of the E modulus are observed for the hydrogels F and I due to the influence of longer polyester grafts with 16 and 8 repeating units, respectively, combined with the higher degree of grafting (DG_{the} 20%) which results in the highest crosslinking density. Thus, the E modulus of the hydrogel F approaches the value of a thermoplastic polymer modulus (>100 MPa) ^[145]. Hydrogels B, J and P with 8 or 9 repeating units in polyester chains show higher E modulus relative to the other hydrogels which have only short polyester chains with 4 repeating units. Hydrogels I and J have the same lactide to glycolide ratio and number of repeating units in the grafts, but their DG_{the} differs (20% and 15%) and consequently, their E modulus differs by more than a factor of 4. All this indicates the strong influence of graft length which is followed by the influence of crosslinking density. The hydrogels with the shortest grafts (C, E, L, M, N, Q and S) are

soft and the degree of grafting does not influence their rigidity significantly. Since the samples with the shortest polyester chains and with similar degree of grafting but different composition regarding the lactide/glycolide ratio, show a similar E modulus, the conclusion can be drawn that the composition has negligible influence on the mechanical properties.

The influence of the glycolide portion in the polymer on mechanical properties was shown to be small in literature ^[141,146]. Moreover, it was reported that poly(lactide-*co*-glycolide) shows a faster loss of mechanical integrity than poly(lactide) upon hydrolysis; this, however, may be due to the difference in molecular weight ^[147]. The mechanical properties of aliphatic polyesters depend greatly on molecular weight. The bending strength of a poly(lactide) sample with $M_w = 160\,000$ is 50-60 MPa and the modulus of elasticity is ≈ 3 GPa. Poly(lactide) with $M_w = 250\,000$ has a modulus of elasticity of 7 GPa ^[148]. Thus, high molecular weight semi-crystalline poly(lactide)s have excellent mechanical properties, but exhibit long degradation periods and might induce long term complications in vivo. Poly(L-lactide) is a chiral crystalline polymer that is preferred in the production of surgical implants for internal fixation due to its high initial strength and good strength retention ^[31]. On the other hand, low molecular weight amorphous poly(D,L-lactide) fully degrades at much faster rate but suffers from poor mechanical properties ^[38]. Poly(L-lactide) ($M_w = 137\,000$) displays an elastic modulus of $\approx 20 \pm 3$ MPa, while its 40/60 w/w blend with poly(D-lactide) displays an elastic modulus of 22 ± 3.4 MPa and poly(D,L-lactide) displays an elastic modulus of 2.8 ± 0.4 MPa ^[149]. Young's modulus, and elongation-at-break of blended poly(L-lactide) and poly(D-lactide) films were reported to be higher than those of non-blended films. These films of blends show an E modulus between 1440 and 1780 MPa ^[150] and the molecular weight of the chiral poly(lactide)s is in the range of 10^5 to 10^6 .

Poly(vinyl alcohol) (PVA) hydrogels were proposed as promising biomaterials to replace diseased or damaged articular cartilage. A critical barrier to their use as load-bearing tissue replacement is a lack of mechanical properties. When measured over a strain range of 10-60%, the compressive modulus of PVA hydrogels increases from approximately 1-18 MPa, which is within the range of the modulus of articular cartilage ^[95]. The shear tangent modulus (0.1-0.4 MPa) was also found to be strain dependent and within the range of normal human articular cartilage ^[95].

Natural and synthetic hydrogels retain water within a three-dimensional network of polymer chains. Kobayashi et al. ^[96] performed mechanical tests on PVA hydrogels of different water content. They showed that by adjusting the water content in the gel production process PVA provides viscoelastic characteristics similar to those of human soft tissues. The stress-strain

curves in their work showed an E modulus of 5 MPa of the PVA hydrogel containing 20% of water, an E modulus of 0.45 MPa of the PVA hydrogel with 45% water content, an E modulus of 0.30 MPa of the PVA hydrogel with 60% water content, and an E modulus of 0.27 MPa of the PVA hydrogel with 90% water content which presents a value very close to the value of the human meniscus ($E \approx 0.20$ MPa). Sudhamani et al. ^[138] found that the tensile strength of PVA films is ≈ 2 MPa which is in the same range as obtained by Kobayashi et al. ^[96]. When mechanical properties of blended films of chitosan and PVA were measured ^[151] the E modulus was found to decrease with increasing amount of PVA in the blend. The E modulus of the dry PVA films was found to be 120 ± 56 MPa. This value is much higher than the E -values of hydrogels swollen to a different extent (0.27-5 MPa) ^[96].

The mechanical test proved the possibility of obtaining materials with different mechanical properties for diverse applications through variation of the composition and structure of hydrogels.

4.5 Surface properties of hydrogels

Knowledge of the surface properties of a material that has a potential to be used as a biomaterial is very important ^[152]. Hydrophilicity is most important for the cell adhesion process. The hydrophobicity/hydrophilicity of the uppermost surface layer of a solid is expressed usually in terms of wettability with water which can be quantified by contact angle measurements. In order to study highly hydrated polymer films, the *captive-bubble* contact angle technique was used. When applying this technique, using water as measuring medium, a smaller contact angle value means higher hydrophilicity.

In Fig. 4-11 and in Tab. 9-3 values of the contact angle of swollen hydrogels, using the *captive-bubble* method are given.

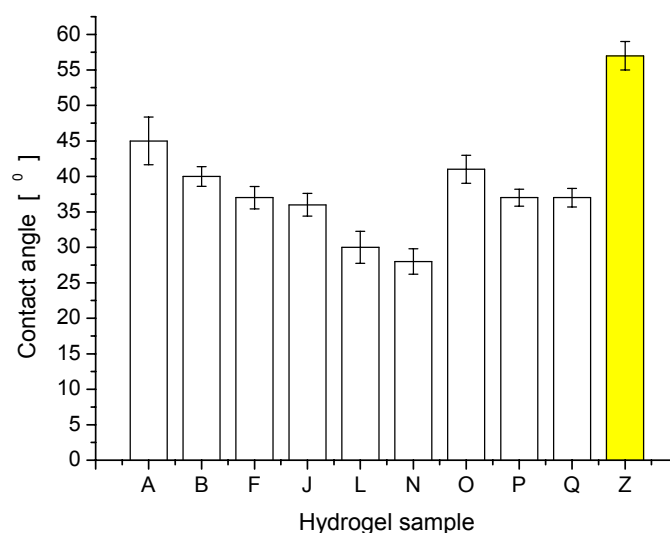


Fig. 4-11 Contact angle of different hydrogels measured in water using the *captive-bubble* method.

Hydrogels A, B	100 mol% lactide	$N = 16, 8$	$DG_{the} 15\%$
Hydrogel F	75 mol% lactide	$N = 16$	$DG_{the} 20\%$
Hydrogel J	75 mol% lactide	$N = 8$	$DG_{the} 15\%$
Hydrogels L, N	75 mol% lactide	$N = 4$	$DG_{the} 15\%, 10\%$
Hydrogels O, P	50 mol% lactide	$N = 18, 9$	$DG_{the} 15\%$
Hydrogel Q	50 mol% lactide	$N = 4$	$DG_{the} 15\%$
Copolymer Z	poly(D,L)lactide		

The values of the contact angle lie between 27° and 45° . Only poly(*rac*-lactide) (Z), used here as a kind of standard, has a value of 57° , which shows its lower hydrophilicity. From Fig. 4-11 one can conclude that samples with longer polyester chains have higher contact angles (networks A relative to B, F relative to L, O relative to P). Hydrogels with pure lactide grafts have higher contact angles compared to those having some glycolide in the polyester chains. Thus hydrogel A has a higher contact angle than hydrogel O, as well as B relative to P. Hydrogels L and N with the shortest polyester grafts exhibit the lowest contact angles among all samples.

4.6 Biocompatibility

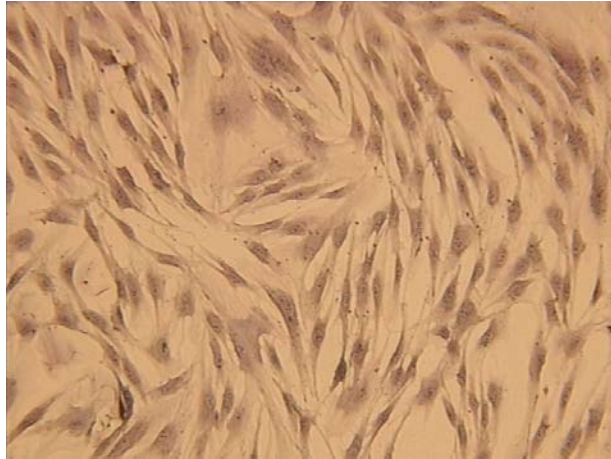
Biocompatibility is a very important property of a material in case of its intended medical use. In order to evaluate the biocompatibility of the materials obtained here, hydrogel type P was examined concerning the cells adhesion, viability and proliferation. Hydrogel P was selected for its composition: lactide to glycolide ratio 50:50 mol% in the polyester chain with 9

repeating ester units and an experimental degree of grafting of 13% (theoretical degree of grafting DG_{the} 15%).

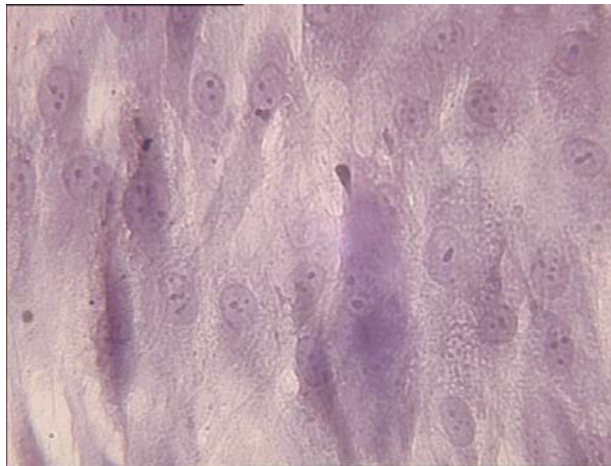
The test of the biocompatibility was performed in cell culture media with primary human dermal fibroblasts (hF) following the procedure described in more detail in Chapter 7.3.7.

Fig. 4-12 presents a photo of the sample surface after 4 days of incubation, showing vital, densely arranged cells on the sample surface.

The surface properties of a biomaterial applied in implant technology (and tissue engineering) are a key element in controlling the interaction with attaching cells and the surrounding tissue. Networks within the scope of this work consist of both hydrophilic and hydrophobic chains which enable tuning of the final hydrophilic/hydrophobic balance. Aliphatic polyesters such as polylactide (PLA), polyglycolide (PGA) and their copolymers (PLGA) are among the few synthetic polymers that have been used to construct temporary scaffolds for tissue engineering on the basis of their biodegradation properties, biocompatibility, high mechanical strength and excellent processing properties. However, these materials have poor hydrophilicity and are free of cell recognition sites on their surfaces, which leads to poor mass transport in scaffolds and poor cell affinity of the materials ^[153]. In order to improve the cell affinity of aliphatic polyesters, many efforts have been made to modify their surface properties and adjust the hydrophilicity/hydrophobicity balance ^[154,155] simply by introducing hydrophilic segments. We have used the approach to introduce the hydrophilic poly(vinyl alcohol) backbone in order to improve cell affinity. It is documented in literature that poly(vinyl alcohol) is biocompatible apart from many other good properties such as similarity to natural cartilage tissue in terms of water content in the hydrogel ^[95,156]. It has been already observed that cells adhere, spread, and grow more on surfaces with moderate hydrophilicity, regardless of the cell types used, than on the more hydrophobic or even more hydrophilic surfaces ^[156]. Fig. 4-12/a shows cells on the hydrogel P surface after 4 days' culture at a magnification of 134, while Fig. 4-12/b shows a sample at a higher magnification (x400). It can be seen that cells adhere evenly to the sample surface. This demonstrates that the hydrophilic/hydrophobic balance of the material is suitable for cell adhesion even without additional surface treatment.



a)



b)

Fig. 4-12 Representative images depicting the shape of primary human dermal fibroblasts (hF) attached to the surface of the hydrogel type P after 4 days culture: a) at MAG x 134 b) at MAG x 400

5 Controlled degradation of hydrogels

(Bio)degradability was accomplished by synthesizing polymers with hydrolytically instable ester groups. In the poly(vinyl alcohol)-g-poly(aliphatic ester) hydrogel, control of the hydrogel structure and consequently of observable material properties such as mass loss, mass swelling ratio and mechanical properties, was made possible by changing the composition of polyester grafts and their proportion to the poly(vinyl alcohol) backbone. The properties as well as the morphological changes were analyzed over a long degradation period (Chapter 7.3.8). Contact angle measurements, IR, TGA and DSC analyses were also performed in the same manner as with samples before the degradation.

5.1 Mass loss of degraded hydrogels

The mass loss is an indicator of the degradation process. For these experiments, a series of samples of each hydrogel was prepared having circular shape with defined diameter using a punch cutter. The circular shaped samples were exposed to hydrolytical degradation in aqueous buffer solution (pH 7.4) at room temperature. Hydrogel P was also degraded at 37 °C for comparison reasons. The weight loss was calculated as the ratio between the mass of the sample before degradation and the mass after hydrolytical degradation, both in dry state.

The influence of structure and composition of a hydrogel as a result of the different length of the polyester grafts and their ratio relative to PVA on mass loss is given in examples that follow.

5.1.1 Influence of the length of the polyester chains

The percentage of the remaining weight of networks A and B with 16 and 8 repeating ester units of the side chain during degradation is shown in Fig. 5-1.

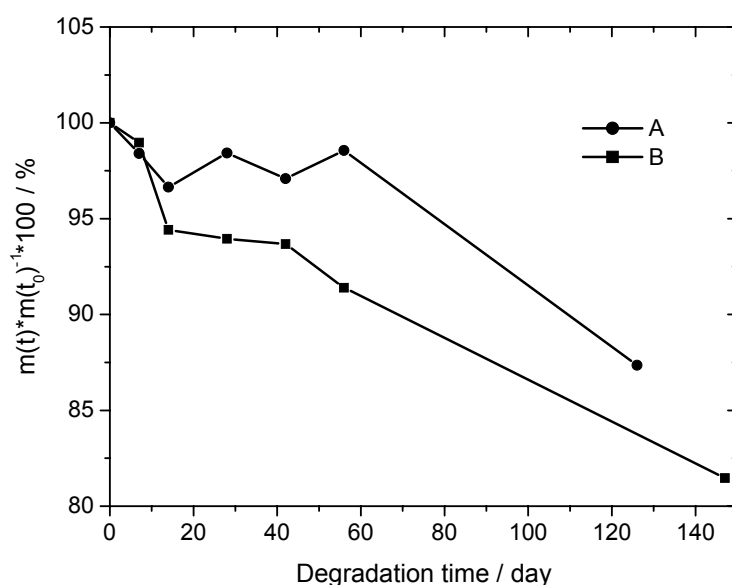


Fig. 5-1 Mass loss of networks A and B in hydrolytical degradation experiments at pH 7.4, room temperature.

- A: 100 mol% LA; $N=16$; DG_{the} 15%
- B: 100 mol% LA; $N=8$; DG_{the} 15%

Mass loss is evident in both samples but it proceeds at a lower rate in hydrogel A. One can conclude that there is a kind of induction period with some irregularities, most probably due to experimental errors. Only after 60 days of degradation the mass loss of hydrogel A increases significantly. Sample B, with shorter polyester grafts, shows a more rapid mass loss as a consequence of its higher hydrophilicity.

Fig. 5-2 shows the percentage of the remaining mass of networks O and P with degradation time. The mass loss starts immediately, indicating good water diffusion into the polymer network. Sample O, with longer polyester grafts, degrades more slowly, particularly initially, as hydrogel A. In sample P, with shorter polyester side chains, the mass loss is more rapid from the onset.

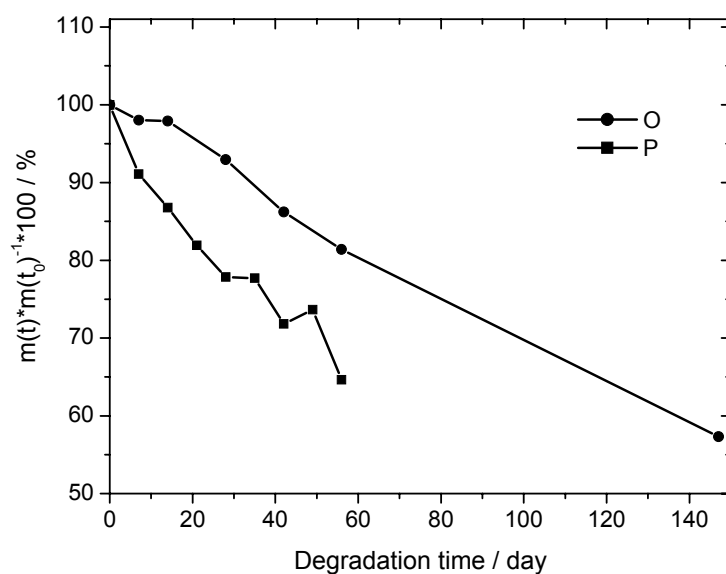


Fig. 5-2 Mass loss of networks O and P in hydrolytical degradation experiments at pH 7.4, room temperature.

- O: 50 mol% LA; $N = 18$; $DG_{\text{the}} 15\%$
- P: 50 mol% LA; $N = 9$; $DG_{\text{the}} 15\%$

Fig. 5-3 gives the remaining mass of samples F, I and L, with 75 mol% lactide and a high degree of grafting ($DG_{\text{the}} 20\%$), during degradation. The mass loss begins immediately, indicating good water diffusion into the polymer network.

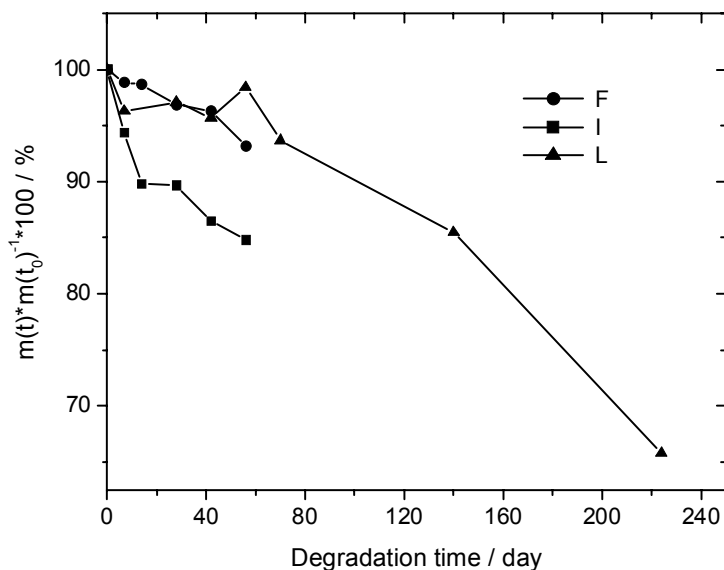


Fig. 5-3 Mass loss of networks F, I and L in hydrolytical degradation experiments at pH 7.4, room temperature.

- F: 75 mol% LA; $N = 16$; DG_{the} 20%
- I: 75 mol% LA; $N = 8$; DG_{the} 20%
- ▲ L: 75 mol% LA; $N = 4$; DG_{the} 20%

The mass loss rate depends on the length of polyester side chains in the network. All samples with shorter polyester grafts show faster mass loss due to their higher hydrophilicity.

5.1.2 Influence of the composition of the polyester chains

Comparing networks A, B, O and P (Fig. 5-1 and Fig. 5-2) one can conclude that samples containing glycolide in the polyester grafts, O and P, show faster degradation compared to hydrogels A and B as a result of higher hydrophilicity and a higher tendency to hydrolyze. Hydrogels A and O show a small weight loss initially, but as degradation proceeds, the mass loss rate increases remarkably. Thus, both hydrogels show less than 5% of mass loss after three weeks of degradation while after eight weeks of degradation hydrogel A shows still less than 5% of mass loss and hydrogel O shows a mass loss of 20%. Samples with shorter side chains, B and P, show a significant influence of composition from the onset.

Samples A and B, having pure lactide grafts, show 10% of mass loss after 110 and 70 days respectively, while samples O and P, having poly(lactide-*co*-glycolide) segments, need only 35 and 10 days, respectively, for the same mass loss. In Fig. 5-4 hydrogels B, J and P are

presented which have about the same number of repeating ester units and degree of grafting, but different composition of the polyester grafts. The mass loss is significantly influenced by the composition. Samples B and J show similar, relatively constant mass loss at first but sample J shows much faster mass loss with time. Hydrogel P with the highest ratio of glycolide shows the most rapid mass loss from the onset, due to its highest hydrophilicity. Network B shows 10% of mass loss after 70 days, network J after 60 days while network P requires only 10 days for 10% of mass loss.

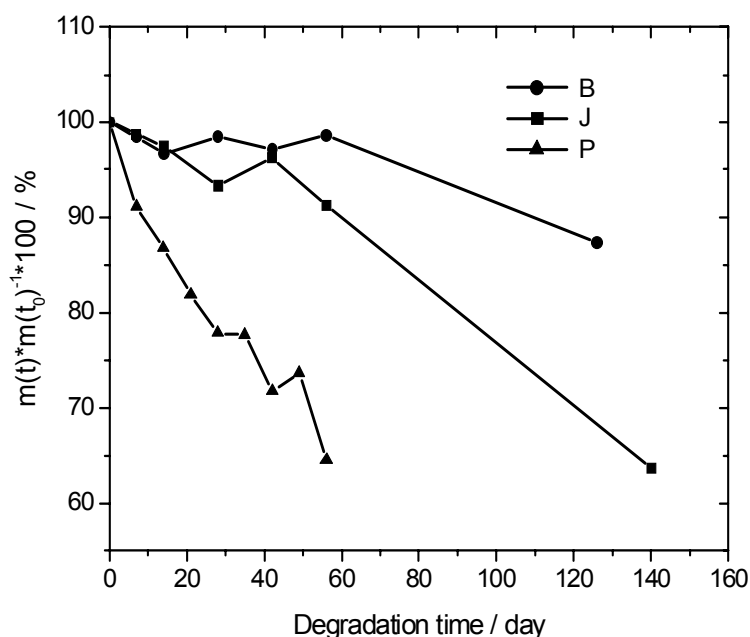


Fig. 5-4 Mass loss of networks B, J and P in hydrolytical degradation experiments at pH 7.4, room temperature.

●	B: 100 mol% LA;	$N = 16$;	$DG_{the} 15\%$
■	J: 75 mol% LA;	$N = 16$;	$DG_{the} 15\%$
▲	P: 50 mol% LA;	$N = 18$;	$DG_{the} 15\%$

The influence of composition in networks that have shorter polyester side chains is stronger than in those having longer chains.

5.1.3 Influence of the degree of grafting

Fig. 5-5 illustrates the mass loss in hydrogels having different composition; L and Q with four polyester repeating units, degree of grafting DG_{the} of 20%, and hydrogels N and S with four polyester repeating units and DG_{the} of 10%.

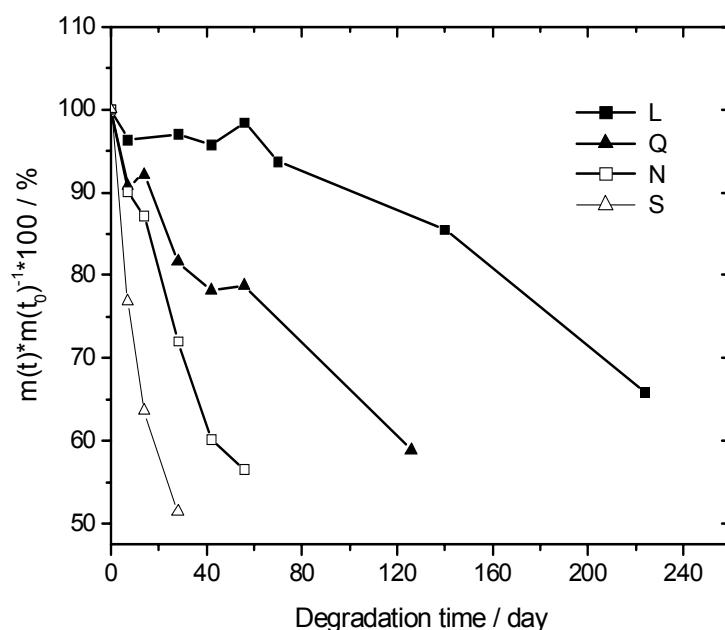


Fig. 5-5 Mass loss of networks L, Q, N and S in hydrolytical degradation experiments at pH 7.4, room temperature.

■ L: 75 mol% LA; $N=4$; DG_{the} 20% ▲ Q: 50 mol% LA; $N=4$; DG_{the} 20%
 □ N: 75 mol% LA; $N=4$; DG_{the} 10% △ S: 50 mol% LA; $N=4$; DG_{the} 10%

For all samples the mass loss starts from the onset except for hydrogel L which shows an induction period. Hydrogel L reaches a value of 90% of the original mass after 100 days, sample Q after 20 days, while samples N and S reach this value only after 8 and 3 days, respectively. Comparing these two sets of samples, it is evident that hydrogels with higher degree of grafting show a much slower rate of mass loss as a consequence of a higher number of crosslinks within the network which makes them denser, more hydrophobic and less susceptible to water diffusion into the polymer matrix and diffusion of oligomers out of the network.

5.1.4 Influence of degradation conditions

The mass loss of sample P degraded in PBS at room temperature and at 37 °C, respectively, is shown in Fig. 5-6.

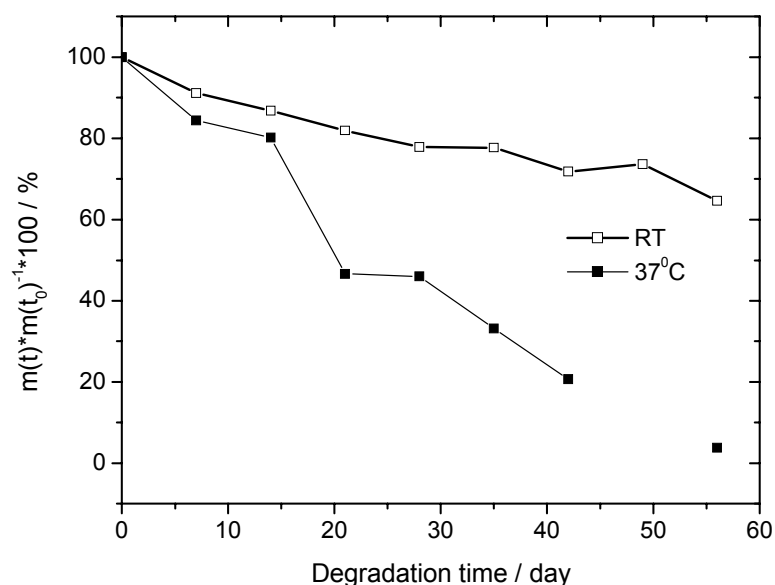


Fig. 5-6 Mass loss of network P in hydrolytical degradation experiments at pH 7.4, at room temperature and at 37 °C.

The sample degraded at RT shows continuous but slow mass loss while the sample degraded at 37 °C shows a much faster mass loss. The sample degraded at 37 °C has 80% of the remaining mass after 14 days and only 40% after 21 days, while the sample degraded at room temperature has 80% of the remaining mass still after 35 days. With time the difference increases and after 56 days of hydrolytical degradation the sample degraded at room temperature shows ≈65% of remaining mass, while the sample degraded at 37 °C shows only around 5% of remaining mass.

Diffusion of eroded products from the network is a function of the network crosslinking density, which also changes with degradation. Thus, in crosslinked systems with long grafts and dense network structures, the mass loss profile has an induction period due to higher hydrophobicity and less accessible ester bonds while in more hydrophilic systems mass loss proceeds straight forward. In the literature ^[95] it is shown that the mass loss behavior is correlated to the rate at which crosslinked polyester grafts hydrolyze and the numbers of crosslink's that need to be degraded before small fragments are released from the hydrogel. In networks with long polyester grafts (A and O) the time needed for a significant mass loss (>10%) is longer than in networks with short polyester grafts due to their hydrophobicity which results in slower water penetration. The influence of hydrophobicity is stronger than the influence of the number of ester bonds present that potentially are hydrolyzed and enable faster hydrolysis.

Davis et al. ^[157] showed that the mass loss of poly(lactic acid-*co*-caproic acid) diethylene glycol based networks is a function of both hydrolysis kinetics and network structure. The degradable polyester bonds are cleaved before diffusing out of the hydrogel. The majority of degradable linkages must be hydrolyzed before the fragments can be released. We can assume that a similar process occurs in hydrogels within the scope of this work where degradable ester bonds need to be hydrolyzed to a large extent before the PVA backbones are released and dissolved.

In the case of α -hydroxy acids based devices the degradation process is completed in four steps ^[132]: the first step starts after water has penetrated the amorphous region of the polymer and disrupts the secondary forces; secondly ester bonds are cleaved, as hydrolysis proceeds, more and more carboxylic end groups autocatalyze the hydrolysis reaction, thirdly significant mass loss begins as a result of massive cleavage of ester bonds and finally the polymer loses weight. This step is called «erosion» which designates the loss of material owing to monomers and oligomers leaving the polymer. Concerning autocatalysis of the hydrolysis reaction, the base-catalyzed hydrolysis of PLA proceeds by a random cleavage mechanism, whereas in the acid-catalyzed hydrolysis of PLA, chain-end cleavage is faster, according to Shih ^[158]. Belbella et al. ^[159] came to the opposite conclusion where a random cleavage takes place at low pH values and a sequential cleavage from the chain end in an alkaline medium.

The glycolide content results in a mass loss increase. Thus, hydrogels O, J and P that contain glycolide in grafts, show higher mass loss when compared with similar hydrogels A and B with pure lactide grafts. Additionally, when hydrogels J with 25 mol% and P with 50 mol% of glycolide are compared, the former loses mass at a slower rate. This is in agreement with the findings on the dynamics of weight loss for PLGA films where it was shown that the PLGA films with a ratio LA:GA of 75:25 and 50:50 mol% were similar to each other except that films with higher glycolide ratio degraded at faster rate ^[132]. Moreover, the weight remained relatively constant for several weeks; then a dramatic decrease in mass was observed ^[132]. Lu et al. ^[82] showed that the thickness of the films also has a significant influence and thin films degrade faster. The hydrolytical degradation of massive, amorphous poly(D,L-lactic acid) devices was shown to proceed heterogeneously and faster inside than at the surface, because in the interior there is a larger contribution of autocatalysis ^[66,76]. Initially, hydrolysis of the ester bonds proceeds homogeneously through the matrix. During degradation, two factors are of importance. First, degradation causes an increase in the number of carboxylic acid chain ends which are known to autocatalyze ester hydrolysis. Secondly, only oligomers, which are soluble in the surrounding aqueous medium, can escape from the matrix. As degradation

advances, soluble oligomers, which are close to the surface, can leach out before they fully degrade, whereas those which are located in the core of the matrix remain entrapped. This yields a low pH value in the core which, in turn, results in accelerated degradation ^[66,76]. The influence of the sample thickness was eliminated regarding the samples in this work since all of them were of about the same thickness. Hydrogels observed in this work display a significant influence of the degree of grafting; whereas samples with higher DG_{the} (e.g. L and Q, Fig. 5-5) exhibit a much slower mass loss due to their denser structure and resulting in higher hydrophobicity, which slows down water diffusion in one direction and oligomers (degradation products) in the other direction, relative to samples with lower DG_{the} (e.g. N and S, Fig. 5-5).

5.2 Swelling of degraded hydrogels

The change in weight related to the degree of swelling, S , (*mass swelling ratio*) is taken as an indicator of hydrolytical degradation. Experiments were conducted to determine the mass ratio of swelling. For these experiments, series of samples of each hydrogel were prepared having circular shape with defined diameter using a punch cutter. The samples were exposed to hydrolytical degradation in aqueous buffer solution (pH 7.4) at room temperature as described in Chapter 7.3.8. Hydrogel P was degraded at 37 °C for comparison reasons. The degree of swelling is the ratio of the weight of the swollen sample and the same sample in the dry state (Chapter 7.3.10).

5.2.1 Influence of the length of the polyester chains

Fig. 5-7 illustrates the weight related degree of swelling of hydrogels A, B and D during the degradation. The swelling increases with degradation time, since the crosslink density decreases.

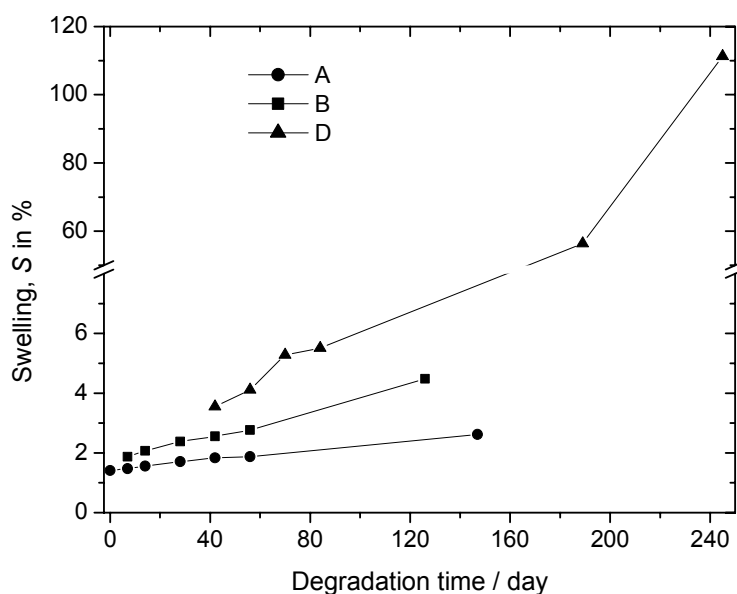


Fig. 5-7 Weight related degree of swelling S in water of hydrogels A, B and D during hydrolytical degradation at pH 7.4, room temperature.

A: 100 mol% LA;	$N = 16$;	$DG_{\text{the}} 15\%$
B: 100 mol% LA;	$N = 8$;	$DG_{\text{the}} 15\%$
D: 100 mol% LA;	$N = 4$;	$DG_{\text{the}} 15\%$

Hydrogel A, with the highest polyester content, shows the lowest degree of swelling and it changes very little during degradation. Hydrogel B with lower polyester content shows a higher degree of swelling while hydrogel D with the lowest polyester content, displays significantly higher values, especially after 70 days. The degree of swelling continues to increase strongly during the whole degradation time indicating the loosening of the network structure.

In Fig. 5-8 the dependence of the degree of swelling on the degradation time of hydrogels O, P and R, containing 50 mol% of glycolide in the grafts is given. The behavior is similar to that of hydrogels A, B and D (Fig. 5-7). Hydrogel O with the highest polyester content shows the lowest degree of swelling, while hydrogel P with a lower polyester content has a higher degree of swelling. Sample R with the lowest polyester content displays high swelling. After 70 days the swelling increases rapidly just before the total disintegration and dissolution of the sample. This shows the strong influence of the polyester content on the swelling behavior of the hydrogel. Even though the hydrogel with longer polyester grafts has more ester bonds capable to be hydrolyzed, it is their hydrophobicity that slows down the process of swelling.

This swelling pattern can be explained as follows: in the initial degradation phase, the long polyester side chains make the hydrogel hydrophobic and the hydrogel remains stable for a longer period of time than the hydrogel with shorter polyester grafts. This leads initially to a lower swelling rate and consequently to a lower degradation rate of the hydrogel.

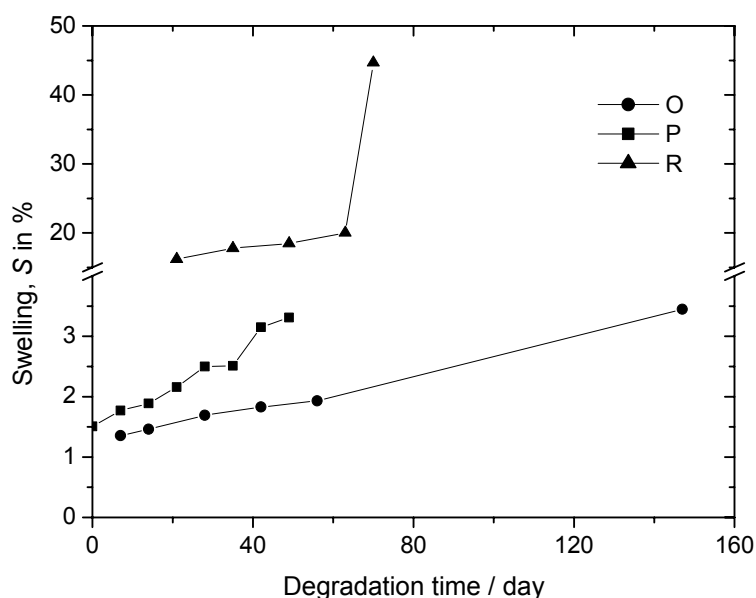


Fig. 5-8 Weight related degree of swelling S in water of hydrogels A, B and D during hydrolytical degradation at pH 7.4, room temperature.

O: 50 mol% LA;	$N = 18$;	$DG_{\text{the}} 15\%$
P: 50 mol% LA;	$N = 9$;	$DG_{\text{the}} 15\%$
R: 50 mol% LA;	$N = 4$;	$DG_{\text{the}} 15\%$

The degree of swelling of the hydrogels F, I and L, having 75 mol% of lactide in the polyester grafts and a high degree of grafting ($DG_{\text{the}} 20\%$) is presented in Fig. 5-9.

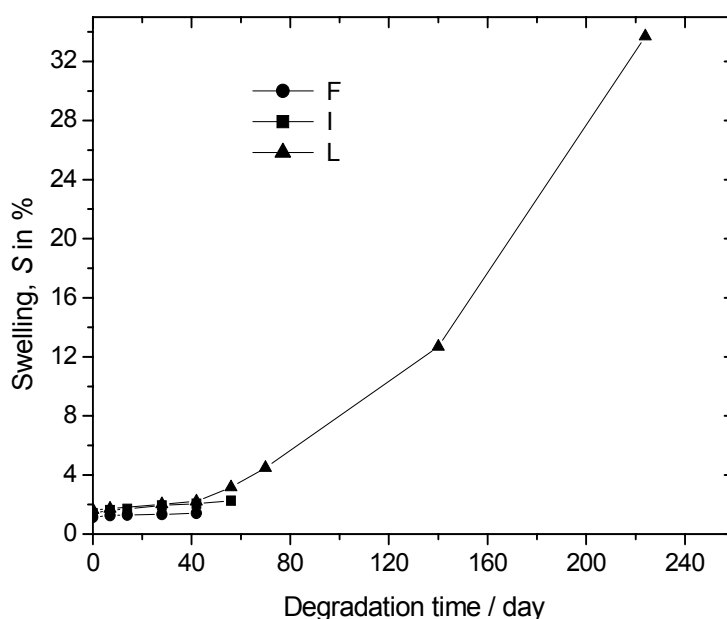


Fig. 5-9 Weight related degree of swelling S in water of hydrogels F, I and L during hydrolytical degradation at pH 7.4, room temperature.

F: 75 mol% LA;	$N = 16$;	DG_{the} 20%
I: 75 mol% LA;	$N = 8$;	DG_{the} 20%
L: 75 mol% LA;	$N = 4$;	DG_{the} 20%

The swelling increases with degradation time in all hydrogels but all of them show low swelling within the first 40 days which is due to a high DG_{the} of 20%. After 60 days, hydrogel L shows a strong increase in the swelling rate. This hydrogel shows the highest swelling because of its lowest polyester content which means the lowest hydrophobicity.

5.2.2 Influence of the composition of the polyester chains

Comparing the hydrogel A with O, B with P and D with R (Fig. 5-7 and Fig. 5-8) it might be assumed that the influence of composition depends on the length of polyester grafts. Thus, hydrogels A, with pure lactide polyester grafts and O, with 50 mol% of lactide in the grafts, did not show any difference in swelling up to 50 days. Hydrogels B and P, with shorter polyester chains, showed a significant influence of composition on swelling after 35 days. Hydrogels D and R, with the shortest chains both showed much higher degrees of swelling than the other hydrogels and from the onset they display a larger deflection of the degree of swelling compared to the other hydrogels.

The degree of swelling of hydrogels B, J and P during degradation is presented in Fig. 5-10.

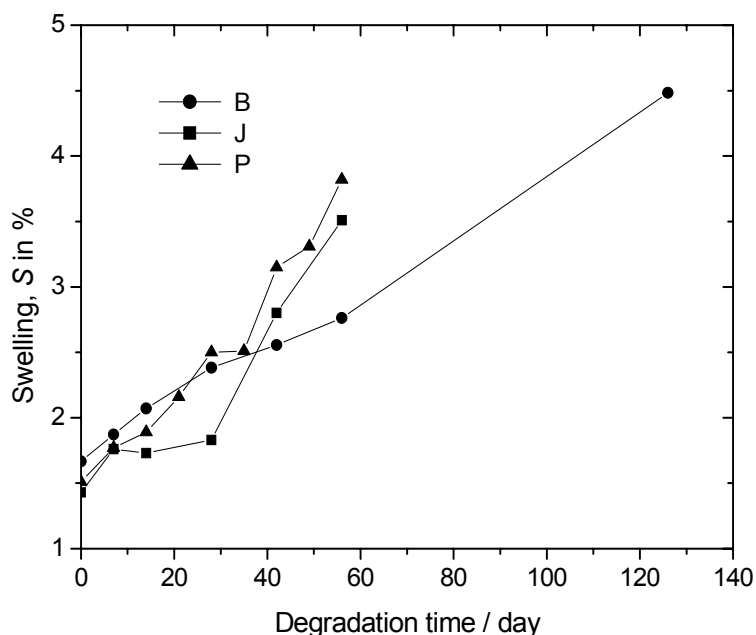


Fig. 5-10 Weight related degree of swelling S in water of hydrogels B, J and P during hydrolytical degradation at pH 7.4, room temperature.

B: 100 mol% LA;	$N = 8$;	$DG_{the} 15\%$
J: 75 mol% LA;	$N = 8$;	$DG_{the} 15\%$
P: 50 mol% LA;	$N = 9$;	$DG_{the} 15\%$

Since all of them have about the same length of polyester grafts, it is possible to observe the influence of their different composition. The swelling increases with degradation time. At first all of them show similar swelling. Hydrogel B, with 100 mol% lactide shows at first, surprisingly, slightly higher values considering its most hydrophobic nature. Up to about 35 days of degradation they all show similar swelling but after that period of time, a significant increase of swelling in the hydrogels J and P, containing glycolide was found.

Hydrogels which have the same length of polyester grafts, i.e. four repeating ester units, but different composition, are shown Fig. 5-11. The swelling increases with degradation time, as it is the case with all other hydrogels. These hydrogels, however, show much higher swelling compared to the other hydrogels as a result of the short polyester grafts which means low hydrophobicity.

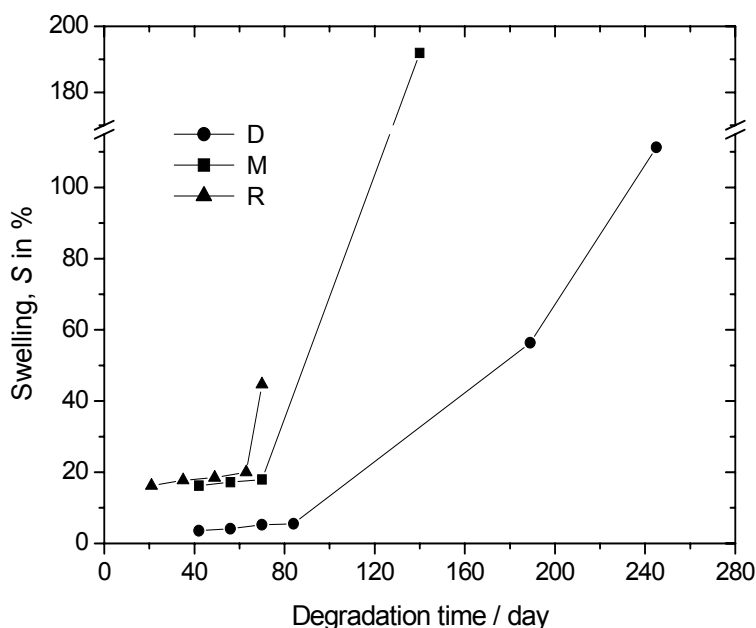


Fig. 5-11 Weight related degree of swelling S in water of hydrogels D, M and R during hydrolytical degradation at pH 7.4, room temperature.

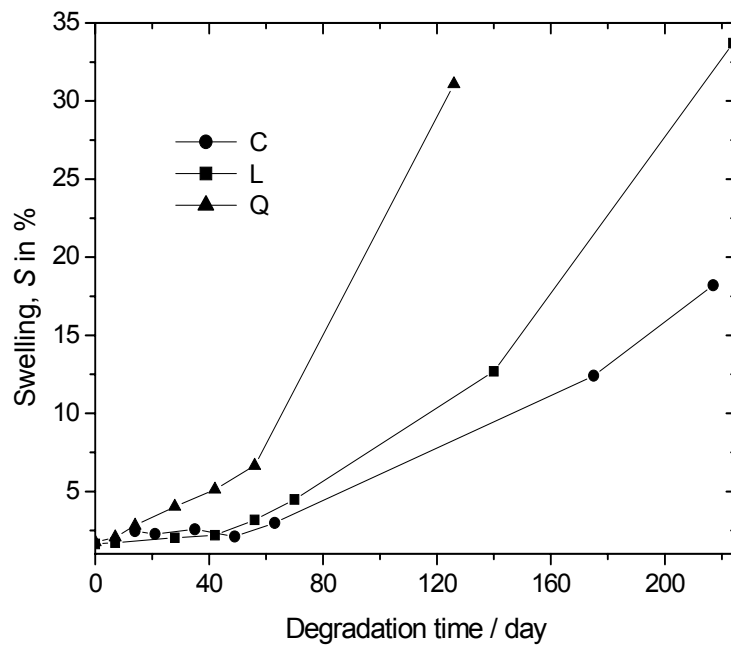
D: 100 mol% LA;	$N = 4$;	$DG_{\text{the}} 15\%$
M: 75 mol% LA;	$N = 4$;	$DG_{\text{the}} 15\%$
R: 50 mol% LA;	$N = 4$;	$DG_{\text{the}} 15\%$

Hydrogels M and R show a much higher degree of swelling than hydrogel D, due to the fact that in these samples the hydrophobicity is reduced not only due to shorter polyester grafts but also due to glycolide present. The more rapid water uptake of hydrogel D starts after 80 days, of hydrogel M after 70 days while for hydrogel R it takes only 65 days until an increased swelling rate was observed. That is a result of the lower crosslinking density and the loosening of the hydrogel structure.

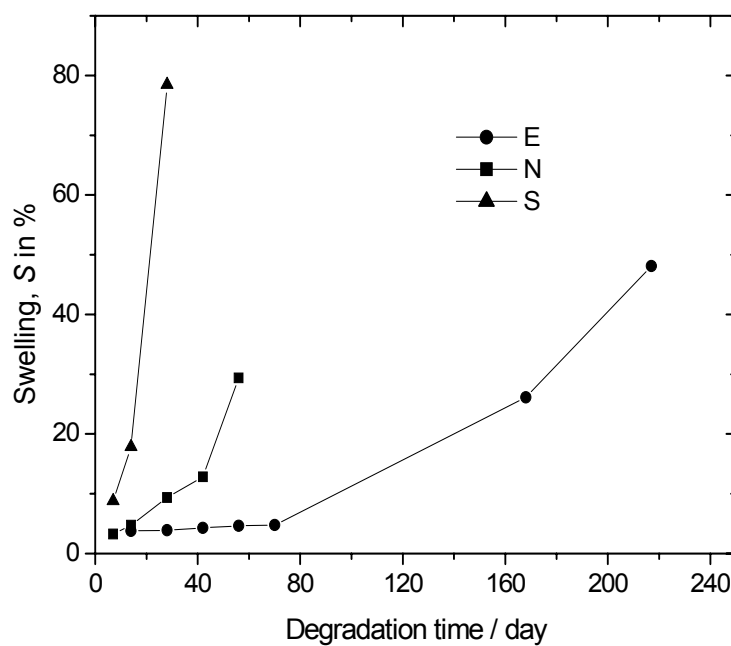
In addition, in hydrogels with shorter polyester grafts the glycolide contributes strongly to the higher hydrophilicity and faster hydrolysis which results in a much higher swelling rate.

5.2.3 Influence of the degree of grafting

The influence of the degree of grafting on the PVA backbone was examined in detail in hydrogels with the shortest grafts, and was shown to be significant. Hydrogels which have analogous composition but different degree of grafting are presented in Fig. 5-12.



a)



b)

Fig. 5-12 Weight related degree of swelling S in water of hydrogels during hydrolytical degradation at pH 7.4, room temperature.

a)			b)		
C:	100 mol% LA;	$N = 4$; $DG_{the} 20\%$	E:	100 mol% LA;	$N = 4$; $DG_{the} 10\%$
L:	75 mol% LA;	$N = 4$; $DG_{the} 20\%$	N:	75 mol% LA;	$N = 4$; $DG_{the} 10\%$
Q:	50 mol% LA;	$N = 4$; $DG_{the} 20\%$	S:	50 mol% LA;	$N = 4$; $DG_{the} 10\%$

Hydrogels C, L and Q show the expected influence of the presence of glycolide on swelling, which causes its increase. Hydrogels E, N and S show similar behavior. When these two sets of hydrogels are compared, hydrogels with higher degrees of grafting, higher crosslinking density and consequently higher hydrophobicity show a smaller degree of swelling. Thus, for a degree of swelling of 10%, hydrogel C needs 150 days, while hydrogel E needs only 95 days. With time, this difference continues to increase. After 220 days of degradation hydrogel C shows a degree of swelling of only 20% and hydrogel E shows a degree of swelling of 50% in the same period of time. The degree of swelling of hydrogel L after 60 days of degradation does not exceed 5%, while that of the analogous hydrogel N, with lower degree of grafting, reaches 30% within the same time. Hydrogel Q requires 65 days for a degree of swelling of 10% and hydrogel S needs only 7 days to reach the same degree of swelling.

As a conclusion, hydrogels with a low degree of grafting (DG_{the} 10%) exhibit a high degree of swelling, the value of which increases continuously and considerably from the onset. At the same time, hydrogels with high DG_{the} (20%) exhibit low swelling, slowly increasing up to 60-80 days of degradation, but during the later degradation stage, the degree of swelling also increases significantly. Yet, they display lower degrees of swelling during the whole period of degradation.

The influence of the degree of grafting on the backbone is combined with the composition of the polyester grafts. Thus, the increasing amount of glycolide in hydrogels of various degrees of grafting causes increase of swelling of different intensity. Since the glycolide content in hydrogels with short polyester grafts contributes significantly to the degree of swelling, hydrogel Q, in spite of a higher DG_{the} (20%) than hydrogel E (DG_{the} 10%), but due to the glycolide present, displays a remarkably higher degree of swelling.

5.2.4 Influence of degradation conditions

The different swelling behavior of sample P, degraded in PBS at room temperature and at 37 °C is presented in Fig. 5-13.

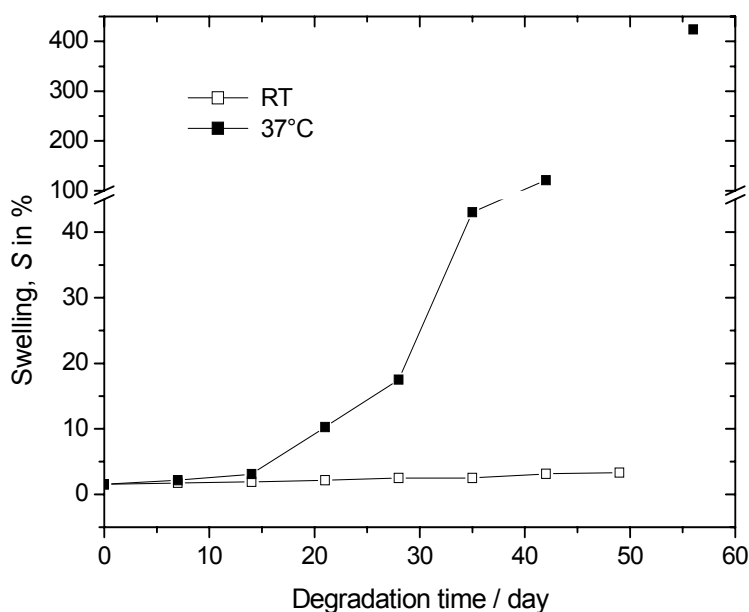


Fig. 5-13 Weight related degree of swelling S in water of hydrogel P during hydrolytical degradation pH 7.4, \square at room temperature, \blacksquare at 37 °C.

The sample degraded at room temperature shows a very small change of swelling in the course of eight weeks. At the same time the sample degraded at 37 °C, after similar behavior within the first two weeks, shows a strong increase of the degree of swelling upon further degradation. Relating the swelling with the mass loss of this sample (Fig. 5-6) a constant and linear mass loss is accompanied with a small, linear swelling increase of the sample degraded at room temperature, which indicates the slow and constant degradation throughout the device. For the sample degraded at 37 °C, the mass loss is approximately linear as well (Fig. 5-6), just much faster, but swelling starts to increase significantly after four weeks of degradation, i.e. after the mass loss has reached about 50 wt%. This indicates that the swelling increases not only due to the decrease of the crosslinking density, but also because of the removal of polyester from the hydrogel resulting in an increase of hydrophilicity.

5.3 Topography of degraded networks

The surface and cross-section morphology of the hydrogels before and during hydrolytical degradation were observed by means of scanning electron microscopy. The cross-sectional samples were prepared by fracturing the samples after being frozen in liquid nitrogen. The samples were gold coated. The SEM images of the cross-section of different types of

hydrogels before and during the hydrolytical degradation are shown in Fig. 5-14 to Fig. 5-20 and Fig. 9-15 to Fig. 9-21. All samples before degradation, at low magnification (x 100, x 200, x 250 or x 300) show a smooth surface. At higher magnification (x 5000) the cross section is also smooth.

During hydrolytical degradation there is a change of thickness and roughness in the sample. Some samples show fairly deteriorated morphology of the surface as well as of the cross section, after only four weeks, while some need much longer for similar changes to occur. Sample A shows a reduction in thickness of ca. 20% (by comparing Fig. 5-14/a-1 and /b-1) but still after eight weeks of hydrolytical degradation a smooth surface and smooth cross section. The comparison between samples under high magnification before degradation (Fig. 5-14/a-2) and after eight weeks of degradation (Fig. 5-14/b-2) show a different cross section where small tiny bubbles a few micrometers in size appear as a result of degradation.

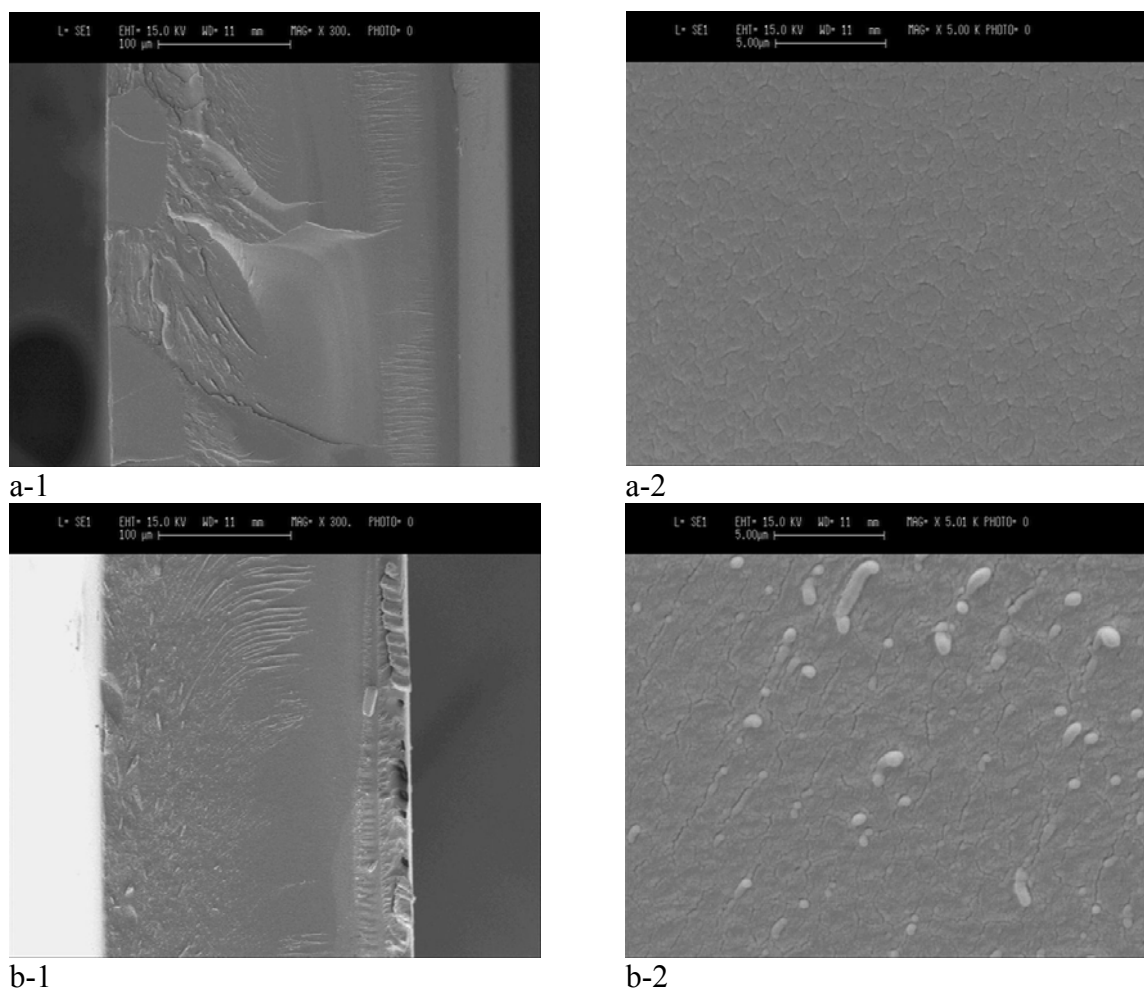


Fig. 5-14 SEM micrographs of network type A
a) before hydrolytical degradation: cross section at MAG x 300 (1) and x 5000 (2)
b) after eight weeks of hydrolytical degradation: cross section at MAG x 300 (1) and x 5000 (2).

Network B exhibits a significant reduction of sample thickness ($\approx 35\%$) after only four weeks of hydrolytical degradation (comparing Fig. 9-15/a-1 and /b-1), but its shape is preserved and the surface and cross section are smooth. The cross section at high magnification does not show any significant difference of the samples before (Fig. 9-15/a-2) and after degradation (Fig. 9-15/b-2). Network C after nine weeks of hydrolytical degradation exhibits large cracks along the cross section. There is, almost, no change in the thickness of the sample ($\approx 7\%$) (Fig. 9-16/a-1 and /b-1). Higher magnification shows a smooth cross section, apart from the cracks (Fig. 9-16/a-2 and /b-2). Network D, after ten weeks of degradation, shows marked deterioration of the surface (Fig. 5-15/a-1 and /b-1). From the shape of the degraded sample and the fact that its thickness does not change significantly, one can conclude that degradation proceeds via the bulk mechanism.

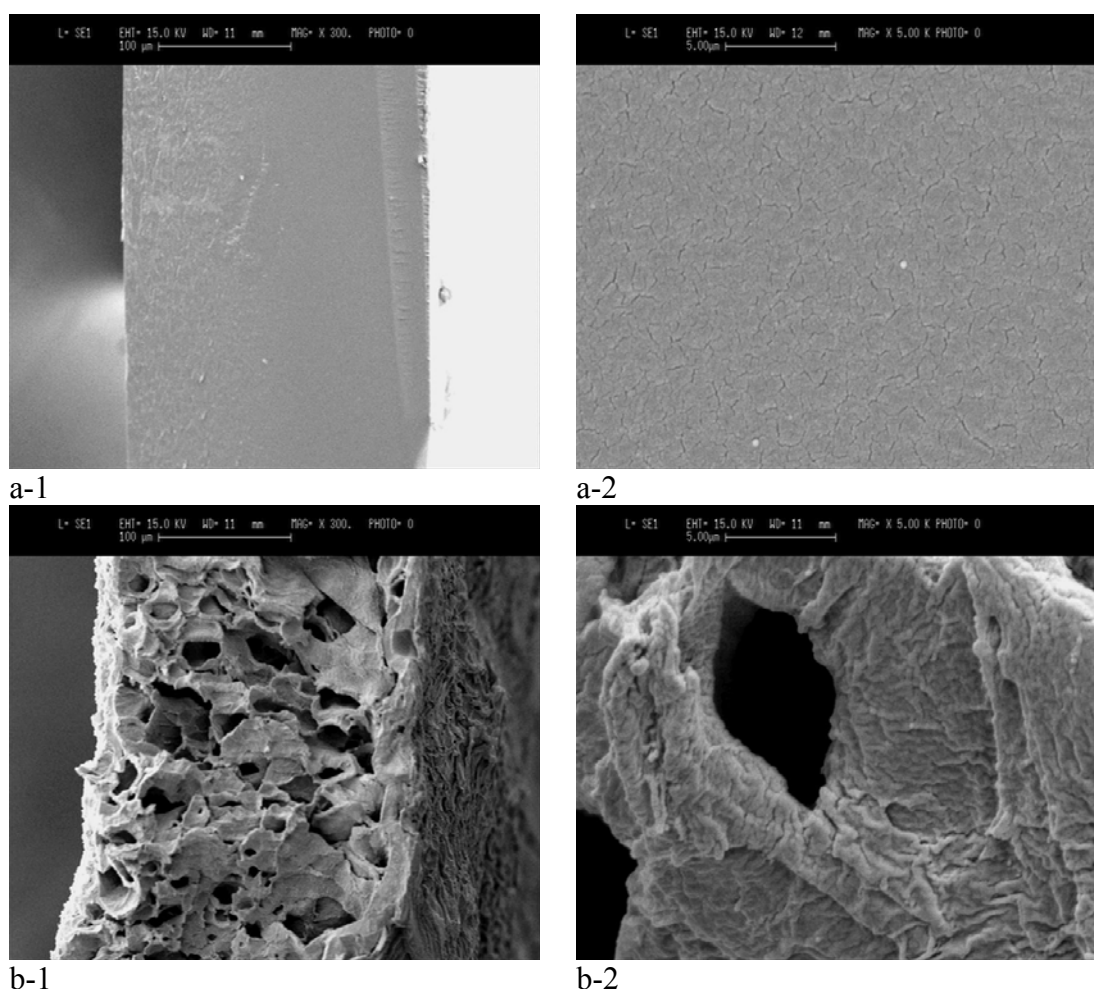


Fig. 5-15 SEM micrographs of network type D
a) before hydrolytical degradation: cross section at MAG x 300 (1) and x 5000 (2)
b) after ten weeks of hydrolytical degradation: cross section at MAG x 300 (1) and x 5000 (2).

This is to be expected, since this sample with the short lactide chains is relatively hydrophilic, which enables rapid water uptake. The cross section of the sample after degradation observed at high magnification (Fig. 5-15/b-2), having an embossed surface with holes, is greatly different from the smooth sample before degradation (Fig. 5-15/a-1). Network E shows a marked decrease in thickness ($\approx 67\%$) (comparing Fig. 9-17/a-1 and /b-1) after ten weeks of hydrolytical degradation, which implies marked degradation on the sample surface rather than in the bulk. Most probably this is due to the looser structure of the network ($DG_{\text{the}} 10\%$). High magnification shows the formation of a small bubble area on the cross section (Fig. 9-17 /b-2) due to degradation absent in the sample before degradation (Fig. 9-17/a-2). Network F after eight weeks of hydrolytical degradation shows smooth surfaces. The sample thickness does not change (comparing Fig. 9-18/a-1 and /b-1). The roughness of the cross section increases just slightly after degradation as it is revealed by pictures taken at high magnification (Fig. 9-18/a-2 and /b-2). Network I shows, after four weeks of hydrolytical degradation, stable shape of the sample and smooth surfaces (Fig. 9-19/a-1 and /b-1). The thickness of the sample changes just slightly, even after eight weeks (Fig. 9-19/a-1 and /c-1). Only pictures taken at high magnification show a rougher surface of the cross section (Fig. 9-19/c-2 relative to /a-2 and /b-2). This indicates a bulk degradation mechanism which takes place at slow rate due to the higher degree of grafting and resulting in a higher cross linking density. Network J, after eight weeks of hydrolytical degradation (Fig. 5-16/a-1), shows stable shape. High magnification (Fig. 5-16/a-2) shows the formation of small bubbles on the cross section. The thickness of the sample is only ca. $160\text{ }\mu\text{m}$ which indicates its decrease (compared to all other samples with a thickness of ca. $300\text{ }\mu\text{m}$ before degradation) implying surface erosion. After twenty weeks of hydrolytical degradation this sample shows an extremely perforated matrix (Fig. 5-16/b-1). The bulk is highly degraded but the sample has the characteristic film shape, yet, and the thickness has even increased relatively to that after eight weeks of degradation ($\approx 30\%$). This indicates that after the initial surface erosion, bulk erosion occurs and becomes the dominant mechanism of degradation. High magnification (Fig. 5-16/b-2) shows advanced degradation and formation of holes on the cross section.

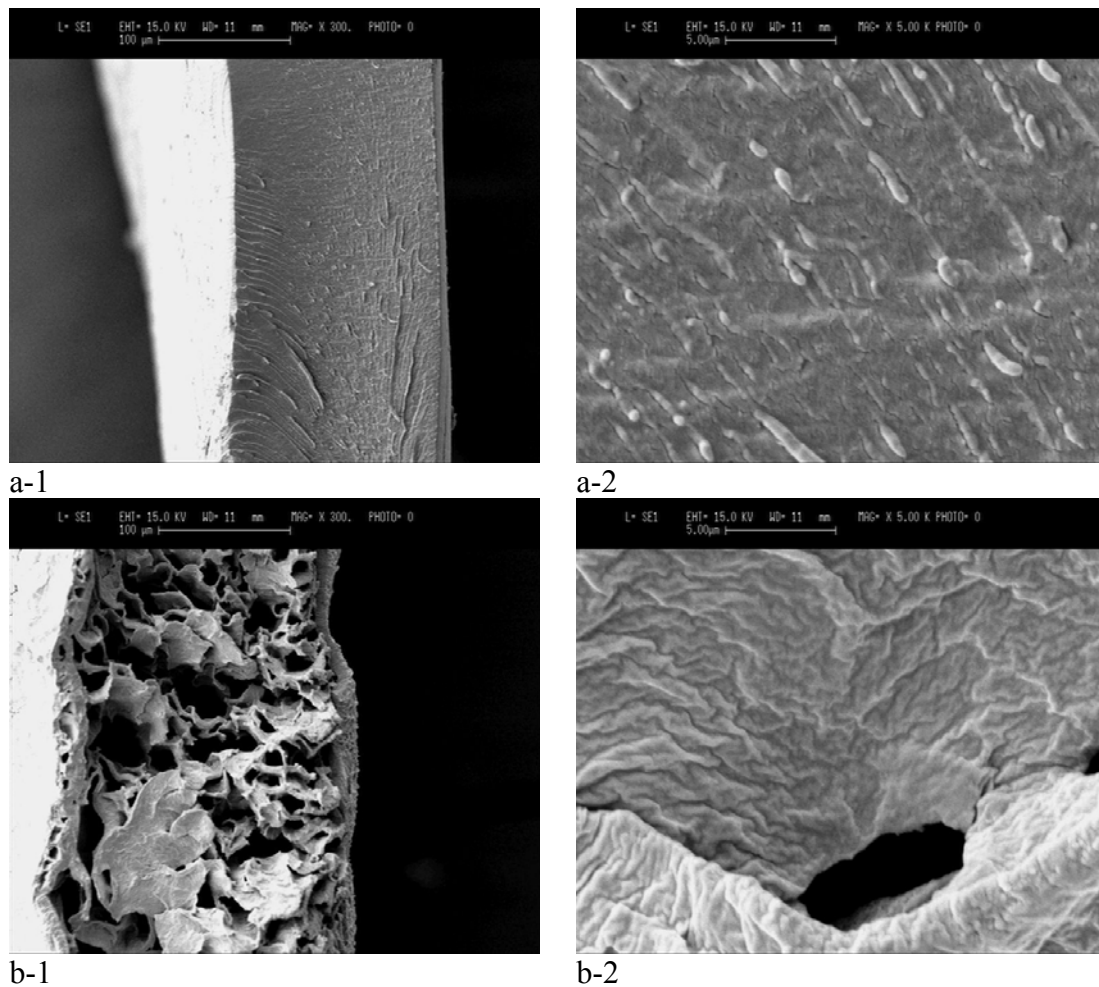
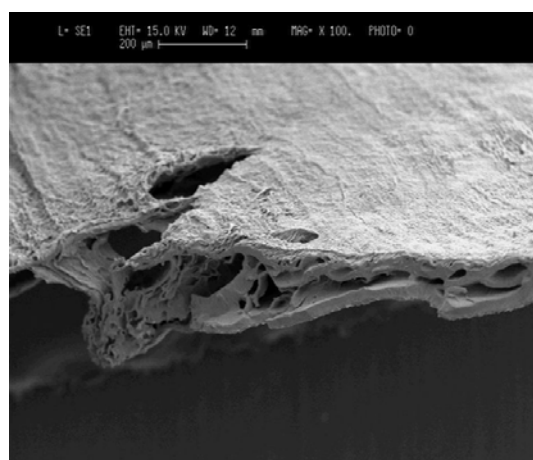


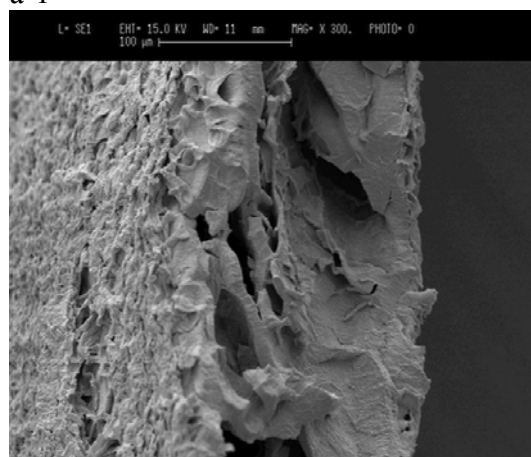
Fig. 5-16 SEM micrographs of network type J
a) after eight weeks of hydrolytical degradation:
cross section at MAG x 300 (1) and MAG x 5000 (2)
b) after twenty weeks of hydrolytical degradation:
cross section at MAG x 300 (1) and MAG x 5000 (2).

Network L after eight weeks of hydrolytical degradation displays an increase in sample thickness by ca. 16% (Fig. 9-20/a-1 relative to /b-1), which implies that bulk degradation occurs. High magnification shows an increase in cross section roughness (comparing Fig. 9-20/a-2 and /b-2). Network N, after only four weeks of degradation, shows a highly degraded structure (Fig. 5-17/a-1 and /a-2). The thickness of the sample (90-160 μm) decreases significantly as a result of the surface degradation mechanism (compared to other samples with a thickness of ca. 300 μm before degradation) but at the same time the cross section is highly deteriorated as a result of bulk degradation. After eight weeks of degradation the sample becomes much thinner (Fig. 5-17/b-1 and /b-2). This indicates that at that stage of degradation surface erosion becomes the dominant mechanism of degradation. Additionally, in the bulk of the sample different layers are distinguished.

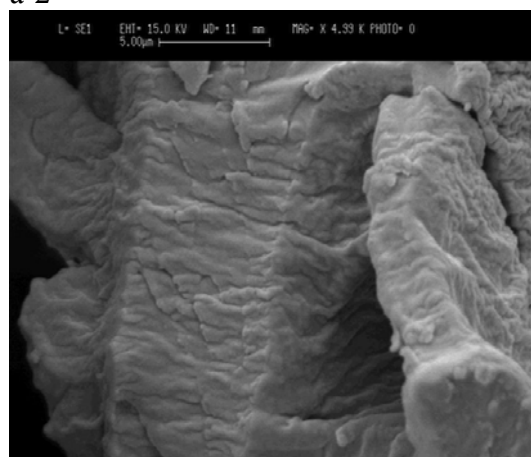
High magnification shows a rough cross section after four weeks of degradation (Fig. 5-17/a-3) and especially after eight weeks (Fig. 5-17/b-3).



a-1



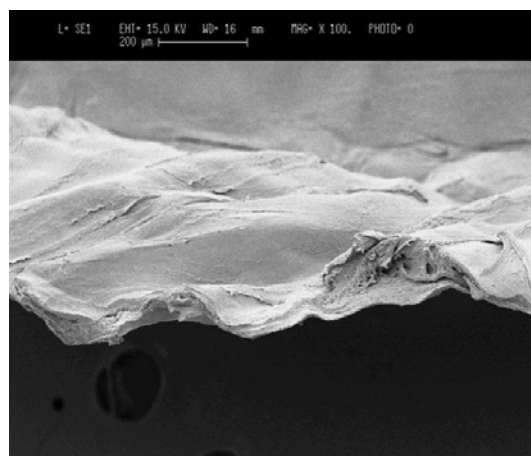
a-2



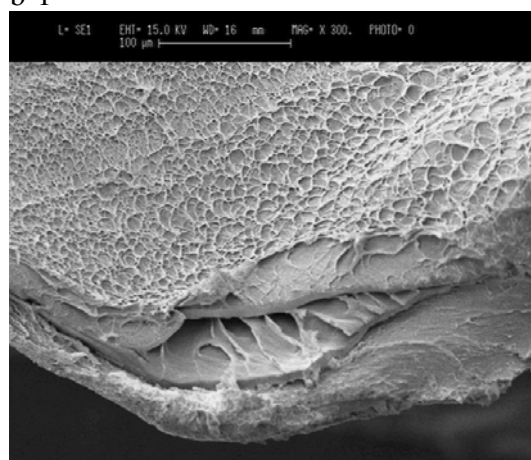
a-3

Fig. 5-17 SEM micrographs of network type N

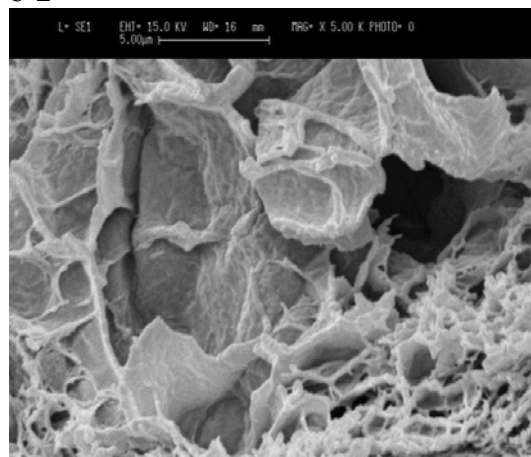
a) After four weeks of hydrolytical degradation: cross section at MAG x 100 (1); x 300 (2) and x 5000 (3).



b-1



b-2



b-3

Fig. 5-17 SEM micrographs of network type N

b) after eight weeks of hydrolytical degradation:
cross section at MAG x 100 (1); x 300 (2) and x 5000 (3).

Network O, after eight weeks of hydrolytical degradation, exhibits a smooth surface. The thickness of the sample decreases only by ca. 10% (comparing Fig. 9-21/a-1 and /b-1) due to the long polyester chains which make it more hydrophobic. High magnification shows a

smooth cross section that does not change during the degradation period of eight weeks (comparing Fig. 9-21/a-2 and /b-2). Network P exhibits significant morphological changes after eight weeks of hydrolytical degradation. The thickness of the network decreases by ca. 30% (Fig. 5-18/a-1 and /b-1). Along the cross section there are cracks and a pattern appears on the surface which is difficult to explain. High magnification shows a smooth cross section with cracks (Fig. 5-18/b-2) which is the only difference to the cross section before degradation (Fig. 5-18/a-2).

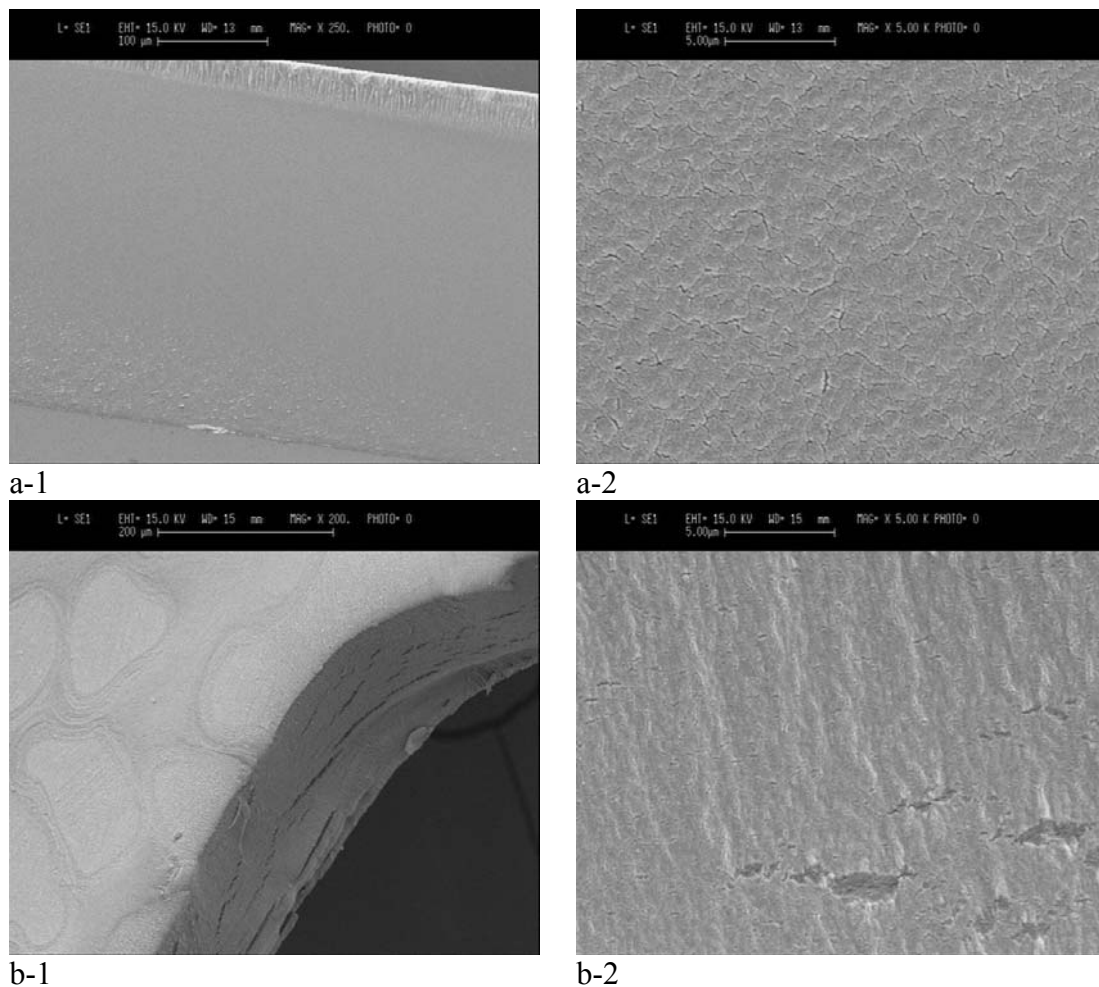


Fig. 5-18 SEM micrographs of network type P
a) before hydrolytical degradation: cross section at MAG x 300 (1) and x 5000 (2)
b) after eight weeks of hydrolytical degradation: cross section and part of side surface at MAG x 300 (1) and x 5000 (2).

Network Q after four weeks of hydrolytical degradation, shows much stronger degradation on the surface than in the bulk (Fig. 5-19/b-1). The surface degradation mechanism leads to the high sample thickness decrease by ca. 47% already after four weeks (by comparing Fig. 5-19

/a-1 and /b-1). Simultaneously degradation occurs in the bulk. The severity of the erosion increases with time. After eight weeks of degradation, the sample is uniformly degraded on the surface as well as in the bulk (Fig. 5-19/c-1 and /c-2), which indicates that after an initial faster surface erosion, at a later stage of degradation, the two mechanisms occur at a similar rate. High magnification shows an increase in cross section roughness (Fig. 5-19/a-2 and /b-2) after four weeks, while after eight weeks of degradation the roughness of the cross section increases extremely (Fig. 5-19/c-2).

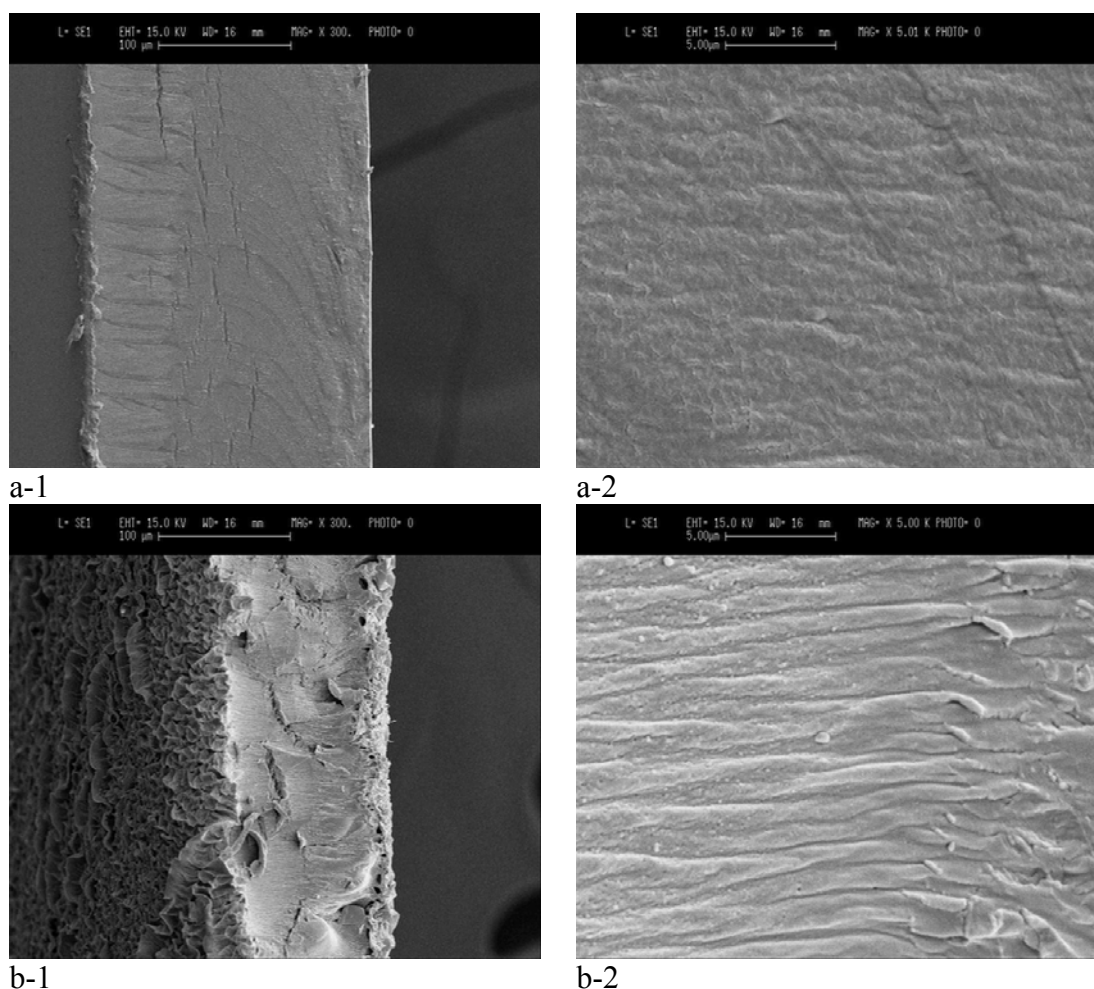
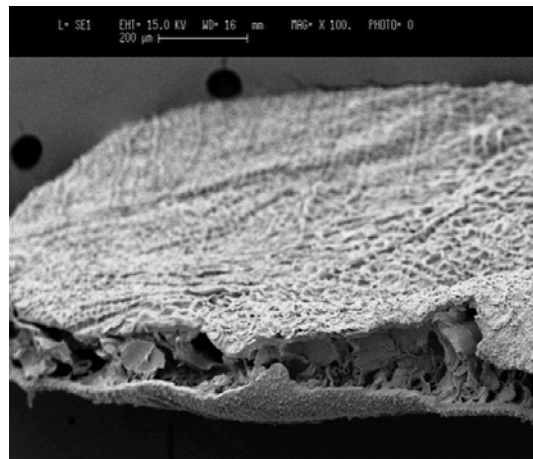
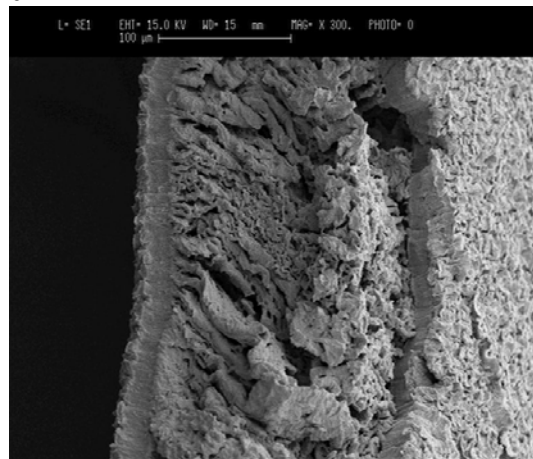


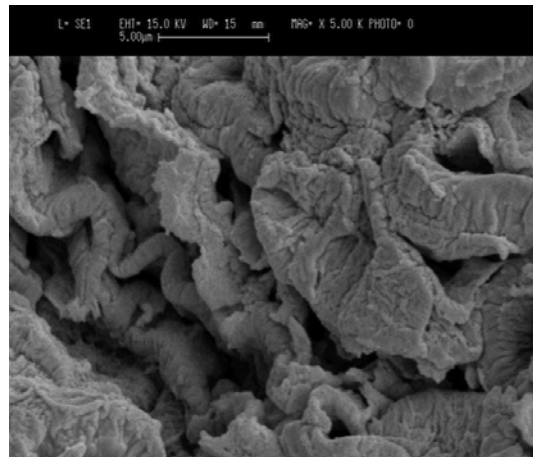
Fig. 5-19 SEM micrographs of network type Q
a) before hydrolytical degradation:
cross section at MAG x 300 (1) and x 5000 (2)
b) after four weeks of hydrolytical degradation:
cross section at MAG x 300 (1) and x 5000 (2).



c-1



c-2



c-3

Fig. 5-19 SEM micrographs of network type Q
c) after eight weeks of hydrolytical degradation:
cross section at MAG x 100 (1), x 300 (2) and x 5000 (3).

5.3.1 Influence of the length of the polyester chains

The influence of the length of the polyester chains can be followed by comparing network A (Fig. 5-14) with 16, network B (Fig. 9-15) with 8 and network D (Fig. 5-15) with 4 ester repeating units. Sample A, with the longest polyester chains, exhibits the most stable structure and the smallest decrease of the sample thickness due to its highest hydrophobicity, which slows down the degradation. The decrease of the sample thickness is ca. 20% after 8 weeks of degradation. Sample B, already after four weeks of degradation, shows a thickness decrease of ca. 35%. This indicates a surface degradation mechanism for both hydrogels. The surface of both samples is surprisingly smooth. Sample D with the shortest polyester grafts, which means small hydrophobicity, consequently shows much faster degradation and faster water uptake. After 8 weeks of degradation the cross section of this sample shows a very deteriorated surface even though the thickness does not change. This indicates a bulk degradation mechanism. Moreover, network O (Fig. 9-21) with 18 and P (Fig. 5-18) with 9 repeating ester units in lactide-*co*-glycolide (50 mol% of lactide) are compared. In hydrogel O the structure stays stable and the thickness decreases by ca. 20% after 8 weeks of degradation. At the same time in network P, with shorter polyester grafts, the thickness decreases by ca. 35% and the cross section shows advanced degradation, large cracks appear. This demonstrates a combined mechanism of degradation.

When the set of networks, F, I and L, with high degree of substitution (DG_{the} of 20%) and decreasing length of the polyester grafts is observed it is evident that they display higher stability relative to the set of networks with DG_{the} of 15%, A, B, D, due to the higher degree of grafting even though the samples contain 25 mol% of glycolide in grafts.

5.3.2 Influence of the composition of the polyester chains

Samples A (Fig. 5-14) and O (Fig. 9-21), with the longest polyester grafts, do not show any significant morphology change after eight weeks of hydrolytical degradation, due to their high hydrophobicity. Network A, containing pure polylactide grafts, shows less stability, which is surprising. It would be expected that sample O, with 50 mol% of glycolide, degrades faster due to its higher hydrophilicity. An explanation might be the longer polyester chains (18 ester units in network O, compared to only 16 in the sample A) which indicates the combined influence of the length and composition of polyester grafts.

Comparing further networks B (Fig. 9-15) and P (Fig. 5-18), similar observation can be made. The initial steady structure is seen still after eight weeks of degradation. Network P shows slightly lower stability due to the presence of glycolide, even though the number of repeating

ester units in grafts is 9, compared to 8 in sample B. The explanation is that the compositional influence depends on the graft length is more expressed in hydrogels with short grafts. Network J (Fig. 5-16) compared with the similar networks B (Fig. 9-15) and P (Fig. 5-18), displays properties between these two: it is less stable than sample B but more than sample P in which cracks appear after eight weeks. This corresponds well with the increasing glycolide content within B, J and P networks which causes higher hydrophilicity. By comparing samples C, L and Q, (Fig. 9-16, Fig. 9-20 and Fig. 5-19), with diverse glycolide content and a DG_{the} of 20%, a different behavior during degradation was observed. Sample C shows only cracks in the bulk after nine weeks of degradation. Network L shows after eight weeks of hydrolytical degradation an increase in the thickness which implies the bulk degradation mechanism. Network Q, with the highest amount of glycolide, already after four weeks of degradation shows strong deterioration of the surface while the degradation that occurs in the bulk is less significant. The thickness of this sample decreases significantly. This indicates that in sample Q both degradation mechanisms occur. After eight weeks of degradation network Q is very much degraded. At that stage of degradation there is no more a difference in morphology between the surface and the bulk of the sample. This demonstrates the “equilibrium” between the two erosion mechanisms.

5.3.3 Influence of the degree of grafting

Comparing samples which have the same composition but different degree of grafting on the backbone, it is evident that an increased degree of grafting results in different hydrophilic/hydrophobic properties which further causes the different rate and mechanism of degradation, bulk or surface. By comparing networks C, D and E, network D (Fig. 5-15) shows much lower stability compared to network C (Fig. 9-16) but both of them display a different degradation mechanism compared to network E (Fig. 9-17). Thus, after eight weeks of degradation network D is very much degraded and highly porous but without significant change of sample thickness which indicates bulk degradation while network E displays surface degradation characterized by a thickness decrease. Networks L (Fig. 9-22) and N (Fig. 5-17) display a behavior similar to that of networks C and E where the higher degree of grafting causes the lower degradation rate. Network L like network C displays the bulk degradation mechanism. In the case of network N, already after four weeks of degradation the sample is highly degraded as the result of the bulk mechanism which during further degradation is transformed to a pure surface erosion. When compared to the similar network E

which degrades by the surface mechanism, network N exhibits faster degradation due to its higher hydrophilicity and both bulk and surface erosion.

The mechanism of degradation is influenced by the degree of grafting. More crosslink's result in the bulk degradation mechanism, while less crosslinked hydrogels show degradation from the surface.

The amount of glycolide influences the rate and mechanism of degradation, additionally. As a conclusion, the presence of glycolide results in higher hydrophilicity and leads to faster degradation.

The difference in sample morphology is the result of the different composition of the polyester grafts and their length, as well as of the different degree of grafting on poly(vinyl alcohol) chains. It reveals the possibility of varying the degradation rate by changing the structure of the hydrogel.

5.3.4 Influence of degradation conditions

When network P, degraded at room temperature, is compared to the same sample degraded at 37 °C, the higher temperature results in a much faster degradation. Sample P after eight weeks of hydrolytical degradation at 37 °C is highly degraded (Fig. 5-20/1 and 5-20/2). This sample displays a very high porosity which is homogenously distributed (Fig. 5-20/3 and 5-20/4).

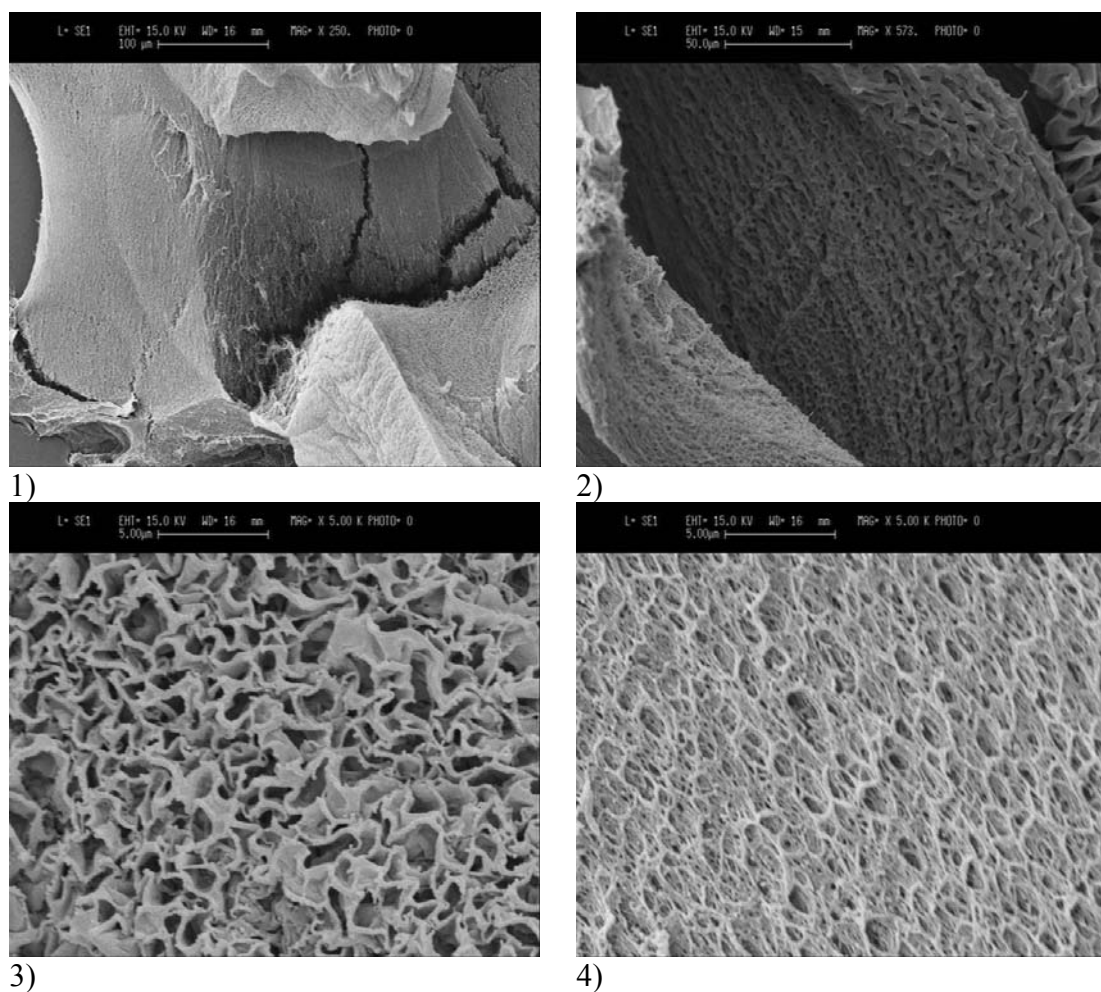


Fig. 5-20 SEM micrographs of network type P after eight weeks of hydrolytical degradation at 37 °C, pH 7.4

- 1) MAG x 250
- 2) MAG x 573
- 3) MAG x 5000
- 4) MAG x 5000.

Since, at higher magnification, two morphology patterns are seen (Fig. 5-20/3 and Fig. 5-20/4), the possible explanation might be the existence of two parallel degradation mechanisms, surface erosion and bulk.

5.4 Mechanical properties of degraded hydrogels

The purpose of this study was to investigate the effect of hydrolytical degradation on the mechanical properties of the hydrogels. The results showed significant mechanical deterioration of the hydrogels and how their elastic behavior is influenced by the mass loss and swelling.

5.4.1 Influence of the length of polyester grafts on the mechanical properties of degraded hydrogels

The change in the E modulus of hydrogels A, B and D during hydrolytical degradation is shown in Fig. 5-21. Tab. 9-4 gives the values of the E modulus and standard deviations. Sample A with the highest portion of lactide due to the longest polyester grafts, shows a high E modulus. This value is 20 times higher than the value of sample B with 8 lactide repeating units, and 90 times higher than that of sample D with only 4 repeating units. The E modulus of all samples decreases with degradation, indicating the loosening of the network structure.

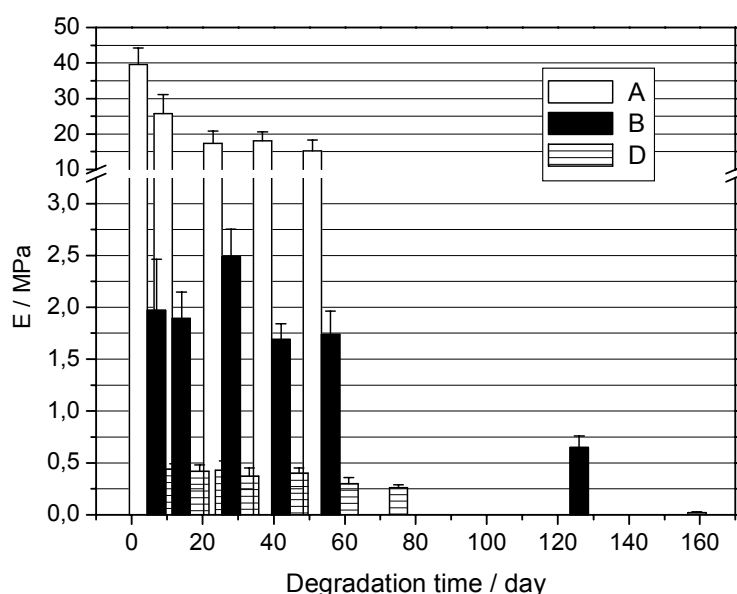


Fig. 5-21 E modulus of the hydrogels during hydrolytical degradation at pH 7.4, room temperature.

A: 100 mol% LA; $N = 16$; DG_{the} 15%
 B: 100 mol% LA; $N = 8$; DG_{the} 15%
 D: 100 mol% LA; $N = 4$; DG_{the} 15%

In Fig. 5-22 the E modulus of hydrogels O, P and R is given. The behavior is similar to that of samples A, B and D. Hydrogel O, with the longest polyester grafts, shows a much higher E modulus than the other two hydrogels with shorter polyester grafts. Thus, hydrogel O with 18 ester repeating units in grafts when compared to hydrogel R, which has only 4 repeating units in polyester, has a 900 times higher E modulus. All samples show a decrease of the E modulus with degradation.

By comparing these two sets of samples (Fig. 5-22 and Fig. 5-21), it is evident that the total polyester portion, relative to the poly(vinyl alcohol), has a strong influence on the mechanical properties. This is in agreement with data in the literature where it was shown that poly(lactide) ^[120,150,160] displays a much higher E modulus than poly(vinyl alcohol) ^[96,138,151]. It is important to emphasize that high values of the E modulus are found typically for poly(lactide) of high molecular weight while the polyester grafts in this work have low molecular weight.

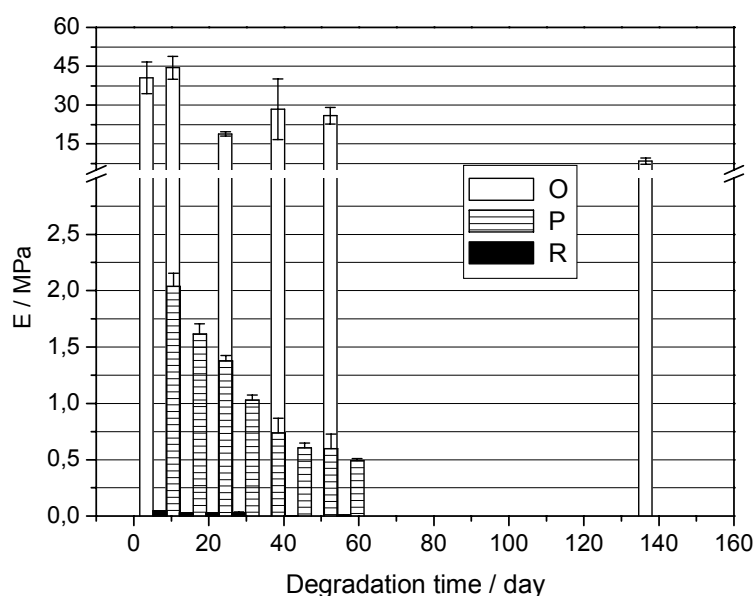


Fig. 5-22 E modulus of the hydrogels during hydrolytical degradation at pH 7.4, room temperature.

O: 50 mol% LA; $N = 18$; DG_{the} 15%
P: 50 mol% LA; $N = 9$; DG_{the} 15%
R: 50 mol% LA; $N = 4$; DG_{the} 15%

The mechanical properties of hydrogels F, I and L with different length of polyester grafts and with a degree of grafting (DG_{the}) of 20%, are given in Fig. 5-23. Hydrogel F, with the longest

polyester grafts, shows a significantly higher E modulus (around 200 MPa) than hydrogels I (8-3 MPa) and L (around 1 MPa). Hydrogel F has the highest E modulus among all hydrogels. This is due to the combined influence of long polyester chains, high degree of grafting and consequently denser network. The polyester chains strengthen the network but the crosslinking density amplifies this influence. The extremely high E modulus of hydrogel F (around 200 MPa) even increases, relative to the E modulus at the onset of the degradation (≈ 100 MPa), and reaches values characteristic of thermoplastic polymers^[145].

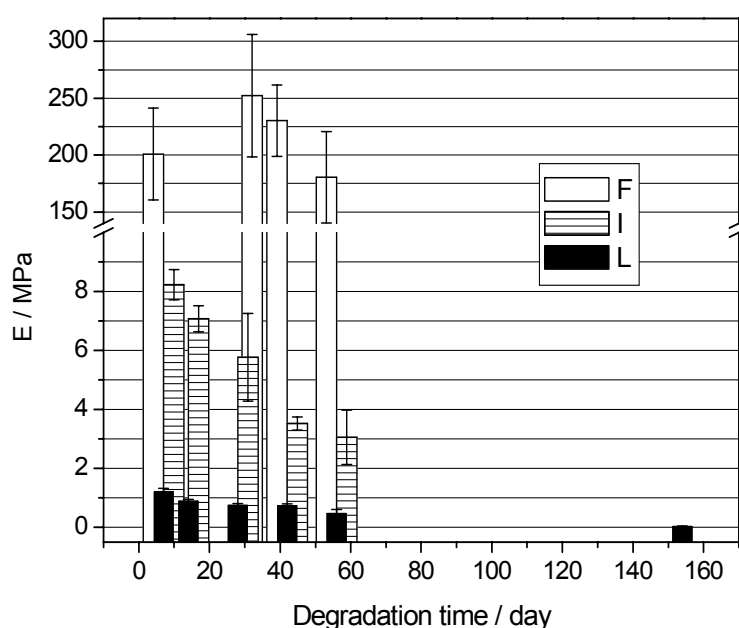


Fig. 5-23 E modulus of the hydrogels during hydrolytical degradation at pH 7.4, room temperature.

F: 75 mol% LA; $N = 16$; $DG_{\text{the}} 20\%$

I: 75 mol% LA; $N = 8$; $DG_{\text{the}} 20\%$

L: 75 mol% LA; $N = 4$; $DG_{\text{the}} 20\%$

5.4.2 Influence of the composition of polyester chains

In order to follow the influence of the composition of the grafts on the mechanical properties, hydrogels A and O, with the longest polyester grafts, already shown in Fig. 5-21 and Fig. 5-22, are compared. Since both of them show similar values of their E moduli during the whole degradation time, composition does not influence the mechanical properties of these hydrogels. In Fig. 5-24 the E moduli of hydrogels B, J and P are shown. The networks have about the same length of polyester graft but different composition. Sample B, with pure lactide grafts, shows the highest E modulus. Unexpectedly, sample P shows higher values of

the E modulus than sample J, even though it has a higher portion of glycolide in the polyester grafts.

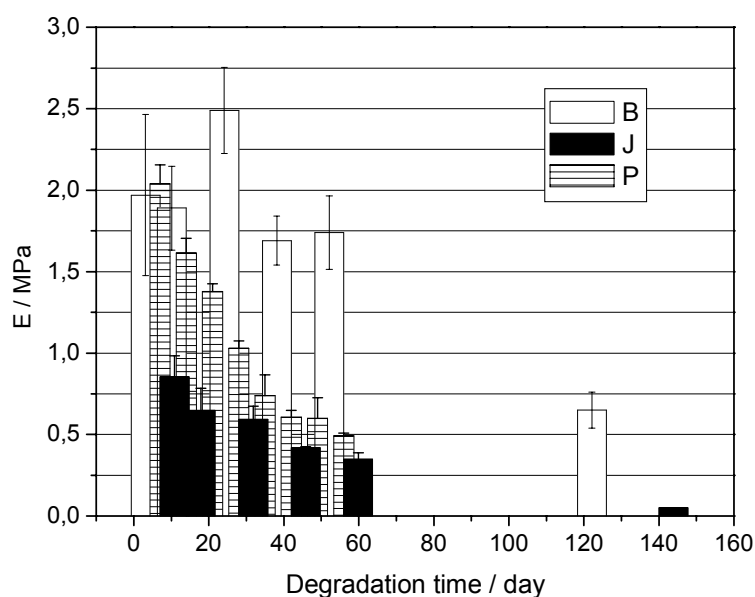


Fig. 5-24 E modulus of the hydrogels during hydrolytical degradation at pH 7.4, room temperature.

B: 100 mol% LA; $N = 8$; DG_{the} 15%
J: 75 mol% LA; $N = 8$; DG_{the} 15%
R: 50 mol% LA; $N = 4$; DG_{the} 15%

In the beginning of degradation (Fig. 4-8) sample P, shows the lowest E modulus in line with the highest glycolide portion. Sample J has 8 repeating ester units, while in sample P there are 9 repeating units. This demonstrates once more the greater influence of the length of polyester chain than of the composition on the E modulus. The influence of the composition gains significance during degradation. Thus, hydrogel P shows an E modulus close to the modulus of hydrogel B in the beginning (values around 2 MPa), as a result of its longer grafts, in spite of the presence of glycolide, but during degradation the E modulus of sample P decreases faster as a consequence of the glycolide portion (50 mol%) that leads to faster degradation, and e.g. after 8 weeks, its E modulus comes close to the value of that of hydrogel J which also contains glycolide (25 mol%) (values 0.65 and 0.5 MPa), while hydrogel B exhibits at the same time a modulus of 1.75 MPa.

The influence of the composition in hydrogels with the shortest polyester grafts is shown in Fig. 5-25.

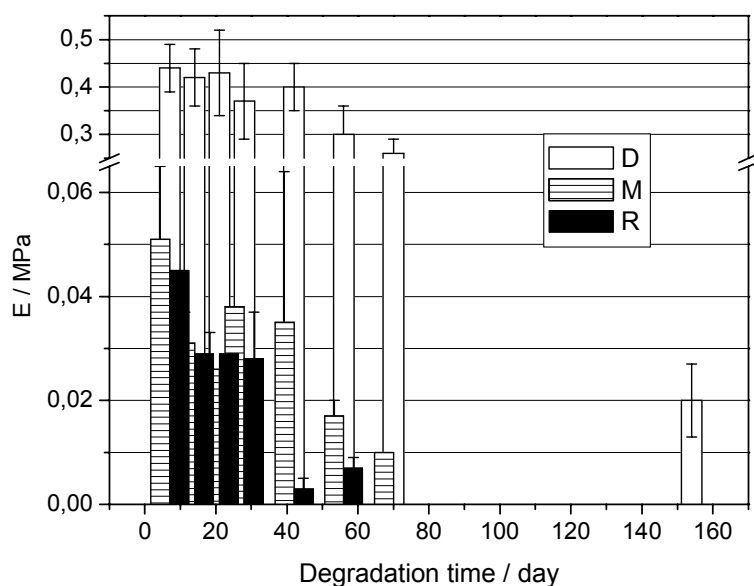


Fig. 5-25 E modulus of the hydrogels during hydrolytical degradation at pH 7.4, room temperature.

D: 100 mol% LA; $N = 4$; DG_{the} 15%

M: 75 mol% LA; $N = 4$; DG_{the} 15%

R: 50 mol% LA; $N = 4$; DG_{the} 15%

A very low E modulus which decreases further due to degradation is a general characteristic of these hydrogels. Sample D shows a much higher value (about 10 times) than hydrogels M and R, which exhibit a similar modulus. Sample D, only after a twice longer degradation time (150 days) approaches the value of the other two. Hydrogel R, after 56 days of degradation, is so weak, that it is impossible to perform mechanical tests. Comparing the E modulus of hydrogels presented in Fig. 5-24 and Fig. 5-25, it is evident that samples B, J and P, with high polyester ratios, as result of longer polyester grafts, shows a higher E modulus and a lower influence of composition compared to the hydrogels with shorter polyester grafts.

The influence of the composition in hydrogels with the shortest grafts and a degree of grafting DG_{the} of 20% is shown in Fig. 5-26. Here, the influence of composition is insignificant. Hydrogel Q with the highest amount of glycolide shows the lowest E modulus, as expected.

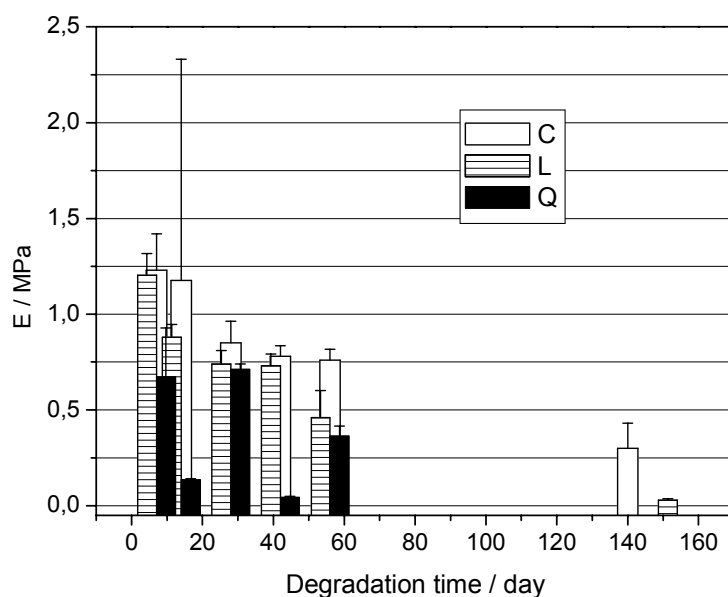


Fig. 5-26 E modulus of the hydrogels during hydrolytical degradation at pH 7.4, room temperature.

C: 100 mol% LA; $N = 4$; DG_{the} 20%

L: 75 mol% LA; $N = 4$; DG_{the} 20%

Q: 50 mol% LA; $N = 4$; DG_{the} 20%

Comparing these hydrogels with those presented in Fig. 5-25, which are similar, except that the degree of grafting is different (DG_{the} 20% vs. 15%), two things can be noticed: samples with a higher degree of grafting show a higher E modulus and at the same time the influence of the glycolide portion is smaller. The mechanical properties of hydrogels belonging to the same kind but having a DG_{the} of 10% are shown in Fig. 5-27. The E values are similar to those of the hydrogels with a DG_{the} of 15% and show a significant influence of composition. Hydrogel S with 50 mol% of glycolide in the grafts, after only one week of degradation is so weak, that it is not possible to perform the mechanical test.

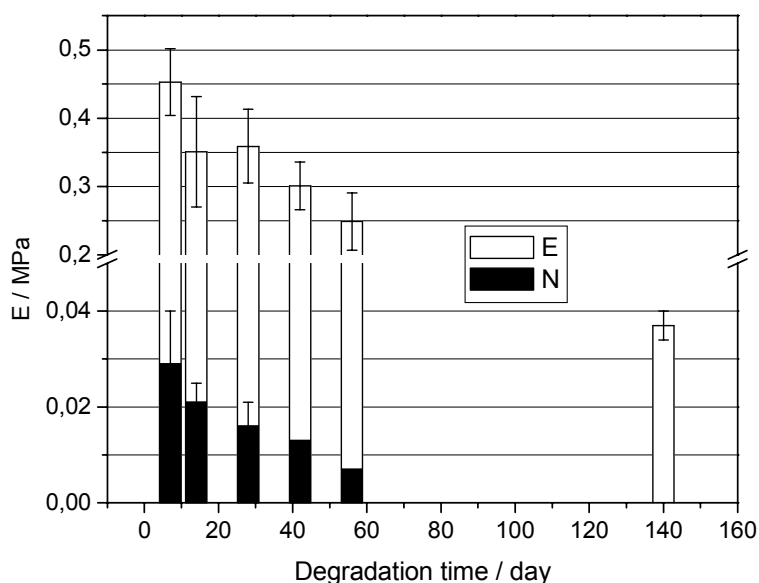


Fig. 5-27 E modulus of the hydrogels during hydrolytical degradation at pH 7.4, room temperature.

E: 100 mol% LA; $N = 4$; DG_{the} 10%

N: 75 mol% LA; $N = 4$; DG_{the} 10%

Generally, hydrogels containing glycolide exhibit a lower E modulus than hydrogels that contain pure polylactide chains. The influence of the lactide to glycolide ratio depends also on the total polyester portion relative to the poly(vinyl alcohol) and is more pronounced for the shorter polyester grafts. The faster deterioration of hydrogels containing glycolide is a consequence of their higher hydrophilicity and hydrolysis susceptibility. This leads to the lower E modulus for the same degradation time for networks containing glycolide and lactide, compared to those containing only lactide grafts. The difference, concerning mechanical properties, between hydrogels with pure lactide or lactide-*co*-glycolide grafts increases with time of hydrolysis.

5.4.3 Influence of the degree of grafting

The influence of the degree of grafting, which eventually means crosslinking density, is discussed for the hydrogels with the shortest polyester grafts, i.e. 4 ester repeating units. In Fig. 5-28 the samples with pure polylactide chains are shown.

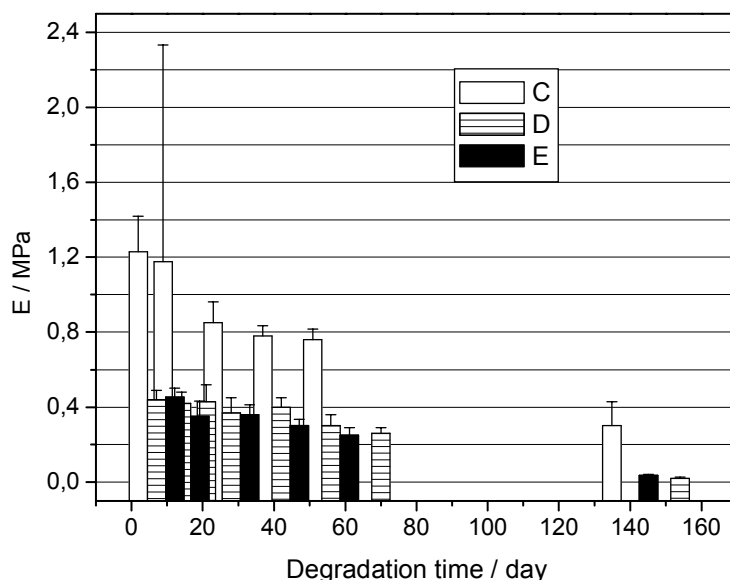


Fig. 5-28 E modulus of the hydrogels during hydrolytical degradation at pH 7.4, room temperature.

C: 100 mol% LA; $N = 4$; DG_{the} 20%

D: 100 mol% LA; $N = 4$; DG_{the} 15%

E: 100 mol% LA; $N = 4$; DG_{the} 10%

Hydrogel C (DG_{the} 20%) has an E modulus twice as high as D (DG_{the} 15%) and E (DG_{the} 10%), which show similar values.

In Fig. 5-29 the hydrogels with 75 mol% of lactide in the grafts are shown. Sample L, with the highest degree of grafting (DG_{the} of 20%) has an E modulus much higher than M (DG_{the} of 15%) and N (DG_{the} of 10%) which have similarly low values of E moduli.

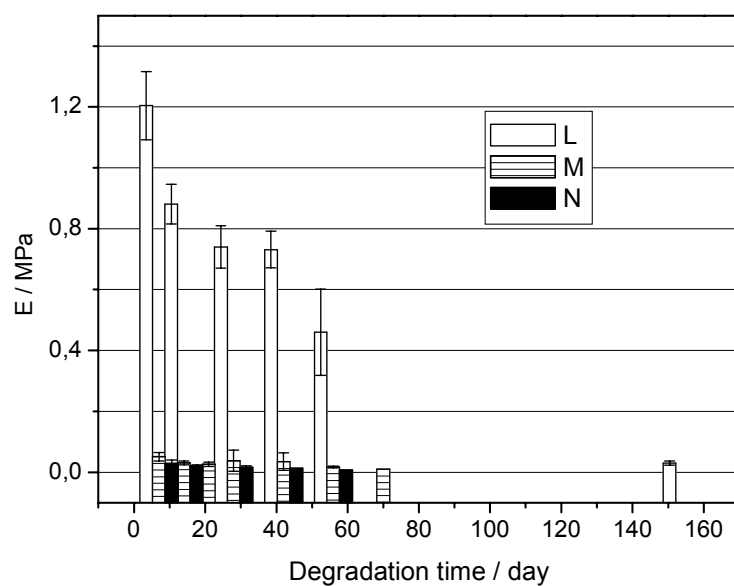


Fig. 5-29 E modulus of the hydrogels during hydrolytical degradation at pH 7.4, room temperature.

L: 75 mol% LA; $N = 4$; DG_{the} 20%

M: 75 mol% LA; $N = 4$; DG_{the} 15%

N: 75 mol% LA; $N = 4$; DG_{the} 10%

Fig. 5-30 shows the E moduli of hydrogels Q and R while sample S, with the lowest degree of grafting, is so weak that it was not possible to perform mechanical testing after 7 days of degradation.

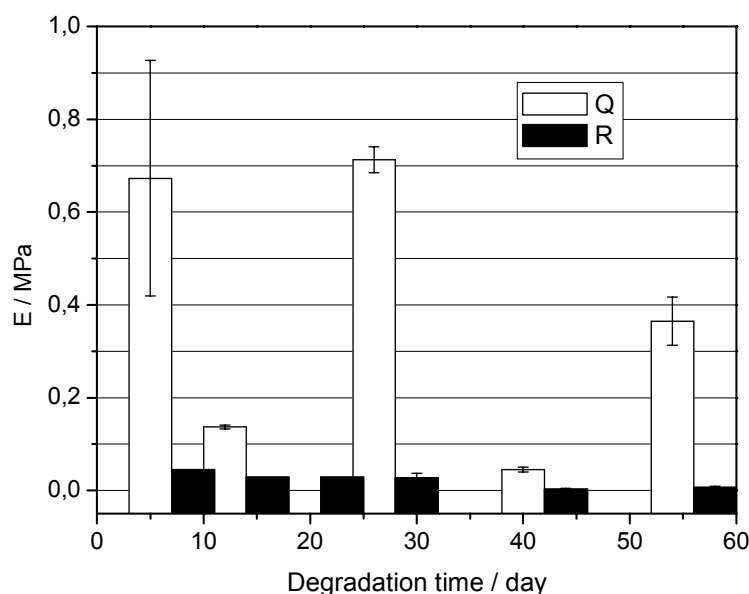


Fig. 5-30 E modulus of the hydrogels during hydrolytical degradation at pH 7.4, room temperature.

Q: 50 mol% LA; $N = 4$; DG_{the} 20%

R: 50 mol% LA; $N = 4$; DG_{the} 15%

A higher degree of grafting results in better mechanical stability. Thus, the hydrogels with a higher degree of grafting and consequently higher crosslinking density show higher E moduli and at the same time smaller influence of glycolide present in polyester chains.

The dependence of the mechanical properties on the degree of grafting of the hydrogels with 8 repeating units is shown in Fig. 5-31. The influence of the crosslinking density on the E modulus is significant, as it is the case with all other hydrogels. Thus, hydrogel I displays a 10 times higher E modulus than hydrogel J and a 30 times higher value than hydrogel K. Comparing these hydrogels with similar ones, which have shorter grafts (shown in Fig. 5-29), analogous behavior is observed. In both sets of samples hydrogels with high DG_{the} show high E moduli. Samples with a high polyester portion show higher E moduli than hydrogels with shorter polyester grafts, as expected.

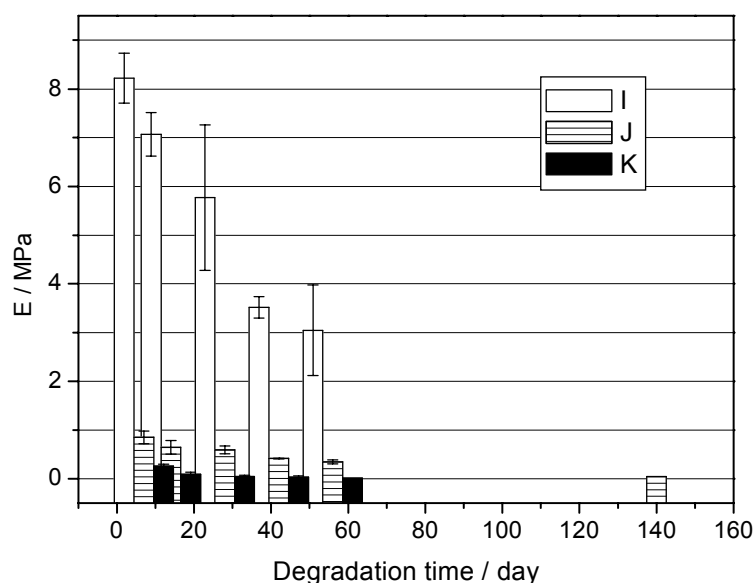


Fig. 5-31 E modulus of the hydrogels during hydrolytical degradation at pH 7.4, room temperature.

I: 75 mol% LA; $N = 8$; $DG_{\text{the}} 20\%$

J: 75 mol% LA; $N = 8$; $DG_{\text{the}} 15\%$

K: 75 mol% LA; $N = 8$; $DG_{\text{the}} 10\%$

Comparing the E modulus during the degradation of 8 weeks, the values are between 180 MPa for hydrogel F and 0.01 MPa for hydrogels K and M. This indicates how the value of the E modulus as well as its decrease during hydrolytical degradation depends on the composition (the polyester portion with respect to the poly(vinyl alcohol) portion). In the case of hydrogel F with the longest polyester grafts and highest degree of grafting the E modulus decreases after 8 weeks of degradation only by 10%, while hydrogel K has a 30 times lower E modulus displaying the largest decrease of the modulus among all. Hydrogels N and R with the shortest grafts, containing glycolide and with a low degree of grafting, are so weak that it was not possible to perform mechanical testing after 7 weeks of degradation, while for hydrogel S it was not possible even after only one week.

5.5 Surface properties of degraded hydrogels

Fig. 5-32 to 5-34 show the contact angle change during hydrolytical degradation of hydrogels, depending on their composition and number of polyester repeating units. The values of the contact angle and standard deviation are given in Tab. 9-5. There is a general tendency of the contact angle to decrease as the degradation process proceeds, which demonstrates the hydrophilicity increase with degradation time. The maximum change was detected within the first week which might be a consequence of the surface group orientation more than of degradation.

Hydrogels with the shortest polyester side chains show a low contact angle of ca. 20°, Fig. 5-32. Hydrogels with short hydrophobic grafts exhibit lower hydrophobicity compared to hydrogels with longer polyester chains from the beginning. Even though the influence of the graft composition on the contact angle is negligible, in case of hydrogel R, with the highest glycolide content, it is not possible to measure the contact angle after six weeks, while it is so hydrophilic that the bubble is not kept on the surface.

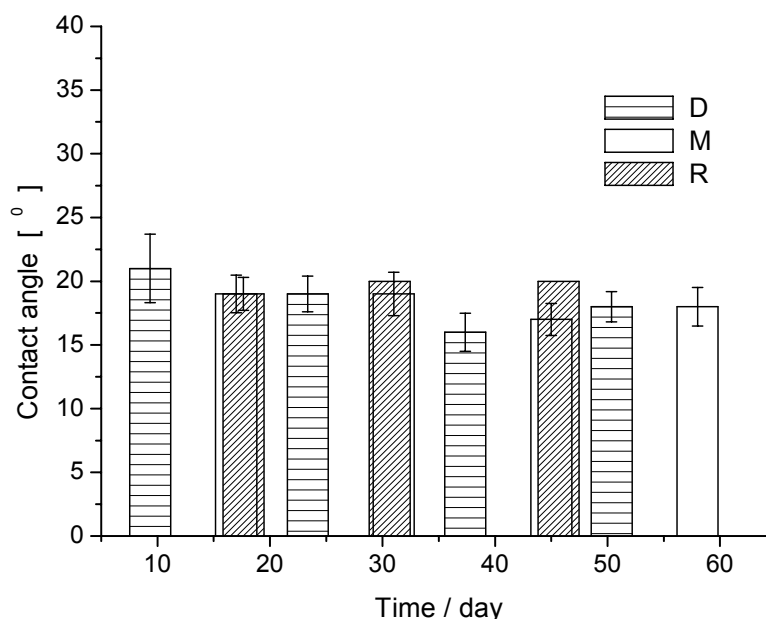


Fig. 5-32 Contact angle of the hydrogels during hydrolytical degradation in water at RT, measured using the *captive-bubble* method. Hydrogels:

D: 100 mol% lactide; $N = 4$; DG_{the} 15%
M: 75 mol% lactide; $N = 4$; DG_{the} 15%
R: 50 mol% lactide; $N = 4$; DG_{the} 15%.

Hydrogels with longer polyester chains (Fig. 5-33) stay hydrophobic for a longer period of time due to a higher portion of hydrophobic regions; consequently, a longer time is needed for their degradation as well as for their surface orientation. Here the influence of composition is noticed. Hence, hydrogel B with pure poly(lactide) grafts shows higher contact during the whole period of degradation. Moreover, hydrogel B has a contact angle of ca. 25° even after eight weeks of degradation while hydrogels J and P that contain glycolide, display contact angles of 20° after only three weeks due to their higher hydrophilicity.

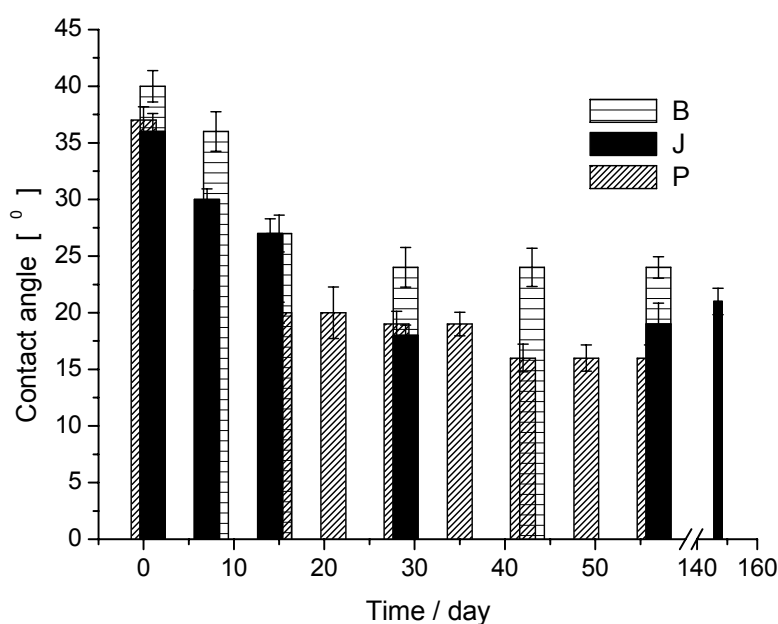


Fig. 5-33 Contact angle of the hydrogels during hydrolytical degradation in water at RT, measured using the *captive-bubble* method. Hydrogels:

B: 100 mol% lactide; $N = 8$; DG_{the} 15%

J: 75 mol% lactide; $N = 8$; DG_{the} 15%

P: 50 mol% lactide; $N = 9$; DG_{the} 15%.

Hydrogels with the longest polyester chains, A and O (Fig. 5-34), do not show a significant influence of the composition. Thus, hydrogel A, having pure poly(lactide) grafts, shows a just slightly higher contact angle than sample O which has 50 mol% of lactide in the grafts. Their hydrophilicity increases initially slowly but after four weeks the contact angle reaches 20°.

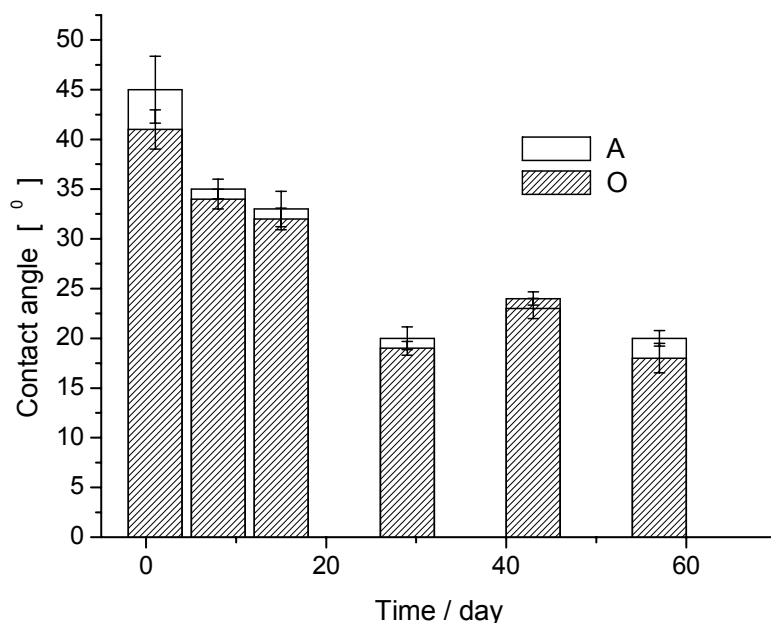


Fig. 5-34 Contact angles of the hydrogels during hydrolytical degradation in water at RT, measured using the *captive-bubble* method. Hydrogels:

A: 100 mol% lactide; $N = 16$; $DG_{\text{the}} 15\%$

O: 50 mol% lactide; $N = 18$; $DG_{\text{the}} 15\%$.

Hydrogels J with 8 and G with 16 repeating units in the grafts Tab. 9-4, that were degraded for a longer period of time (150 or 300 days, respectively), show an increase of the contact angle which means that the hydrophobicity increases slightly with time. A possible explanation could be that the hydrophobic surface became rougher and consequently more hydrophobic ^[166].

Generally, hydrogels with longer polyester grafts exhibit larger contact angles, which means higher hydrophobicity. With increasing glycolide portion in the grafts, there is a decrease of the contact angle as a result of the higher hydrophilicity of the glycolide.

Furthermore, the influence of the length of the polyester chains is combined with their composition, but the former has a stronger influence on the hydrophilic properties of the surface of the hydrogel. Hydrogels with short polyester chains are more hydrophilic, no matter what their composition is.

Examination of the degradation of sample P, which has more or less average values (50 mol % of lactide and number of polyester repeating units 9, $DG_{\text{the}} 15\%$), was performed under different conditions; in water at RT (Tab. 9-6), in water at 37 °C (Tab. 9-7) and under *in vitro*

conditions in PBS (pH 7.4) at 37 °C (Tab. 9-8). The conditions influence the contact angle, as seen from Fig. 5-35. The temperature at which the hydrolytical degradation is performed is of the major influence. Thus, samples degraded in water at room temperature display the main increase in hydrophilicity within the first 7 days and the subsequent change is small.

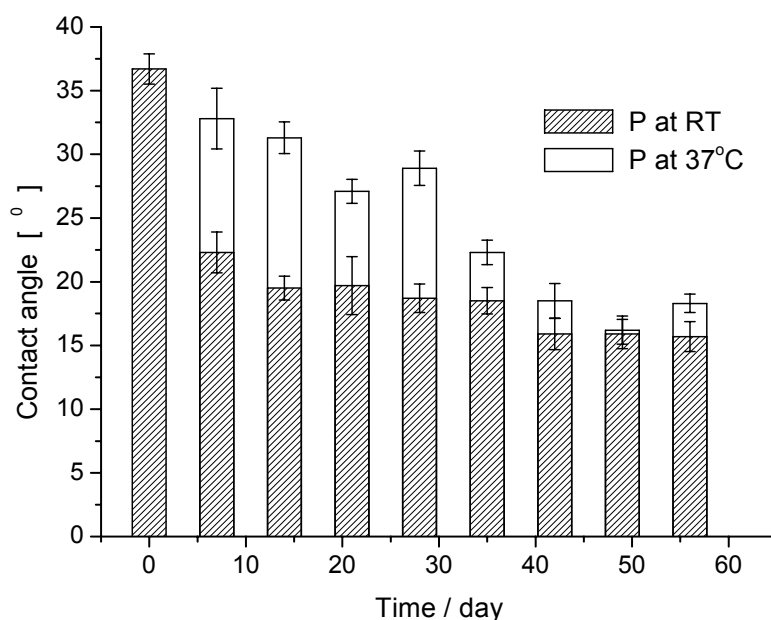


Fig. 5-35 Contact angle of hydrogel P hydrolytically degraded in water at RT and at 37 °C, measured in water using the *captive-bubble* method.

Within the first week, the orientation of OH groups to the surface takes place causing a significant decrease of the contact angle (increase of hydrophilicity). Since degradation at RT is a slow process, the further increase of hydrophilicity proceeds slowly. On the other hand, the contact angle decrease of the sample degraded at 37 °C, due to reorientation, is partially compensated by surface degradation and an increase in surface roughness, resulting in a much slower decrease of the contact angle.

Comparing the degradation of the same hydrogel in two different media, PBS and water at 37 °C, both samples show similar behavior, Fig. 5-36. The surface becomes gradually more hydrophilic, where samples degraded in water stay slightly more hydrophobic during the whole degradation.

After 40 days of hydrolytical degradation all samples show similar hydrophilicity irrespective of the degradation conditions.

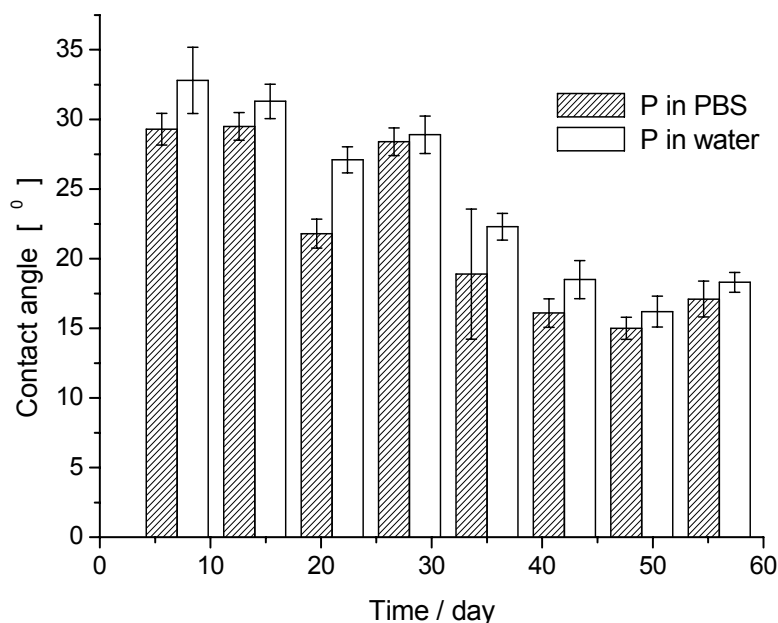


Fig. 5-36 Contact angle of hydrogel P degraded hydrolytically at 37 °C in PBS and in water, measured in water using the *captive-bubble* method.

5.6 IR analysis of degraded networks

Using IR spectroscopy networks A, B, D (100 mol% poly(lactide); number of polyester repeating units: 16, 8, 4; DG_{the} 15%), F, I, L (75 mol% poly(lactide); number of polyester repeating units: 16, 4; DG_{the} 20%), O, P, R (50 mol% poly(lactide); number of polyester repeating units: 18, 9, 4; DG_{the} 15%), after hydrolytical degradation for at least 4 weeks, mostly 8 up to 20 (network L) or 31 (network D) weeks, were analyzed.

Fig. 5-37 shows the spectra of sample D before and after hydrolytical degradation for 4, 10 and 31 weeks in PBS at RT. The characteristic peaks around 3380 cm^{-1} (OH), 2940 cm^{-1} (C-H) and 1750 cm^{-1} (C=O), their intensities and ratios for different networks including sample D after degradation are presented in Tab. 5-1.

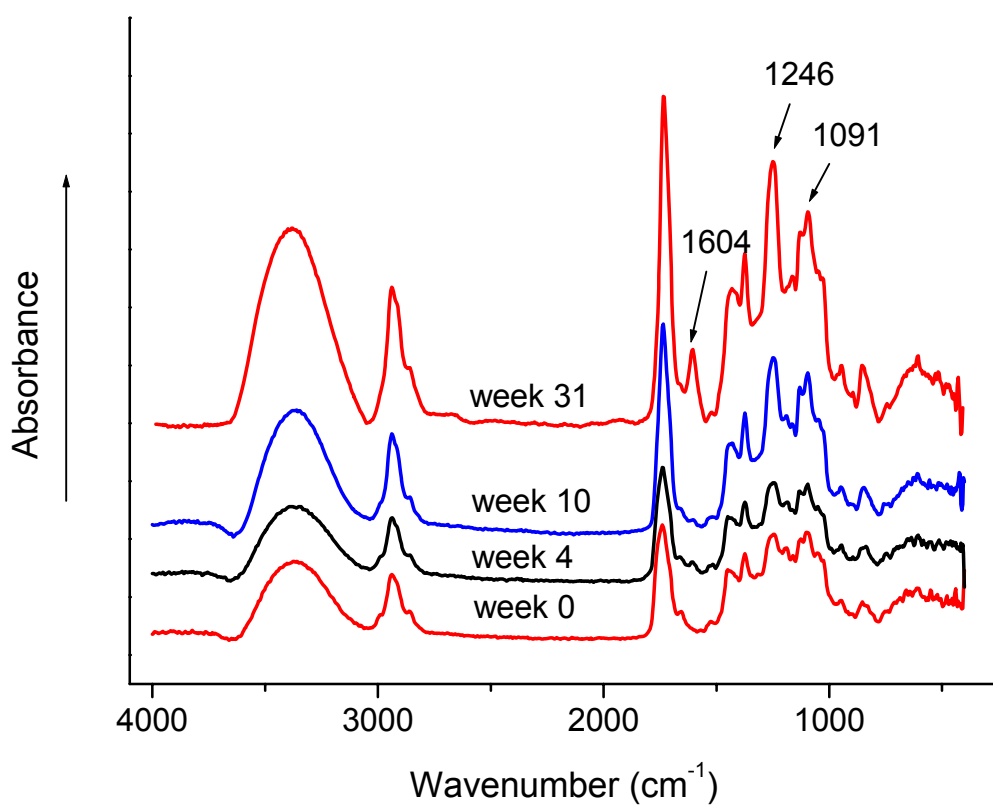


Fig. 5-37 Absorption IR spectra of D type of network, before and after 4, 10 and 31 weeks of hydrolytical degradation in PBS (pH 7.4) at RT.

Tab. 5-1 Characteristic bands around 3380 cm^{-1} , 2940 cm^{-1} and 1750 cm^{-1} , the bands area and their ratios of networks A, B, D, O, P, R, F, I and L after hydrolytical degradation.

Characteristic signals								Area ratio	
Sample	Week	O-H str cm^{-1}	$A_{\text{O-H}}$	C-H str cm^{-1}	$A_{\text{C-H\%}}$	C=O str cm^{-1}	$A_{\text{C=O}}$	$S_{\text{O-H}}/S_{\text{C-H}}$	$S_{\text{O-H}}/S_{\text{C=O}}$
A	4	3413	1813	2939	577	1755	1176	3.142	1.539
	8	3375	3308	2943	983	1755	2193	3.351	1.508
B	4	3379	3946	2939	1047	1743	2061	3.769	1.915
	8	3359	4319	2939	1150	1739	2293	3.756	1.883
D	4	3379	3823	2939	810	1739	1476	4.720	2.590
	10	3375	6362	2939	1284	1736	2190	4.955	2.905
	31	3379	11226	2939	2144	1736	3935	5.236	2.853
O	4	3383	2729	2943	1049	1756	2554	2.600	1.069
	8	3370	2096	2940	755	1760	2108	2.776	0.994
P	4 (RT)	3370	4613	2939	1186	1740	2571	3.889	1.794
	4 (37°C)	3390	6323	2938	1400	1736	3398	4.516	1.861
R	4	3360	3092	2940	752	1736	1664	4.110	1.858
F	0	3380	1910	2940	932	1760	2580	2.049	0.741
	4	3390	1462	2943	667	1759	2100	2.192	0.696
	8	3383	1441	2943	711	1759	2253	2.027	0.640
I	1	3383	3350	2939	1079	1775	2412	3.105	1.389
	4	3375	3528	2939	1085	1755	2486	3.252	1.419
L	0	3378	3104	2935	1221	1739	2052	2.542	1.513
	8	3398	4706	2935	1315	1739	2728	3.579	1.725
	20	3390	4109	2935	1081	1736	2144	3.801	1.917

The wave number of the OH band in the hydrogels is between that of PVA (3360 cm^{-1}) and polyester copolymers (3500 cm^{-1}), Tab. 9-1, and is more or less constant. The increasing amount of polyester in hydrogels moves the C=O band toward higher wave numbers. On the other hand, as a result of degradation this band moves toward lower wave numbers, in each sample, indicating the removal of ester groups from the hydrogel.

The ratios OH/C-H and OH/C=O decrease in the series of samples D, B, A; R, P, O and L, I, F, which is in accordance with the increasing portion of polyester due to longer grafts in the network (Tab. 5-1).

The position of the OH band ($\approx 3380\text{ cm}^{-1}$) and C=O band ($\approx 1740\text{ cm}^{-1}$) changes slightly, while that of the CH band at 2939 cm^{-1} does not change at all during degradation in network D. Comparing the area ratio of characteristic bands OH/C-H before and during degradation it increases constantly (by 8% after 4 weeks, by 14% after 10 and by 20% after 31 weeks). At the same time the area ratio OH/C=O does not change initially, after 10 weeks it increases by 12% and after 31 weeks by 10%. For sample B after hydrolytical degradation, Tab. 5-1, Fig. 9-8, the bands at 3390 cm^{-1} and at 1747 cm^{-1} are moved toward lower wave numbers while the band at 2939 cm^{-1} stays constant during degradation. The area ratio of the characteristic bands OH/C-H decreases by 6% both after 4 and 8 weeks, while at the same time the ratio OH/C=O increases by 14% after 4 weeks and by 12% after 8 weeks.

Sample A, Tab. 5-1, Fig. 9-9, shows pretty constant values of the wave number for the groups C-H and C=O while values for the OH group are fairly different before ($\approx 3390\text{ cm}^{-1}$) and after degradation ($\approx 3413\text{ cm}^{-1}$ and 3375 cm^{-1}). The intensity ratio OH/C-H increases during degradation while the ratio OH/C=O increases significantly at first and then decreases slightly, as it is the case with samples B and D.

The relative change of OH/C-H and OH/C=O band area ratios during degradation is difficult to follow since they indicate the multiplicity of the degradation processes within the sample, a general observation, however, can be made that hydrolysis of the ester bonds leads to an increase in OH groups relative to C=O groups. A slight decrease of the ratio OH/C-H that appears in some samples (e.g. B) might be due to the removal of OH groups together with C=O groups from the system during degradation.

Having insight into the behavior of the same samples before and after hydrolytical degradation, using IR spectroscopy in the fingerprint region certain conclusion can be drawn even though it is difficult because the bands are not well separated. Sample A, before degradation, Fig. 4-6, has a strong band at 1095 cm^{-1} and a weak band at 1264 cm^{-1} which is exactly opposite to PVA, Fig. 9-6. This fact together with the band that appears at 1190 cm^{-1}

demonstrates the present ester portion while the band at 1190 cm^{-1} does not exist in the PVA spectrum. After degradation up to 8 weeks there is no significant change in this region except for the band at 1190 cm^{-1} which slightly decreases, Fig. 9-9. This indicates the slow degradation of this sample within 8 weeks.

The spectra of network A and the spectra of network B, Fig. 9-9 and Fig. 9-8, have similar shape. After 4 weeks of degradation there is a decrease of the band at 1190 cm^{-1} compared to the bands at 1240 cm^{-1} and 1090 cm^{-1} which proves the loss of polyester. In network B the band at 1240 cm^{-1} increases compared to the band at 1090 cm^{-1} during degradation and in that way the ratio becomes more similar to that in PVA. This change happens faster in network B than in A which shows its faster degradation as a result of the shorter polyester grafts and smaller hydrophobicity. In sample D already after 4 weeks of degradation the band at 1245 cm^{-1} is stronger than that at 1099 cm^{-1} , which is opposite to their ratio before degradation, Fig. 5-37. After longer periods of degradation, 10 weeks and especially 31 weeks, the difference becomes much greater and the spectrum resembles that of PVA, Fig. 9-6. At the same time, the band at 1189 cm^{-1} , characteristic of polyester, gradually disappears. The spectrum of sample R, Fig. 9-10, Tab. 5-1, after 4 weeks of degradation, shows the OH band at 3360 cm^{-1} , the C-H band at 2940 cm^{-1} and the C=O band at 1740 cm^{-1} , while the intensity ratio OH/C-H has a value of 4.11 and the ratio OH/C=O has a value of 1.86. After 4 weeks of degradation this sample has a band at 1250 cm^{-1} which is just slightly stronger than that at 1096 cm^{-1} and shows no more a distinct band at 1190 cm^{-1} . All this demonstrates a rapid degradation of this sample having the shortest polyester chains with four repeating units and 50 mol% of glycolide and the resulting highest hydrophilicity.

Sample P, Fig. 5-38, Tab. 5-1, is of the most interest because it was degraded both, at RT and $37\text{ }^{\circ}\text{C}$ in PBS for 4 weeks in order to follow the influence of the different conditions. Thus, the sample before degradation has an OH band at 3380 cm^{-1} , Tab. 4-9, while the sample degraded at RT shows the same band at 3370 cm^{-1} and the sample degraded at $37\text{ }^{\circ}\text{C}$ displays it at 3390 cm^{-1} .

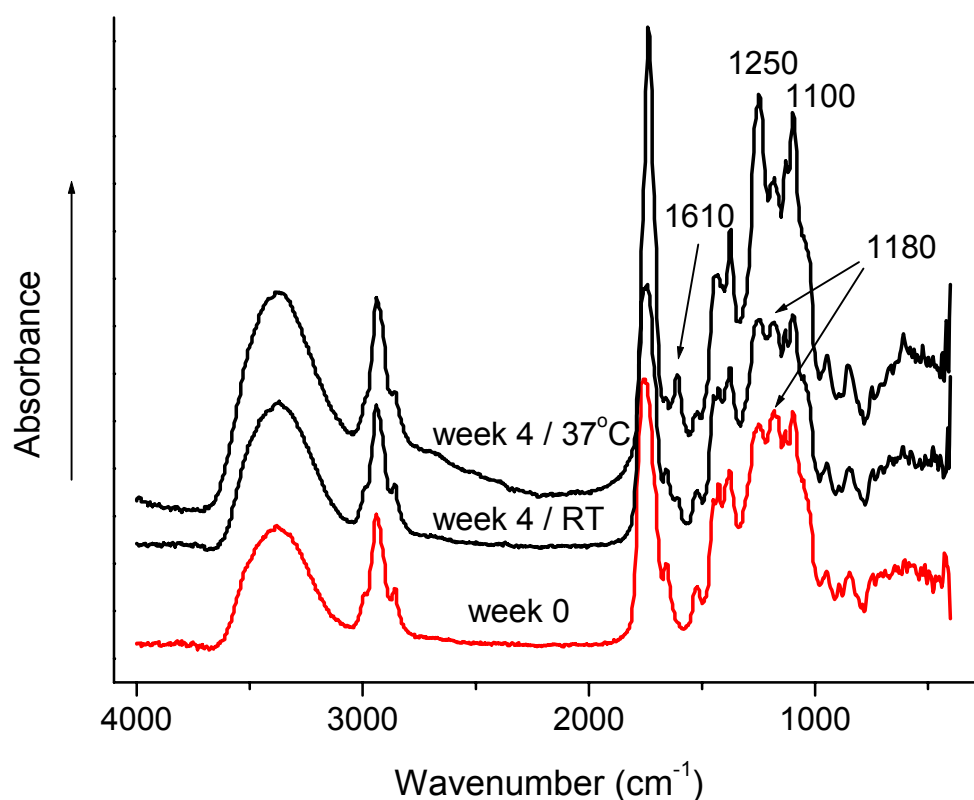


Fig. 5-38 IR spectra of network P after 4 weeks of hydrolytical degradation in PBS (pH 7.4) at RT and at 37 °C.

The absorption band characteristic of the C-H group shows the smallest deviation (2939 ± 1 cm⁻¹). The intensity ratio OH/C-H in the sample before degradation has a value of 3.30 and OH/C=O of 1.43. In the sample degraded at RT the ratio OH/C-H increases by 18% (3.89) and the ratio OH/C=O increases by 25% (1.79). In the sample degraded at 37 °C the ratio OH/C-H increases by 40% (4.52) and the ratio OH/C=O increases by 30% (1.86). This indicates that at higher temperature the rate of degradation increases.

In the fingerprint region sample P has bands of the same intensity at 1180 cm⁻¹ and at 1100 cm⁻¹ and a slightly weaker band at 1250 cm⁻¹ (the band strongly expressed in the PVA spectrum, coming from acetate groups present, Fig. 9-6) which confirms the lower portion of polyester in comparison, e.g., to network O which contains 18 repeating ester units and has a much weaker band at 1250 cm⁻¹ relative to the other two (Fig. 9-11). The band around 1450 cm⁻¹ is split as a consequence of the glycolide content in the copolyester chain ^[51,165]. The sample degraded at RT shows a decrease of the intensity of the band at 1184 cm⁻¹ and its intensity is slightly below that of the band at 1248 cm⁻¹ and 1096 cm⁻¹. The band around 1450 cm⁻¹ is still split. On the other hand, the spectrum of the sample degraded at 37 °C shows a

much larger decrease of the band at 1180 cm^{-1} relative to the bands at 1246 cm^{-1} and at 1095 cm^{-1} . The band at 1246 cm^{-1} in this sample is significantly stronger than the band at 1095 cm^{-1} and resembles the PVA spectrum indicating the reduction of the ester portion relative to the PVA backbone. The band around 1440 cm^{-1} shows a weak shoulder. In this highly degraded sample a new band appears at 1610 cm^{-1} which is difficult to assign.

Sample O, Fig. 9-11, Tab. 5-1, shows the largest shift of the OH band i.e. from 3390 cm^{-1} before degradation, Tab. 4-9, to 3370 cm^{-1} after degradation, while the two bands C-H and C=O do not show shifts (2940 cm^{-1} and 1760 cm^{-1}) during degradation. The area ratio OH/C-H increases during degradation, by 11% after 4 weeks and by 18% after 8 weeks. The ratio OH/C=O increases by 22% after 4 weeks and by 13% after 8 weeks. A possible explanation is that initially the number of OH groups increases relative to the number of C=O groups due to hydrolysis, while with the progress of degradation there is a decrease in both C=O and OH groups owing to a larger mass loss. Generally, with an increasing polyesters portion in the polymer networks (R, P, O) there is a decrease in the area ratios OH/C-H and OH/C=O, Tab. 5-1. For each sample after degradation there is an increase of the ratio OH/C-H which indicates an increase of the number of OH groups resulting from the hydrolysis of the polyester chains.

Sample O in the fingerprint region before degradation shows the strongest band at 1170 cm^{-1} belonging to the polyester content and a band at 1250 cm^{-1} which is not only much weaker but also not well separated, Fig. 4-6. After degradation the band at 1170 cm^{-1} has decreased relative to the band at 1250 cm^{-1} , Fig. 9-11 which confirms a slow degradation of the polyester. The band around 1450 cm^{-1} is split as a consequence of the glycolide content in the polyester grafts.

In Tab. 5-1 are given the wave numbers of characteristic absorption bands and their relative areas for networks F, I and L ($DG_{\text{the}} 20\%$) before as well as after hydrolytical degradation in PBS at RT. Their IR spectra are shown in Fig. 9-12 to Fig. 9-14. The increasing content of polyesters in the networks shifts the C=O band toward higher wave numbers, as it is the case with all other networks. During degradation, this band shifts slightly toward lower values, as in case of other samples. The area ratio OH/C-H increases during degradation, as well as the ratio OH/C=O, indicating the decrease of the polyester portion.

In the fingerprint region, network F, Fig. 9-12, after four weeks of degradation, shows a split band at $1452/1424\text{ cm}^{-1}$ as a consequence of the glycolide content in the grafts. The strongest band is at 1093 cm^{-1} , followed by a slightly weaker band at 1190 cm^{-1} while the band at 1245 cm^{-1} is much weaker and is not so well separated. After another four weeks of degradation

(week 8) there is no significant difference between the spectra: the band at $1452/1424\text{ cm}^{-1}$ is still split, the differences between the bands at 1240 cm^{-1} , 1190 cm^{-1} and 1090 cm^{-1} are similar to the differences in the former sample, which demonstrates its slow degradation as a consequence of its long polyester grafts and high degree of substitution ($DG_{\text{the}} 20\%$). Network I, Fig. 9-13, after one week of degradation, shows a slightly split band at 1452 cm^{-1} due to the glycolide content. The strongest band is at 1097 cm^{-1} and two smaller bands are at 1190 cm^{-1} and at 1245 cm^{-1} . After 4 weeks of degradation the band at 1190 cm^{-1} is smaller relative to the band at 1097 cm^{-1} , while the band at 1245 cm^{-1} has increased. This is a confirmation of slow degradation which is still faster than that of sample F. Network L, Fig. 9-14, in the fingerprint region does not show a split band at 1452 cm^{-1} , there is only a shoulder due to the glycolide portion. The strongest band occurs at 1246 cm^{-1} while the band at 1097 cm^{-1} is weaker which resembles the PVA spectrum (Fig. 9-6). The band at 1185 cm^{-1} is very weak as an evidence of the short polyester chains. After 8 weeks of degradation the band at 1185 cm^{-1} has diminished significantly relative to the neighboring bands (1250 cm^{-1} and 1090 cm^{-1}), similarly as the band at 1450 cm^{-1} relative to the band at 1380 cm^{-1} , due to the removal of ester units. At the same time, the band at 1245 cm^{-1} has increased relative to the band at 1096 cm^{-1} . This is a confirmation of the much faster degradation of network L compared to network F. The performed observations reveal the possibility of using IR analysis for qualitatively following the degradation process in networks.

5.7 Thermal properties of degraded networks

In order to investigate their thermal properties TGA and DSC analyses were performed on the networks during their hydrolytical degradation. Prior to those measurements samples were freeze-dried. This enables the influence of the degradation on the thermal properties due to the destruction of crosslinked structure as well as mass loss to be followed.

5.7.1 Thermogravimetry (TGA)

The thermal analysis was used to see the influence of hydrolytical degradation on thermal properties of hydrogels. There was no significant change in the shape of TGA and DTGA curves of networks before and after degradation as shown in Fig. 5-39 to Fig. 5-41, except for the degradation onset. After an initial small weight loss which is caused by water evaporation, there is a two stages decomposition process. In Tab. 5-2 thermal analysis data for networks A (Fig. 5-39), B (Fig. 5-40) and D (Fig. 5-41) are given.

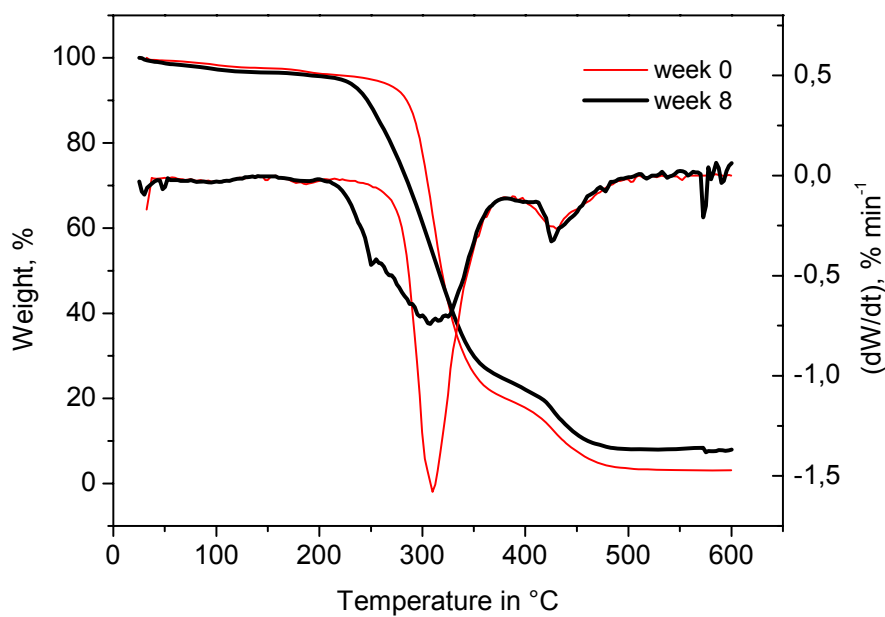


Fig. 5-39 TGA and DTGA plots of network A before and after hydrolytical degradation, measured at a heating rate of 10 °C min⁻¹.

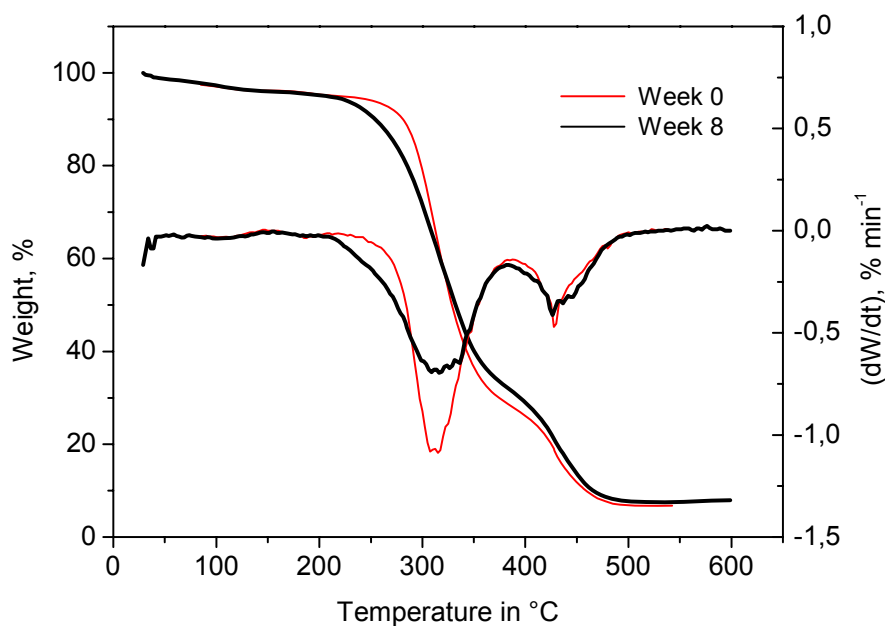


Fig. 5-40 TGA and DTGA plots of network B before and after hydrolytical degradation, measured at a heating rate of 10 °C min⁻¹.

The difference in the onset of the decomposition process before and after hydrolytical degradation depends on the composition of the network; it is more pronounced in networks with longer polyester chains.

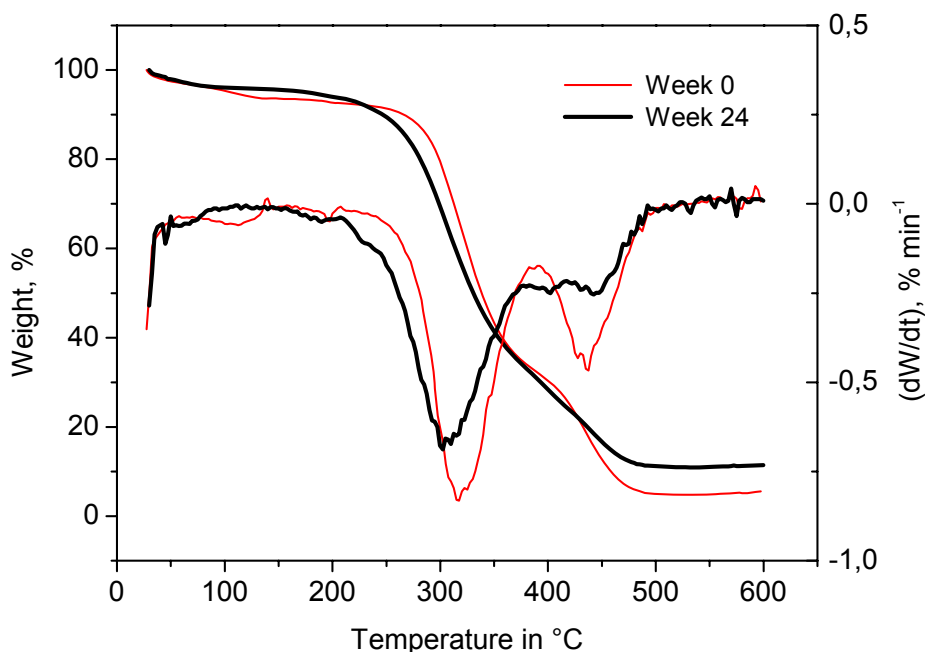


Fig. 5-41 TGA and DTGA plots of network D before and after hydrolytical degradation, measured at a heating rate of $10\text{ }^{\circ}\text{C min}^{-1}$.

The main difference that appears in the thermographs of network D, before and after hydrolytical degradation, is seen at the third decomposition stage, where the differentiated curve shows multiple peaks which implies different volatile degradation products ^[68,135,136].

Tab. 5-2 Thermal characterization of networks A, B and D after hydrolytical degradation, obtained by TGA at a heating rate of $10\text{ }^{\circ}\text{C min}^{-1}$; $T_{10\%}$, 10% loss of weight temperature; $T_{\max 1}$ and $T_{\max 2}$, temperature of maximum rate of weight loss; ΔW_1 and ΔW_2 , weight loss at $T_{\max 1}$ and $T_{\max 2}$; $Y_{600\text{ }^{\circ}\text{C}}$, residue at $T = 600\text{ }^{\circ}\text{C}$.

	A *	B *	D **
$T_{10\%}\text{ }^{\circ}\text{C}$	247	254	245
$T_{\max 1}\text{ }^{\circ}\text{C}$	309	315	305
$\Delta W_1\text{ }^{\circ}\text{C}$	72	63	62
$T_{\max 2}\text{ }^{\circ}\text{C}$	427	427	444
$\Delta W_2\text{ }^{\circ}\text{C}$	15	25	21
$Y_{600\text{ }^{\circ}\text{C}}$	8	7	11

* Measured after 8 weeks of hydrolytical degradation
 ** Measured after 24 weeks of hydrolytical degradation

When comparing the temperature values at 10% of weight loss before (Tab. 4-10) and after (Tab. 5-2) degradation of networks A, B and D, a shift toward lower values becomes evident: 38 °C for network A, 27 °C for network B, both degraded for eight weeks, and only 21 °C for network D, even though it was degraded for a longer period of time, for 24 weeks. The other characteristic value, T_{\max} , does not change significantly, except for network D with the shortest grafts, which make it the least stable one.

Network P, after 4 weeks of degradation, shows only a slightly steeper onset of thermal decomposition while the same sample, after 8 weeks of hydrolytical degradation (Fig. 5-42), shows immediate weight loss, but the main decomposition process takes place at about the same rate as in the sample before degradation.

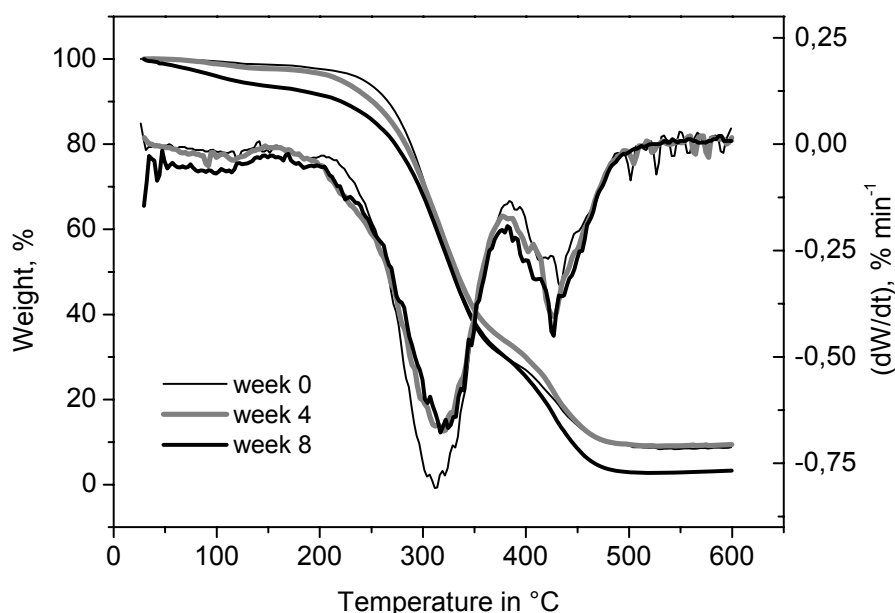


Fig. 5-42 TGA and DTGA plots of network P before and after hydrolytical degradation, measured at a heating rate of 10 °C min⁻¹.

The thermal analysis of network P, after 4 weeks of hydrolytical degradation at room temperature and at 37 °C is shown in Fig. 5-43.

In Tab. 5-3 the characteristic values of network P, degraded under different conditions, and obtained by thermal analysis are given.

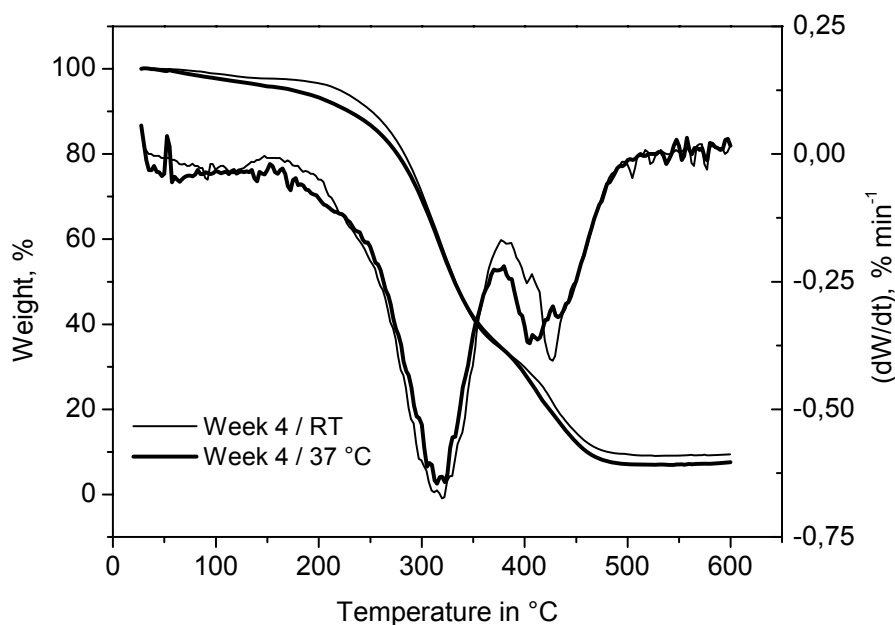


Fig. 5-43 TGA and DTGA plots of network P after four weeks of hydrolytical degradation at room temperature and at 37 °C, measured at a heating rate of 10 °C min⁻¹.

Tab. 5-3 Thermal characterization of network P hydrolytically degraded at room temperature 4 and 8 weeks and 4 weeks at 37 °C, obtained by TGA at a heating rate of 10 °C min⁻¹; $T_{10\%}$, 10% loss of weight temperature; $T_{\max 1}$ and $T_{\max 2}$, temperature of maximum rate of weight loss; ΔW_1 and ΔW_2 , weight loss at $T_{\max 1}$ and $T_{\max 2}$; $Y_{600\text{ °C}}$, residuum at $T = 600\text{ °C}$.

	P (37 °C)*	P (RT)*	P (RT)**
$T_{10\%} / \text{°C}$	229	251	221
$T_{\max 1} / \text{°C}$	317	317	322
$\Delta W_1 / \%$	60	64	61
$T_{\max 2} / \text{°C}$	405	426	426
$\Delta W_2 / \%$	28	24	27
$Y_{600\text{ °C}}$	7	9	3

* Measured after 4 weeks of hydrolytical degradation

** Measured after 8 weeks of hydrolytical degradation

As seen from Fig. 5-43, the curves have similar shape. In the first degradation region of the sample degraded at 37 °C, $T_{10\%}$ is located at 229 °C compared to 251 °C for the copolymer degraded at RT. At the second range of the main mass loss, the two curves have similar shape. The difference between them is most evident when their differentiated curves in the third decomposition range are observed. Thus, the curve of sample P degraded for 4 weeks at RT

displays in this region one smaller peak that appears at a lower temperature of 402 °C and the main peak at 426 °C. In the sample degraded for 4 weeks at 37 °C, the main transformation in the third region appears at 405 °C, but a new smaller peak appears at higher temperature of 432 °C. This indicates different volatile degradation products ^[68,135,136].

5.7.2 Differential scanning calorimetry (DSC)

DSC measurements were performed in the range of 20 °C to 150 °C. The second run was taken because the thermal history is erased by the first run. All samples show only one glass transition temperature. There is no sign of crystallization or melting at all, which shows that during hydrolytical degradation there is no formation of crystalline products. This is the advantage of these materials in cases of application as degradable implant materials, since crystalline particles may cause the formation of fibrous capsules in vivo ^[162,163].

The change of the glass transition temperature of the networks, depending on the degradation time, is shown in Fig. 5-44.

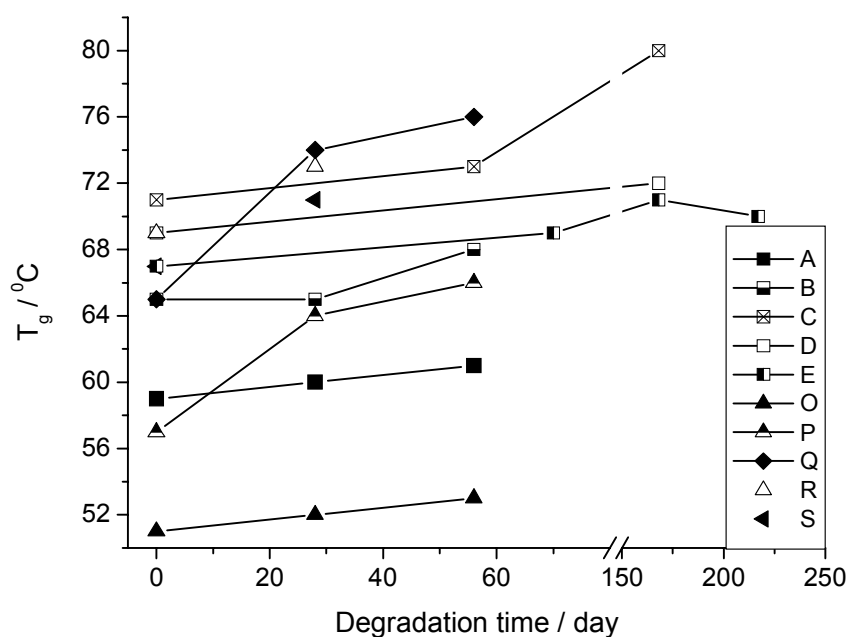


Fig. 5-44 Dependence of T_g on the degradation time of different networks.

A: 100 mol% LA; $N = 16$; DG_{the} 15%	O: 50 mol% LA; $N = 18$; DG_{the} 15%
B: 100 mol% LA; $N = 8$; DG_{the} 15%	P: 50 mol% LA; $N = 9$; DG_{the} 15%
C: 100 mol% LA; $N = 4$; DG_{the} 20%	Q: 50 mol% LA; $N = 4$; DG_{the} 20%
D: 100 mol% LA; $N = 4$; DG_{the} 15%	R: 50 mol% LA; $N = 4$; DG_{the} 15%
E: 100 mo % LA; $N = 4$; DG_{the} 10%	S: 50 mol % LA; $N = 4$; DG_{the} 10%

All networks show an increase of the glass transition temperature with degradation time. In Tab. 9-9 the values of T_g and ΔC_p of the network during hydrolytical degradation are given. There is no significant difference in ΔC_p of all networks which means that there is no difference in short range order of the amorphous samples. The increase of T_g is smaller in networks with longer polyester chains as a result of their higher stability due to their higher hydrophobicity. The increase of the glass transition temperature in network A with 16 ester repeating units in poly(*rac*-lactide), after four and eight weeks of degradation, is smaller than in network B with 8, or in network D with 4 ester repeating units. In network A there is an increase of T_g of 2 °C after eight weeks of degradation. Sample B shows after the same degradation time an increase of 3 °C. Network O with 18 repeating units in the grafts shows an increase of 2 °C like network A, while network P, with 9 ester repeating units, shows a T_g increase of 9 °C after eight weeks of degradation. The glass transition temperatures of the samples that contain glycolide grafts are lower than those containing pure lactide and stay lower during the whole degradation period, but they exhibit a greater increase of T_g during degradation. The glycolide content results in a lower T_g value and faster degradation as a consequence of its higher hydrophilicity.

6. Summary

The present work describes the synthesis and characterization of amorphous and covalently crosslinked polymer systems based on poly(vinyl alcohol) and polyesters. With regard to medical applications, for the synthesized materials only components are used that are already established as biomaterials. The hydrogels prepared are biocompatible and hydrolytically degradable. The chemical composition and the crosslinking density of the polymer networks can be controlled by variation of the monomer/initiator ratio and by the amount of polyester grafts relative to the amount of the poly(vinyl alcohol) backbone. The macroscopic properties, primarily the degradation rate, mass loss, water uptake, mechanical properties of the hydrogels can be tailored by variation of the polyester composition and the network structure. Covalently crosslinked polymer networks were synthesized via a three step reaction. Short polyester chains were initially prepared by ring opening polymerization of lactide and glycolide. Hydroxyethyl methacrylate was used as an initiator which enables the simultaneous introduction of double bonds into the system. In the second step the hydroxy end groups of the polyesters were transferred into carboxylic groups by reaction with succinic anhydride. The third step was the grafting of the polyester chains onto the poly(vinyl alcohol) chain. Finally, crosslinking was accomplished through reaction of the double bonds using a free radical initiator.

The chemical composition and structure of the networks was controlled by varying the stoichiometric ratio of components in the reaction mixture. The chemical composition of the networks was investigated by means of IR and NMR spectroscopy, whereas NMR was used to pursue each step of synthesis. It revealed agreement between the theoretical and experimental values concerning the length and composition of polyester grafts, which indicated a good control over the synthesis. Polyesters with 4, 8, 9, 16 and 18, repeating units were obtained. The ratio of lactide to glycolide in the polyester chains was varied between the molar ratios 100:0; 75:25; 50:50 and experimental values confirmed that. The theoretical degree of grafting on the backbone was 10%, 15% and 20%. Generally, the experimentally determined degree of grafting revealed lower values. The major deviation displayed the grafted copolymer Q (experimental degree of grafting DG_{exp} of 11% compared to the theoretical DG_{the} of 20%), and the best match showed copolymer P (DG_{exp} of 13% compared to the DG_{the} of 15%). The IR spectroscopy gave insight into the composition of the networks by means of the characteristic bands at 3300 cm^{-1} for OH, 1750 cm^{-1} for C=O, as well as in the fingerprint region.

Thermogravimetry revealed the onset of a small mass loss in the temperature range between 265 °C and 285 °C. The major mass loss occurs in the temperature range between 301 °C and 318 °C. Networks with longer polyester chains showed the onset of the first small loss ($T_{10\%}$) at higher temperature when compared to networks with shorter grafts. The same networks display the major mass loss at lower temperature than the networks with shorter grafts. The glycolide amount showed only small influence on the thermal decomposition. DSC measurements showed only one characteristic transition temperature, the glass transition temperature T_g . All networks showed a glass transition temperature in the range between 51 °C and 71 °C. Networks with longer polyester chains showed a lower glass transition temperature. Moreover, networks with a glycolide content of 50 mol% display significantly lower glass transition temperature T_g relative to networks that contain pure polylactide grafts, especially networks with longer polyester grafts.

The surface properties of hydrogel films were investigated using the *captive-bubble* method. Statistic contact angles were found to be between 28° and 45°, which demonstrates the possibility of obtaining materials of diverse hydrophilicity by varying the comonomers ratio.

The mechanical properties of hydrogels clearly depend on the composition and structure. Mechanical testing showed Young's modulus E to have values between 0.01 and 103 MPa, however, the values of most of the hydrogels were below 4 MPa. Hydrogels with higher polyester content and higher crosslinking density have higher E moduli. Thus, variation of the length of polyester grafts and their number enables preparation of materials in a large range of mechanical properties.

Biocompatibility was tested on hydrogel type P as an example with the assistance of primary human dermal fibroblasts (hF) cells. After four days of incubation the cells displayed good adhesion and viability, confirming the good biocompatibility of the material.

Hydrolytical degradation experiments were carried out in an aqueous phosphate buffer solution at pH 7.4 and room temperature.

The mass loss that accompanies the degradation of hydrogels was determined gravimetrically. The mass loss is influenced by the composition of the hydrogel. More hydrophilic hydrogels, as a result of shorter polyester grafts or a fewer number of grafts, show a faster mass loss. Glycolide in the polyester chains additionally contributes to a faster mass loss due to its more hydrophilic nature. Thus, the hydrogel with the longest polylactide grafts showed 10% of mass loss after 110 days of hydrolytical degradation while hydrogels with the shortest polyester chains, containing lactide and glycolide, showed 10% of mass loss within the first week of degradation. A hydrogel that was degraded both at room temperature and at 37 °C

exhibits a continuous mass loss, but a faster one in the sample degraded at 37 °C, particularly after 14 days. The sample degraded at 37 °C has 80% of residual mass after 14 days while the sample degraded at RT still has 80% residual mass after 35 days.

All hydrogels exhibit an increase in swelling in the course of hydrolytical degradation although at different rate. Within the first eight weeks of degradation, the hydrogels display a weight related degree of swelling, S , in the range from less than 2% up to 30%. Hydrogels that were submitted to degradation for a longer period of time, showed a degree of swelling of up to 190%. The swelling behavior of the hydrogels depends strongly on composition and structure. Hydrogels with shorter polyester grafts show more rapid and more intensive swelling due to their more hydrophilic nature. Thus, samples with shorter polyester grafts initially display a several times higher degree of swelling and moreover the swelling increases at a higher rate. The influence of glycolide present in the polyester chains depends on the number of repeating units: it is more significant in hydrogels with shorter polyester grafts. The degree of substitution on the backbone has a strong influence on the swelling behavior. Therefore, hydrogels with a DG_{the} of 10% display an increase of swelling immediately which continues to increase at high rate, while hydrogels with a DG_{the} of 20% show a linear, small swelling at first which increases significantly after 60 days of degradation. The dependence of swelling on the degree of grafting is combined with the influence of the composition of the polyester chains. Thus glycolide present in the polyester grafts causes greater swelling than hydrogels with pure lactide grafts, this influence being intensified with time.

The morphology change of hydrogels during hydrolytical degradation was examined by means of scanning electron microscopy. This method enables the surface and the cross section of the sample as a consequence of different mechanisms of degradation to be followed. It is difficult to follow separately each single influence: structure, composition and degree of grafting, while their influences combine. Thus, hydrogels with long polyester chains (e.g. F and I with DG_{the} of 20% or A and O with DG_{the} of 15%), show a conserved shape after eight weeks of degradation accompanied by a significant reduction of sample thickness in A and O. On the other hand, hydrogels with short polyester chains, during a degradation period of similar duration, exhibit a significant change in the sample shape, where the nature of the change depends on the degradation mechanism. Thus, some samples display a significant decrease of thickness characteristic of a surface erosion mechanisms (e.g. E, DG_{the} of 10%), while others display a highly deteriorated cross section due to a bulk degradation mechanism (e.g. D, DG_{the} of 15%) or large cracks were observed along the cross section (e.g. C, DG_{the} of 20%). Hydrogels with short polyester chains, containing both lactide and glycolide (N and Q),

after only four weeks of degradation show highly deteriorated samples and both mechanisms of degradation: erosion and bulk.

The decrease of the E modulus as a result of hydrolytical degradation is immanent to all hydrogels. Hydrogels with the shortest grafts (4 repeating units) exhibit an E modulus below 1 MPa after eight weeks of degradation. Some of these samples became so swollen and weak that it was not possible to measure their tensile strength after eight weeks of degradation (N and R). Hydrogels with medium length of polyester grafts (8 or 9 repeating units) have a modulus of 1.7-3 MPa while hydrogels with the longest polyester grafts have values between 15-175 MPa during the same course of degradation time.

The contact angles of degraded hydrogels were measured. After eight weeks of degradation all hydrogels showed about the same value of 20° . A difference was seen only when the time is considered within this value is reached. Therefore, hydrogels which were more hydrophobic initially due to higher polyester content need a longer period of time to become so hydrophilic as to have a contact angle around 20° . Hydrogels with the longest polyester grafts need up to eight weeks, while hydrogels with the shortest polyester grafts and resulting higher hydrophilicity show a contact angle of 20° after only the first week of degradation.

The investigation of the degradation process by means of IR spectroscopy was possible through the observation of characteristic IR bands. The area ratio of the bands OH/C-H and OH/C=O which increases indicates the decrease of the polyester content. The existence and relative intensity of characteristic bands in the fingerprint region give evidence for different compositions of the networks as well as for the change that occurs in networks during the degradation.

Thermogravimetry was performed on several networks degraded for eight weeks or longer. After degradation, the networks with longer polyester chains show an earlier mass loss onset. All networks show an increase of the glass transition temperature with degradation time. The glass transition temperatures of samples which contain glycolide are lower than that of networks containing only lactide repeating units and stay lower during the whole period of degradation, but they exhibit a larger increase of T_g during degradation. Thus, network B after eight weeks of degradation shows an increase of 3°C , while network P, during the same time shows an increase of 9°C .

All the analyses and tests performed confirm the possibility of tailoring the properties, predisposition and tendency of the materials to hydrolyze depending on their composition and structure.

7 Experimental part

7.1 Materials

Poly(vinyl alcohol) (PVA) (Polysciences) with $M_w = 6000$ and a degree of hydrolysis of 80%, was dried in an oven at 80 °C until constant weight. D,L-Lactide (*rac*-lactide) (Sigma Aldrich) and glycolide (glycolide A) (Boehringer Ingelheim) dimers were recrystallized from dry ethylacetate. Ethylacetate (99.5%) (Merck) was refluxed over calcium hydroxide (95%) (Aldrich). Hydroquinone (Merck), 2-hydroxyethyl methacrylate (HEMA, 99%) (Fluka), stannous octoate (tin(II) bis (2-ethylhexanoate), SnOct_2 , 95%) (Sigma Chemicals), 4-(*N,N*-dimethylamino)pyridine (DMAP, 99%) (Aldrich), pyridine (99%) (Aldrich), dicyclohexyl carbodiimide (DCC, 99%) (Fluka), 2,2'-azobis(2-methylpropionitrile) (AIBN, 98%) (Aldrich), dimethyl sulfoxide (DMSO, 99%) (Fluka), diethyl ether (DEE, 99.9%) (Fluka) were used as received.

Deuterated dimethyl sulfoxide ($\text{DMSO-}d_6$, 99.9% D, 0.1 v/v% tetramethyl silane) and chloroform-*d* (CDCl_3 , 99.8% D, 0.1 v/v% tetramethyl silane) (Sigma Aldrich) were used for NMR measurements.

7.2 Synthesis

7.2.1 Ring opening polymerization

The synthesis of the (*rac*-lactide) and (*rac*-lactide-*co*-glycolide) oligomers of different composition and number of repeating units, was performed by ring opening polymerization with 2-hydroxyethyl methacrylate as the initiator.

The *rac*-lactide and glycolide dimers and the initiator, together with a small amount of hydroquinone (HQ) which was added in order to prevent premature free-radical polymerization of the methacrylate double bonds, were placed in glass flask in nitrogen atmosphere, stirred and left to melt at 110 °C. Then, SnOct_2 was added as a catalyst in a concentration of 0.005 mol/mol dimer. After 1 h of reacting, the resulting mixture was left to cool down to 50 °C.

The recipe with the masses of all reactants is given in Tab. 7-1.

The experiments are assigned with letters A-S which finally result in the respective hydrogels (see Tab. 3-1). Roman signs as index in Tab. 7-1 to 7-4 present the corresponding oligomers

on the first synthesis level (I), functionalized oligomers (II), grafted copolymers (III) and precipitated and diluted copolymers before crosslinking (IV).

Tab. 7-1 Reactants in the ring opening reactions.

Experiment	<i>rac</i> -Dilactide		Diglycolide		HEMA		Sn(Oct) ₂		HQ	
	mmol	g	mmol	g	mmol	g	mmol	mg	μmol	mg
A_I	76.0	10.94	-	-	9.5	1.23	0.38	162.0	4.37	0.54
B_I	57.0	8.21	-	-	14.3	1.85	0.29	121.5	6.55	0.80
C_I	25.3	3.65	-	-	12.7	1.65	0.08	36.0	3.89	0.48
D_I	16.9	2.43	-	-	8.5	1.09	0.13	54.0	5.83	0.72
E_I	12.7	3.65	-	-	12.7	1.65	0.13	54.0	5.83	0.72
F_I	57.0	8.21	19.0	2.20	9.5	1.23	0.38	162.0	4.37	0.54
G_I	38.0	5.47	12.7	1.47	6.3	0.82	0.25	108.0	2.91	0.36
H_I	38.0	5.47	12.7	1.47	6.3	0.82	0.25	108.0	2.91	0.36
I_I	57.0	8.21	19	2.20	19	2.47	0.38	162.0	8.74	1.08
J_I	28.5	4.10	9.5	1.10	9.5	1.23	0.19	81.0	4.37	0.54
K_I	28.5	4.10	9.5	1.10	9.5	1.23	0.19	81.0	4.37	0.54
L_I	28.5	4.10	9.5	1.10	19	2.47	0.19	81.0	8.74	1.08
M_I	12.7	1.82	4.2	0.49	8.5	1.09	0.08	36.0	3.89	0.48
N_I	21.3	3.08	7.1	0.83	14.3	1.85	0.14	60.7	6.55	0.80
O_I	38.0	5.47	38.0	4.41	9.5	1.23	0.38	162.0	4.37	0.54
P_I	57.0	8.21	57.0	6.612	28.5	3.71	0.57	243.0	13.11	1.63
Q_I	24.7	3.56	24.7	2.87	24.7	3.21	0.25	105.3	11.36	1.41
R_I	12.7	1.82	12.7	1.47	12.7	1.65	0.13	54.0	5.83	0.72
S_I	12.7	1.82	12.7	1.47	12.7	1.65	0.13	54.0	5.83	0.72

7.2.2 Transformation of hydroxy end groups into carboxylic end groups

Succinic anhydride, pyridine and DMAP (Tab. 7-2) were added to the mixture that was left to cool, from the previous step, and let to react for 18 h at 50 °C in order to transfer the hydroxy into carboxylic end groups. Unreacted succinic anhydride was removed by adding partially crosslinked poly(vinyl alcohol) film-pieces, at room temperature during 24 h. Afterwards, PVA pieces were removed from the system.

Tab. 7-2 Reactants in the transformation reaction of oligomers from hydroxy to carboxy end groups.

Experiment	Succinic anhydride		DMAP		Pyridine
	mmol	g	mmol	mg	mL
A_{II}	9.5	0.95	1.025	125	6.0
B_{II}	14.3	1.43	1.533	187	9.0
C_{II}	12.7	1.27	1.369	167	8.3
D_{II}	8.5	0.85	0.910	111	5.5
E_{II}	12.7	1.27	1.369	167	8.3
F_{II}	9.5	0.95	1.533	187	6.3
G_{II}	6.3	0.63	0.680	83	4.0
H_{II}	6.3	0.63	0.680	83	4.0
I_{II}	19.0	1.90	0.205	25	12.5
J_{II}	9.5	0.95	1.025	125	6.3
K_{II}	9.5	0.95	1.025	125	6.3
L_{II}	19.0	1.90	0.205	25	12.5
M_{II}	8.5	0.85	0.090	11	5.6
N_{II}	14.3	1.43	1.533	187	9.4
O_{II}	9.5	0.95	1.025	125	6.0
P_{II}	28.5	2.85	3.074	375	18.7
Q_{II}	24.7	2.47	2.664	325	16.3
R_{II}	12.7	1.27	1.369	167	8.3
S_{II}	12.7	1.27	1.369	167	8.3

7.2.3 Grafting of poly(*rac*-lactide) or poly(*rac*-lactide-*co*-glycolide) chains onto the poly(vinyl alcohol) backbone

The grafting of *rac*-lactide or *rac*-lactide-*co*-glycolide oligomers (index II) with carboxylic acid end groups onto the PVA backbone through reacting of hydroxy groups was performed with the assistance of the commonly used coupling reagent dicyclohexyl carbodiimide (DCC) [66]. The reaction was conducted at room temperature for 24 h. The masses of reactants used, which were added directly to the product of the former synthesis step, are given in Tab. 7-3.

Tab. 7-3 Reactants in the grafting reaction of *rac*-lactide or *rac*-lactide-*co*-glycolide oligomers onto the PVA backbone.

Experiment	DCC		PVA		Solution of PVA (15 wt%) in DMSO
	mmol	g	mmol	g	g
A_{III}	14.3	2.93	79.2	3.48	23.22
B_{III}	21.4	4.40	118.7	5.23	34.83
C_{III}	19.0	3.91	79.2	3.48	23.22
D_{III}	12.7	2.61	70.4	3.10	20.64
E_{III}	19.0	3.91	158.3	6.97	46.44
F_{III}	14.3	2.93	59.3	2.61	17.42
G_{III}	9.5	1.96	52.8	2.32	15.47
H_{III}	9.5	1.96	79.0	3.48	23.25
I_{III}	28.5	5.87	118.9	5.23	34.83
J_{III}	28.5	5.87	79.2	3.48	23.22
K_{III}	14.3	2.93	118.7	5.23	34.83
L_{III}	28.5	5.87	118.7	5.23	34.83
M_{III}	12.7	2.61	70.4	3.10	20.64
N_{III}	21.4	4.40	178.1	7.84	52.25
O_{III}	14.3	2.93	79.2	3.48	23.22
P_{III}	42.7	8.81	237.5	10.45	69.67
Q_{III}	37.0	7.63	154.4	6.79	45.28
R_{III}	19.0	3.91	105.5	4.64	30.96
S_{III}	19.0	3.91	158.3	6.97	46.44

The resulting mixture was filtered in order to remove the formed dicyclohexyl urea and precipitated into cold DEE.

7.2.4 Crosslinking of hydrogels

The obtained precipitate was dissolved in DMSO, keeping the ratio precipitate/DMSO 50/50 wt/wt. The additional dissolution was necessary in order to prevent physical crosslinking which might take place in a concentrated solution of the grafted copolymer in DMSO ^[65]. Remaining DEE was removed using vacuum. 2,2'-Azobis(2-methylpropionitrile) was added as initiator, 0.167 wt% relative to the precipitate in DMSO solution (Tab. 7-4), in order to crosslink the hydrogels via reaction of the methacrylate double bonds. The mixture was cast between two glass slides and placed in an oven at 50 °C for 24 h. As a result, crosslinked PVA-g-poly(*rac*-lactide) or PVA-g-poly(*rac*-lactide-*co*-glycolide) hydrogels (A-S, Tab. 3-1) in sheet form were obtained.

Tab. 7-4 Reactants in the crosslinking reaction of grafted copolymers.

Experiment	Mass of wet precipitate (1)	Mass of added DMSO (2)	Mass of (1)+(2) after removal of DEE (3)	Mass of AIBN, 0.167 wt% of (3)
	g	g	g	mg
A_{IV}	11.2	11.3	16.92	28.2
B_{IV}	14.6	14.6	24.74	41.2
C_{IV}	7.8	7.8	13.29	22.2
D_{IV}	6.9	7.0	10.49	17.5
E_{IV}	10.5	10.0	16.24	27.1
F_{IV}	9.9	10.0	17.22	28.7
G_{III}	9.4	9.0	16.93	28.2
H_{IV}	16.5	17.0	30.02	50.0
I_{IV}	12.7	12.7	21.58	36.0
J_{IV}	13.6	13.5	23.11	38.6
K_{IV}	10.5	10.5	18.36	30.7
L_{IV}	11.3	11.5	17.18	28.6
M_{IV}	8.7	8.7	14.22	23.7
N_{IV}	18.0	18.0	30.97	51.7
O_{IV}	14.0	14.0	24.04	40.1
P_{IV}	24.7	24.7	42.28	70.6
Q_{IV}	14.3	14.3	24.80	41.3
R_{IV}	13.5	13.0	22.30	37.2
S_{IV}	16.5	16.5	29.05	48.5

7.3 Characterization methods

7.3.1 Nuclear magnetic resonance (NMR)

¹H-NMR spectra were recorded on the Inova 400 or Mercury 300 spectrometer (400 MHz or 300MHz, Varian Associates Nuclear Magnetic Resonance Instruments) in CDCl₃ or DMSO-*d*₆ at room temperature. Tetramethylsilane was used as an internal standard. The mode of the composition calculation from the obtained spectra is given in Chapter 4.1.

7.3.2 Infrared spectroscopy (IR)

IR spectra are recorded on a NEXUS FT-IR spectrometer using the photoacoustic method (FTIR-PAS). For each sample, scans were recorded between 4000 and 400 cm⁻¹ with a resolution of 8 cm⁻¹.

7.3.3 Thermogravimetry (TGA)

TGA measurements were performed on a Netzsch TG 209 instrument in nitrogen atmosphere. In order to monitor the weight loss of the sample as a function of temperature the samples with 5-10 mg of weight were heated with a rate of $10\text{ }^{\circ}\text{C min}^{-1}$. Thermograms were taken in the range of $30\text{ }^{\circ}\text{C}$ to $600\text{ }^{\circ}\text{C}$.

7.3.4 Differential scanning calorimetry (DSC)

DSC measurements were carried out on a Netzsch DSC 204 calorimeter. The temperature range was $20\text{ }^{\circ}\text{C}$ to $150\text{ }^{\circ}\text{C}$. The sample was contained in a small aluminum dish with lid. One empty dish with lid was used as a reference. A nitrogen flow of 20 mL/min was used for washing the cells. The heating and cooling rates were $10\text{ }^{\circ}\text{C min}^{-1}$. The sample chamber is cooled with liquid nitrogen. The samples with 5-10 mg of weight were first heated to $150\text{ }^{\circ}\text{C}$, kept for 5 min at that temperature and cooled to $20\text{ }^{\circ}\text{C}$, kept 5 min at that temperature and heated to $150\text{ }^{\circ}\text{C}$. The phase transitions were evaluated from this second heating run. The glass transition temperature was calculated as halfway value between onset and end point of the glass transition temperature interval. The onset value was taken as the intersection of the extrapolated tangent at the first limit and the extrapolated tangent at the inflection point. The end point was taken as the intersection of the extrapolated tangent at the second limit and the extrapolated tangent at the inflection point.

7.3.5 Tensile strength measurements

The tensile tests were performed with the low-load horizontal tensile test machine Minimat 2000 (Rheometric Scientific). The strain rate was 10 mm/min . The tests for each measuring point are performed on five samples.

7.3.6 Contact angle measurements

The hydrophobicity/hydrophilicity balance of a solid surface is usually expressed in terms of wettability which can be quantified by contact angle measurements. The contact angle provides information on the relative hydrophobicity of the uppermost surface layer of a solid.

In order to study the highly hydrated polymers, the *captive bubble* contact angle technique was used. An air bubble, released from a syringe, was introduced into a liquid reservoir beneath a submerged sample and traveled upward onto the hydrated hydrogel surface where it became trapped, or “captive”. A hydrophobic material would cause the bubble to spread over

the sample surface since water is excluded from the bubble-polymer interface. A hydrophilic surface, on the other hand, would result in a sphere-like bubble. The smaller the contact angle is, the greater is the hydrophilicity of the polymer surface.

For measuring purpose the swollen hydrogels were cut into pieces of ca. 2-3 cm² and fixed on microscope slides. Thereafter, they were introduced into a liquid reservoir filled with water, leaning onto two spaced teflon supports above the U-shaped needle of the syringe.

7.3.7 Biocompatibility test

The biocompatibility test was performed on the hydrogel type P. *In vitro* cell culture experiments were carried out in order to evaluate the cellular interaction of the hydrogel surface with primary human dermal fibroblasts (hF). The isolation procedure was initiated within 3 h following surgery according to methods described by van den Bogaerd ^[164]. Individual skin biopsy from a 39 year old female patient was harvested and split into the papillary dermal layer (with the help of a dermatome) and the subcutaneous adipose tissue layer (with surgical scissors). After removing the epidermis from split skin, upon 20 min incubation in a 0.25% (w/v) dispase II-phosphate-buffered saline (PBS) solution (Roche Diagnostics, FRG), a thin papillary dermis was obtained. The obtained papillary dermis and adipose tissue were incubated for 2 h at 37 °C in PBS solution containing 0.25% (w/v) dispase II (Roche Diagnostics) and collagenase type II (GIBCO-BRL, UK). After digestion, cells were washed, collected, and cultured in a fibroblast culture medium. Dulbecco's modified Eagle's medium (DMEM) was used supplemented with L-glutamine, 10 vol% fetal calf serum (FCS), 1 U/mol penicillin, and 1 mg/mol streptomycin (PAA, FRG). When the cells reached 70-80% confluence (approximately 6-8 days), they were split and subcultured until passage 3. The cultures were maintained at 37 °C in humidified atmosphere containing 5% CO₂.

The polymer disc specimens were sterilized by immersing them into 70 vol% ethanol for 2 h and then rinsed with distilled and sterile water. To measure the cellular interactions of different polymer materials, cells suspended in DMEM were dropped onto each disc specimen. Tissue-culture grade polystyrene (TCPS) from Greiner Bio-One GmbH (Frickhausen, FRG) served as control substrates. HF's (4×10^4 cells ml⁻¹) of the fourth passage were seeded onto each material and cultured at 37 °C. On day 4, the morphology was investigated by inspection under a light microscope (LM). Light microscopy was performed using an Axioplan2 Imaging microscope (Zeiss, FRG) combined with a HAL 100 lamp (Zeiss, FRG) and with an appropriate set of objectives. The samples were treated with 4%

formaldehyde in PBS (pH 7.4) and subsequently stained with Mayers' haemalaun at room temperature to study the cells' morphology.

7.3.8 Hydrolytical degradation experiment

Samples for degradation experiments were prepared either by punch cutting into circular disks of 15 mm diameter, or they were cut into ribbons of ca. 8 mm width and 30-50 mm length. The thickness of samples was around 0.3 mm. All dimensions were measured in swollen state. The discs were placed in glass vials of 20 mol volume. These vials were filled with 10 mol of pH 7.4 phosphate buffer solution (PBS). In order to prevent the growth of microorganisms, sodium azide was added. Samples in ribbon shape, used for mechanical tests, were placed into poly(propylene) centrifugation tubes of 50 mol volume and filled with 20 mol of PBS. The pH values were measured after four to seven days and as the value sank below 7.2, the buffer solution was exchanged. Samples were degraded at room temperature. Sample P was degraded additionally under the following conditions: PBS of pH 7.4 in a mechanical stirring incubator with 40 turns per min at 37 ± 0.1 °C, for comparison reason. During the degradation, after certain periods of time, samples were taken (3 discs at each point).

7.3.9 Weight loss of hydrogels during degradation

The weight loss of disc samples was determined during hydrolytical degradation. The relative weight (m_{rel}) presents the ratio between the weight of the dry sample after degradation (m_d) and the weight of the dry sample before the degradation (m_0) (Eq. 7-1).

$$m_{rel} = \frac{m_d}{m_0} \quad (7-1)$$

7.3.10 Gravimetrical determination of the degree of swelling

In cases where the density of the network could not be determined, as in the degradation experiments, the weight related degree of swelling S was determined as the ratio between the weight of the swollen disc m_s and the weight of the disc in the dry state m_d (Eq. 7-2).

$$S = \frac{m_s}{m_d} \quad (7-2)$$

7.3.11 Scanning electron microscopy (SEM)

SEM images were taken using a scanning electron microscope (Cambridge S360, Leica), operated at an accelerating voltage of 15 kV and different magnification (x 100, x 250, x 300, x 573, x 5000). The cross-sectional samples were prepared by fracturing the scaffolds after being frozen in liquid nitrogen. The films of samples were mounted on the top surface of metal studs. Double sided tape was used to keep the film attached. Before morphology observations, the samples were coated in argon atmosphere with gold using a sputter coater (S 150B Sputter Coater, Edwards). The surface and cross-section morphologies of different types of network before and during hydrolytical degradation were observed with the scanning electron microscope.

8 Literature

1. Williams DF. Definitions in Biomaterials. Proceedings of a Consensus Conference of the European Society for Biomaterials, Chester, England, March 3-5 1986.
2. Williams DF, Black J, Doherty PJ. Biomaterial-Tissue Interfaces. Second Consensus Conference on Definitions in Biomaterials, Chester, England, September 7-8 1991.
3. Rattner BD, Hoffman AS, Schoen FJ, Lemons JE. Biomaterials Science. An Introduction to Materials in Medicine. New York: Academic Press; 1996.
4. Cheng M, Deng J, Jang F, Gong Y, Zhao N, Zhang X. Biomaterials 2003;24:2871-2880.
5. Hoffman AS. Macromolecules. Oxford: Pergamon Press; 1982. p. 321.
6. Yamaoka T, Kimura Y. Biodegradable copolymers comprising poly(L- lactide acid). The Polymer Materials Encyclopedia. CRC Press Inc; 1996.
7. Kopeček J, Ubrich K. Prog Polym Sci 1983;9:1-58.
8. Bizzarri R, Chellini F, Solaro R, Chiellini E, Cammas-Marion S, Guerin P. Macromolecules 2002;35:1215-1223.
9. Jacoby M. Sci Techno 2001;79:30-35.
10. Singh S, Woerly S, McLaughlin BJ. Biomaterials 2001;22:3337-3343.
11. Serrano MC, Pagani R, Vallet-Regí M, Peña J, Rámila A, Izquierdo I, Portolés A. Biomaterials 2004;25:5603-5611.
12. Burdick JA, Frankel D, Dernel WS, Anseth KS. Biomaterials 2003;24:1613-1620.
13. Hubbell JA. Curr Opin Biotech 1999;10:123-129.
14. Hsu S-H, Tang C-M, Lin C-C. Biomaterials 2004;25:5593-5601.
15. Koyano T, Minoura N, Nagura M, Kobayashi K. J Biomed Mater Res 1998;39:486-490.
16. Lu L, Nyalakonda K, Kam L, Bizios R, Göpferich A, Mikos AG. Biomaterials 2001;22:291-297.
17. Cai K, Yao K, Lin S, Yang Z, Li X, Xie H, Qing T, Gao L. Biomaterials 2002;23:1153-1160.
18. Giordano GG, Thomson RC, Ishaug SL, Mikos AG, Cumber S, Garcia CA, Lahiri-Munir D. Retinal J Biomed Mater Res 1997;34:87-93.
19. Hern DL, Hubbell JA. J Biomed Mater Res 1998;39:266-276.
20. Drumheller PD, Hubbell JA. Anal Biochem 1994;222:380-388.
21. Yamada KM. J Biol Chem 1991;266:12809-12812.
22. Evans GRD, Brandt K, Katz S, Chauvin P, Otto L, Bogle M, Wang B, Meszlenyi RK, Lu L, Mikos AG, Patrick CW. Biomaterials 2002;23:841-848.
23. Lu L, Yaszemski MJ, Mikos AG. Biomaterials 2001;22:3345-3355.
24. West JL, Hubbell JA. Macromolecules 1999;32:241-244.
25. Mann BK, Gobin AS, Tsai AT, Schmedlen RH, West JL. Biomaterials 2001;22:3045-3051.
26. Shin H, Jo S, Mikos AG. Biomaterials 2003;24:4353-4364.
27. Masters KS, Shah DN, Leinwand LA, Anseth KS. Biomaterials 2005;26:2517-2525.
28. Wichterle O and Lim D. Nature 1960;185:117-118.
29. Wong HM, Mooney DJ. In: Atala A, Mooney D editors. Synthetic Biodegradable Polymer Scaffolds. Boston: Birkhauser; 1997.
30. Suggs LJ, Mikos AG. Synthetic biodegradable polymers for medical applications. In: Mark JE editor. Physical Properties of Polymers Handbook. New York: AIP Press; 1996. p. 615-624.
31. Amecke B, Bendix D, Entenmann G. Synthetic Resorbable Polymers Based on Glycolide, Lactides and Similar Monomers. In: Wiese DL editor. Encyclopedic Handbook of Biomaterials and Bioengineering. Boston: Marcel Dekker Inc; 1995. p.977-1007.
32. Chu CC. Recent advancements in suture fibres for wound closure. ACS Symp. Ser 1991;475:167-211.
33. Benicewicz BC, Hopper PK. J Bioact Compat Polymers 1990;5:453-472.
34. Benicewicz BC, Hopper PK. J Bioact Compat Polymers 1991;6:64-94.
35. Lostocco MR, Huang SJ. The Synthesis and Characterization of Polyesters Derived from L-Lactide

- and Variably-Sized Poly(Caprolactone.) In: Swift G, Carraher CE, Bowman C. New York: Plenum Pub Corp Published; 1997. p.45-61.
36. Çatiker E, Gümüşderelioğlu M, Güner A. Polym Inter 2000;49:728-734.
 37. Li SM, Rashkov I, Espartero JL, Manolova N, Vert M. Macromolecules 1996;29:57-62.
 38. Joziassse CAP, Veenstra H, Topp MDC, Grijpma DW, Pennings AJ. Polymer 1998;39:467-473.
 39. Kim SH, Kim Y. Macromol Symp 1999;144:277-287.
 40. Frazza EJ, Schmitt EE. J Biomed Mater Res Symposium 1971;1:43-58.
 41. Farina SM, Mohammadi-Rovshaden J, Sarbolouki MN. J Appl Polym Sci 1999;73:633-637.
 42. Breitenbach A, Kissel T. Polymer 1998;39:3261-3271.
 43. Degée P, Dubois P, Jérôme R, Jacobsen S, and Fritz HG. Macromol Symp 1999;144:289-302.
 44. Dobrzynski P, J. Kasperczyk J, Bero M. Macromolecules 1999;32:4735-4737.
 45. Stridsberg K, M. Ryner M, Albertsso AC. Macromolecules 2000;33:2862-2869.
 46. Bero M, Czapla B, Dobrzynski P, Kasperczyk J. Macromol Chem. Phys 1999;200:911-916.
 47. Lee S-H, Kim S-H, Han Y-K, Kim YH. J Polym Sci Part A-Polym Chem 2001;39:973-985.
 48. Breitenbach A, Li YX, Kissel T. J Control Release 2000;64:167-178.
 49. Pistel KF, Breitenbach A, Zange-Volland R, Kissel T. J Control Release 2001;73:7-20.
 50. Cohn D, Lando G. Biomaterials 2004;25:5875-5884.
 51. Hile DD, Pishko MV. Macromol Rapid Commun 1999;20:511-514.
 52. Wu XS. Encyclopedic handbook of biomaterials and bioengineering. New York: Marcel Dekker;1995. p.1015.
 53. Tice TR, Tabibi ES. Treatise on controlled drug delivery: fundamentals optimization, applications. In: A Kydonieus editor. New York: Marcel Dekker; 1992. p. 315.
 54. Mikos AG, Bao Y, Cima LG, Ingber DE, Vacanti JP, Langer R. J Biomed Mater Res 1993;27:183-189.
 55. Arvanitoyannis I, Nakayama A, Psomiadou E, Yamamoto N. Polymer 1995;36:2947-2956.
 56. Pitt CG, Gu ZW, Ingram P, Hendren RW. J Polym Sci A-Polym Chem 1987;25:955-966.
 57. Li Y, Nothnagel J, Kissel T. Polymer 1997;38:6197-6206.
 58. Breitenbach A, Pistel KF, Kissel T. Polymer 2000; 41:4781-4792.
 59. Breitenbach A, Mohr D, Kissel T. J Control Release 2000;63:53-68.
 60. Carlotti SJ, Giani-Beaune O, Schué F. J Appl Polym Sci 2001;80:142-147.
 61. Kissel T, Jung T, Kamm W, Breitenbach A. Macromol Symp 2001;172:113-125.
 62. Breitenbach A, Jung T, Kamm W, Kissel T. Polym Adv Technol 2002;13:938-950.
 63. Arvanitoyannis I, Nakayama A, Psomiadou E, Yamamoto N. Polymer 1996;37:651-660.
 64. Rashkov I, Manolova N, Li SM, Espartero JL, Vert M. Macromolecules 1996;29:50-56.
 65. Nuttelman CR, Henry SM, Anseth KS. Biomaterials 2002;23:3617-3626.
 66. Van Dijk-Wolthuis WNE, Tsang SKY, Kettenes-van den Bosch JJ, Hennink WE. Polymer 1997;38:6235-6242.
 67. Gimenez V, Reina JA, Mantecon A, Cadiz V. Polymer 1999;40:2759-2767.
 68. Gilding DK, Reed AM. Polymer 1979;20:1459-1464.
 69. Pitt CG, Gratzl MM, Kimmel GL, Surles J, Schindler A. Biomaterials 1981;2:215-220.
 70. Höcker H, Keul H. Macromol Symp 2001;174:231-240.
 71. Feng Y, Klee D, Höcker H. J Appl Polym Sci 2002;86:2916-2919.
 72. Han K, Hubbell JA. Macromolecules 1996;29:5233-5235.
 73. Hu DS-G, Liu H-J. J Appl Polym Sci 1994;51:473-482.
 74. Kim K, Yu M, Zong X, Chiu J, Fang D, Seo Y-S, Hsiao BS, Chu B, Hadjiargyrou M. Biomaterials 2003;24:4977-4985.
 75. Chabot F, Vert M. Polym Int 1994;33:37-41.
 76. Li S, Vert M. Macromolecules 1994;27:3107-3110.
 77. Frazza EJ, Schmitt EE. J Biomed Mater Res Symposium 1971;1:43-58.

78. US Patent 1,332.505, assignet to Ethicon Inc; New Jersey, 1973.
79. Storey RF, Warren SC, Allison CJ, Puckett AD. *Polymer* 1997;38:6295-6301
80. Kister G, Cassanas G, Bergounhon M, Hoarau D, Vert M. *Polymer* 2000;41:925-932.
81. De jong SJ, Arieas ER, Rijkers DTS, van Nostrum CF, Kettenes-van den Bosch JJ, Hennink WE. *Polymer* 2001;42:2795-2802.
82. Lu L, Garcia CA, Mikos G. *J Biomed Mater Res* 1999;46:236-244.
83. Peppas AN. *Hydrogels in medicine and pharmacy*. Boca Raton: CRC Press; 1987.
84. Hoffman AS. *Adv Drug Deliv Rev* 2002;54:3-12.
85. Lee KY, Mooney DJ. *Chem Rev* 2001;101:1869-1879.
86. Nuttelman CR, Mortisen DJ, Henry SM, Anseth KS. *J Biomed Mater Res* 2001;57:217-223.
87. Hoffman AS, Stayton PS. *Macromol Symp* 2004;207:139-151.
88. Mason MN, Metters AT, Bowman CN, Anseth KS. *Macromolecules* 2001;34:4630-4635.
89. Elliot JE, Bowman CN. *Macromolecules* 2001;34:4642-4649.
90. Bruining MJ, Blaauwgeers HGT, Pels E, Nuijts RMMA, Koole LH. *Biomaterials* 2000;21:595-604.
91. Cruise GM, Scharp DS, Hubbell JA. *Biomaterials* 1998;19:1287-1294.
92. Alsberg E, Anderson KW, Albeiruti A, Franceschi RT, Mooney DJ. *J Dent Res* 2001;80:2025-2029.
93. Schmedlen RH, Masters KS, West JL. *Biomaterials* 2002;23:4325-4332.
94. Burdick JA, Anseth KS. *Biomaterials* 2002;23:4315-4323.
95. Stammen JA, Williams S, Ku DN, Guldborg RE. *Biomaterials* 2001;22:799-806.
96. Kobayashi M, Toguchida J, Oka M. *Knee* 2003;10:47-51.
97. Peppas NA, Merrill EW. *J Biomed Mater Res* 1977;11:423-434.
98. Corkhill PH, Trevett AS, Tighe BJ. *Proc Inst Mech Engrs* 1990;204:147-155.
99. Zheng-Qiu G, Jiu-Mei X, Xiang-Hong Z. *Biomed Mater Engng* 1998;8:75-81.
100. Anseth KS, Bowman CN, Brannon-Peppas L. *Biomaterials* 1996;17:1647-1657.
101. Middleton JC, Tipton AJ. *Biomaterials* 2000;21:2335-2346.
102. Kricheldorf HR, Lee S-R. *Polymer* 1995;36:2995-3003.
103. Leenslag JW, Pennings AJ. *Macromol Chem* 1987;188:1809-1814.
104. Vert M, Schwach G, Engel R, Coudane J. *J Control Release* 1998;53:85-92.
105. Dobrzynski P, Kasperczyk J, Janczek H, Bero M. *Macromolecules*; 2001;34:5090-5098.
106. Schwach G, Coudane J, Engel R, Vert M. *Biomaterials* 2002;23:993-1002.
107. Dubois P, Jacobs C, Jérôme R, Teyssé P. *Macromolecules* 1991;24:2266-2270.
108. Kreiser-Saunders I, Kricheldorf HR. *Macromol Chem Phys* 1988;199:1081-1087.
109. Bero M, Dobrzynski P, Kasperczyk J. *Polymer Bulletin* 1999;42:131-139.
110. Lowe CE, (Du Pont) U.S. Pat. 2668162. 1954.
111. Tonelli AE, Flory PJ. *Macromolecules* 1969;2:225-227.
112. F. Chabot, M. Vert, M. Chapelle, S. Granger. *Polymer* 1983;24:53-59.
113. Dittrich W, Schulz RC. *Angew Makromol Chem* 1971;15:109-126.
114. Lillie E, Schulz RC. *Makromol Chem* 1975;176:1901-1906.
115. Kricheldorf HR, Sumbel M. *Eur Polym J* 1989;25:585-591.
116. Kricheldorf HR, *Polym Bull (Berlin)* 1985;14:497-502.
117. Schindler A, Jeffcoat R, Kimmel GL, Pitt CG, Wall ME, Zweidinger R. In Pearce EM, Schaefgen JR, Eds. *Contemporary Topics in Polymer Science*. New York: Plenum press; 1977. p.251.
118. Deasy PB, Finan MP, Meegan MJ. *J Microencapsulation* 1989;6:369-378.
119. Van Dijk JAPP, Smit JAM, Kohn FE, Feijen J. *J Polym Sci A-Polym Chem* 1983;21:197-208.
120. Grijpma DW, Nijenhuis AJ, Pennings AJ. *Polymer* 1990;31:2201-2206.
121. Andini S, Ferrara L, Maglio G, Palumbo R. *Macromol Chem Rapid Commun* 1988;9:119-124.
122. Lee S-H, Kim S-H, Han Y-K, Kim YH. *J Polym Sci Part A-Polym Chem* 2001;39:973-985.

123. Kohn FE, Van Ommen JG, J. Feijen J. *Eur Polym J* 1983;19:1081-1088.
124. Kricheldorf HR, Berl M, Scharnagl N. *Macromolecules* 1988;21:286-293.
125. Jedlinski Z, Walach W. *Makromol Chem* 1991;192:2051-2057.
126. Kurocok P, Panczek J, Franek J, Jedlinski Z. *Macromolecules* 1992;25:2285-2289.
127. Degée P, Dubois P, Jérôme R. *Macromol Symp* 1997;123:67-84.
128. Kricheldorf HR, Keiser-Saunders I, Boettcher C. *Polymer* 1995;36:1253-1259.
129. Kowalski AK, Duda A, Penczek S. *Macromol Rapid Commun* 1998;19:567-572.
130. Reyner M, Stridsberg K, Albertsson A-C, Von Schenck H, Svensson M. *Macromolecules* 2001;34:3877-3881.
131. Skoog DA, Holler FJ, Nieman TA. *Principles of Instrumental Analysis*, 5th Ed, London: Sanders College Publishers;1998. p. 411.
132. Çatiker E, Gümüşderelioglu M, Güner A. *Polym Inter* 2000;49:728-734.
133. Tosh A, Saikia CN, Dass NN. *J Appl Polym Sci* 1999;74:663-669.
134. Gilman JW, VanderHart DL, Kashiwagi T. In: *Fire and Polymers II: Materials and Test for Hazard Prevention*. Washington DC: ACS; 1994. p. 161.
135. Chatterjee PK. *J Polym Sci* 1968;6:3217-3233.
136. El-Kalyoubi SF, El-Shinnawy NA. *J Appl Polym Sci* 1985;30:4793-4799.
137. Vargas RA, Zapata VH, Matallana BE, Vargas MA. *Electrochim Acta* 2001;46:1699-1702.
138. Sudhamani SR, Prasad MS, Udaya Sankar K. *Food Hydrocolloids* 2003;17:245-250.
139. Ullmann's Encyclopedia of Industrial Chemistry. Online. Wiley-VCH Verlag GmbH & Co; 2002. p.377.
140. Sakai W, Kinoshita M, Nagata M, Tsutsumi N. *J Polym Sci A-Polym Chem* 2001;39:706-714.
142. Santoveña A, Álvarez-Lorenzo C, Concheiro A, Llabrés M, Fariña JB. *Biomaterials* 2004;25:925-931.
143. Altheld A. Dissertation, RWTH-Aachen 2003.
144. Odian G. *Principles of Polymerization*, 3rd Ed, New York: J. Wiley; 1991. p.34.
145. Janović Z. *Polimerizacije i polimeri*. Zagreb:HDKI-Kemija u industriji; 1997. p. 111.
146. Sander EA, Alb AM, Nauman EA, Reed WF, Dee KC. *J Biomed Mater Res* 2004;70A:506-513.
147. Kranz H, Ubrich N, Maincent P, Bodmeier R. *J Pharm Sci* 2000;89:1558-1566.
148. Kasuga T, Ota Y, Nogami M, Abe Y. *Biomaterials* 2001;22:19-23.
149. Chen C-C, Chueh J-Y, Tseng H, Huang H-M, Lee S-Y. *Biomaterials* 2003;24:1167-1173.
150. Tsuji H, Ikada Y. *Polymer* 1999;40:6699-6708.
151. Srinivasa PC, Ramesh MN, Kumar KR, Tharanathan RN. *Polymer* 2003;53:431-438.
152. Khang G, Choe J-H, Rhee JM, Lee HB. *J Appl Polym Sci* 2002;85:1253-1262.
153. Cai Q, Wan Y, Bei J, Wang S. *Biomaterials* 2003;24:3555-3562.
154. Webb K, Hlady V, Trosco PA. *J Biomed Mater Res* 1998;41:422-430.
155. Yang J, Bei JZ, Wang SG. *Polym Adv Technol* 2002;13:220-226.
156. Oh SH, Kang SG, Kim ES, Cho SH, Lee JH. *Biomaterials* 2003;24:4011-4021.
157. Davis KA, Burdick JA, Anseth KS. *Biomaterials* 2003;24:2485-2495.
158. Shih C. *Pharm Res* 1995;12:2063-2070.
159. Belbella A, Vauthier C, Fessei H, Devissaguet J-P, Puisieux F. *Int J Pharm* 1996;129:95-102.
160. Fischer EW, Sterzel HJ, Wegner G. *Kolloid Z Z Polym* 1973;251:980-990.
161. Chen C-C, Chueh J-Y, Tseng H, Huang H-M, Lee S-Y. *Biomaterials* 2003;24:1167-1173.
162. Williams DF. *J Mater Sci* 1987;22:3421-3445.
163. Woodward SC, Brewer PS, Moatamed F, Pitt CG. *J Biomed Mater Res* 1985;19:437-444.
164. Van Den Bogaerdt AJ, Van Zuijlen PP, Van Galen M, Lamme EN, Middelkoop E. *Arch Dermatol Res* 2002;294:135-142.
165. Kreitz MR, Domm JA, Mathiowitz E. *Biomaterials* 1997;18:1645-1651.
166. Jayasekara R, Harding I, Bowater I, Christie GBY, Lonergan GT. *Polym Testing* 2004;23:17-27.
167. Feng Y, Klee D, Höcker H. *Macromol Chem Phys* 2002;203:819-824.

9 Appendix

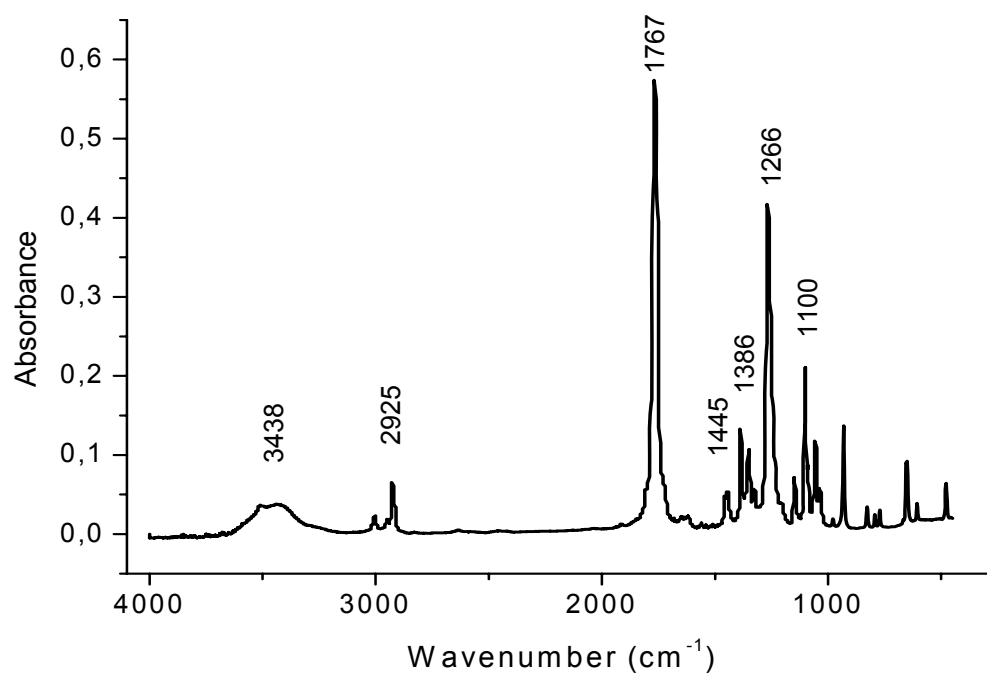


Fig. 9-1 Absorption IR spectrum of *rac*-lactide dimer. The group frequencies are given in Tab. 9-1.

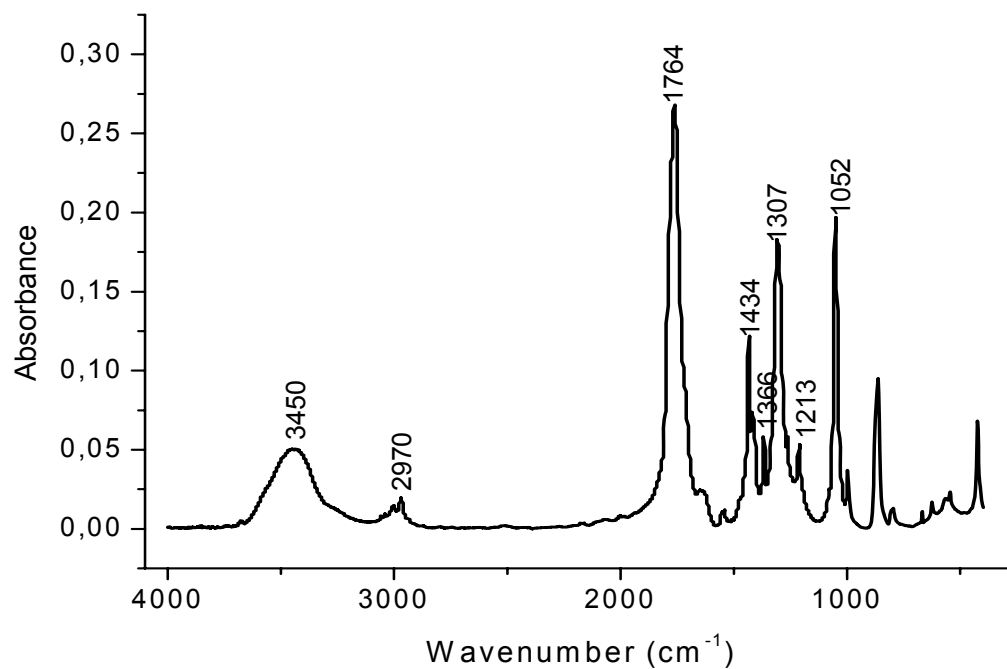


Fig. 9-2 Absorption IR spectrum of glycolide dimer. The group frequencies are given in Tab. 9-1.

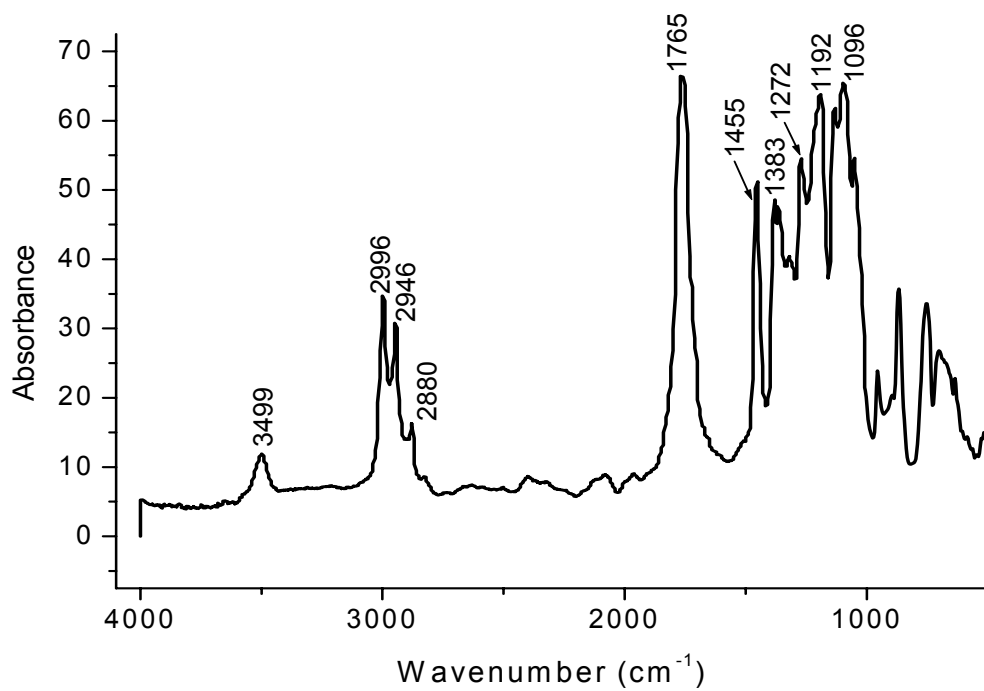


Fig. 9-3 Absorption IR spectrum of poly(D,L-lactide). The group frequencies are given in Tab. 9-1.

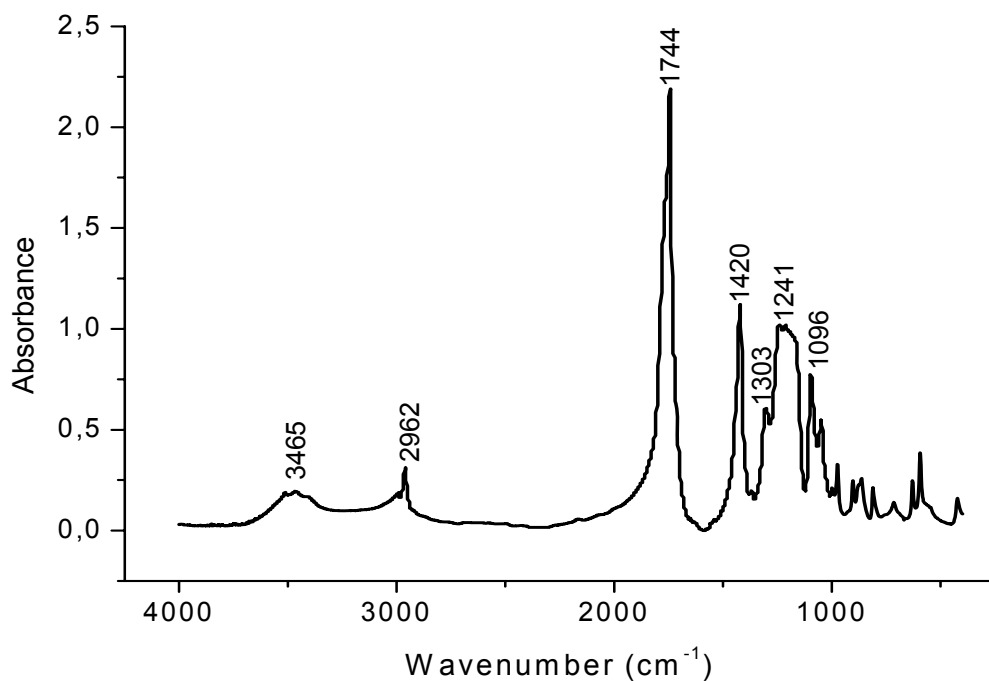


Fig. 9-4 Absorption IR spectrum of polyglycolide. The group frequencies are given in Tab. 9-1.

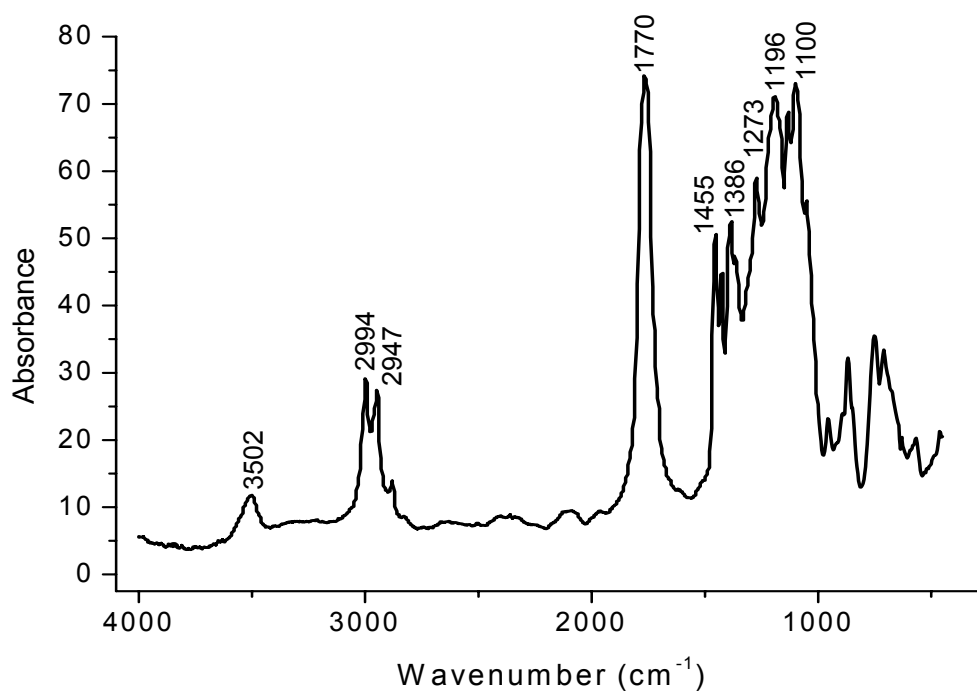


Fig. 9-5 Absorption IR spectrum of poly(lactide-*co*-glycolide) copolymer (lactide : glycolide 75 : 25 mol% / mol%). The group frequencies are given in Tab. 9-1.

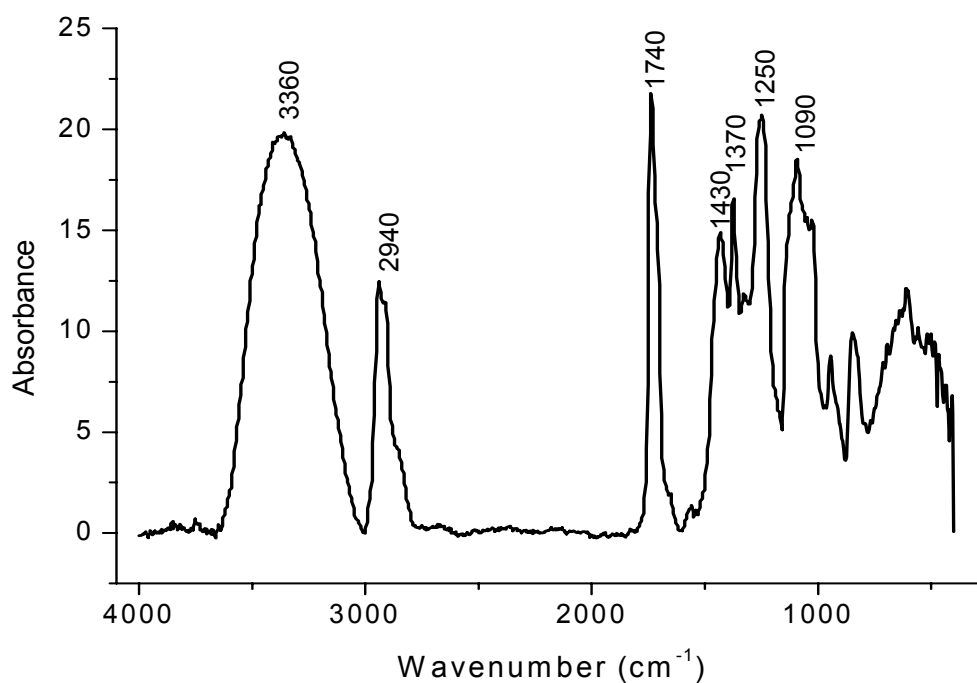


Fig. 9-6 Absorption IR spectrum of poly(vinyl alcohol) 6 ($M_w=6\,000$, 80% hydrolyzed). The group frequencies are given in Tab. 9-1.

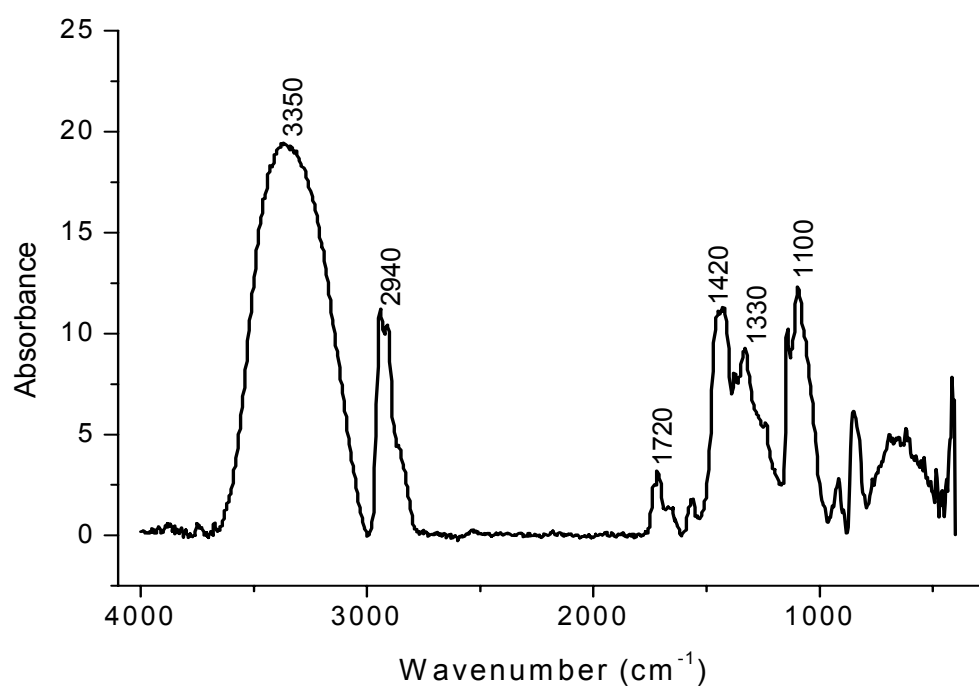


Fig. 9-7 Absorption IR spectrum of poly(vinyl alcohol) 16 ($M_w=16\ 000$, 98% hydrolyzed).

Tab. 9-1 Characteristic peaks of *rac*-lactide and glycolide dimers, their homopolymers, copolymer and poly(vinyl alcohol).

Bond	Frequency range, cm^{-1}	PVA	PLGA	PLA	PGA	<i>rac</i> -dilactide	diglycolide
O-H	3200-3600	3360	3502	3499	3465	3438	3450
C-H	2850-2970	2940/ 2860	2994/ 2947	2996/ 2946/ 2880	2962	2925	2970
C=O	1690-1760	1740	1770	1765	1744	1767	1764
C-H	1340-1470	1430	1455/ 1426	1455	1420	1445	1434/ 1417
C-O	1050-1300	1370	1386	1383/ 1365	1303	1386/ 1352	1366/ 1307
	1260	1250	1273	1272	1241	1266	1264/
	1190		1196	1192			1213
	1150		1136	1134		1148	
	1100	1090	1100	1096	1096	1100	
	1050			1053	1049	1057	1052

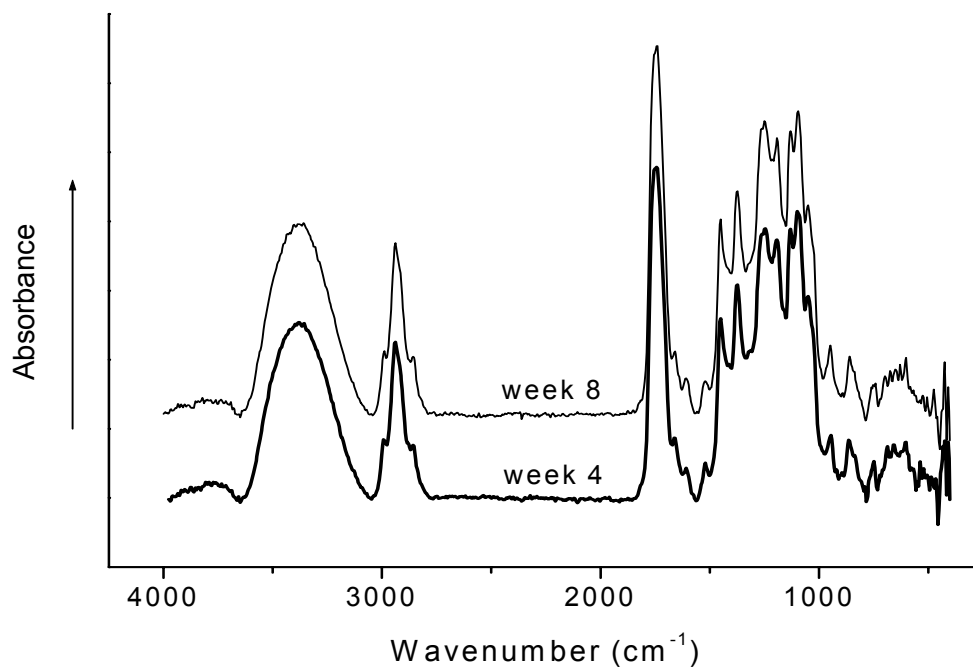


Fig. 9-8 Absorption IR spectra of network type B after 4 and 8 weeks of hydrolytical degradation in PBS (pH 7.4) at RT.

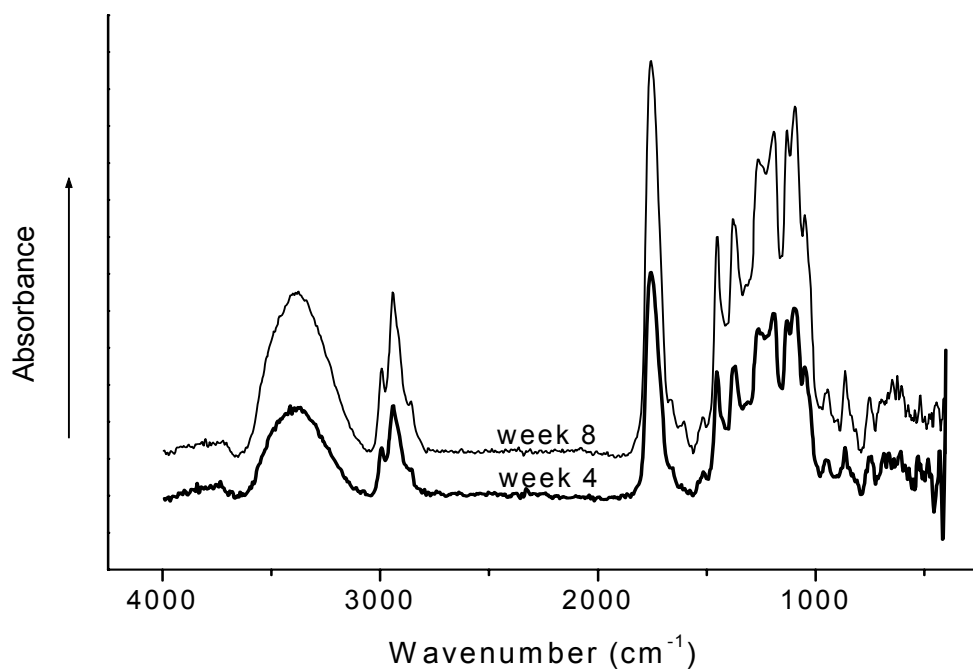


Fig. 9-9 Absorption IR spectra of network type A after 4 and 8 weeks of hydrolytical degradation in PBS (pH 7.4) at RT.

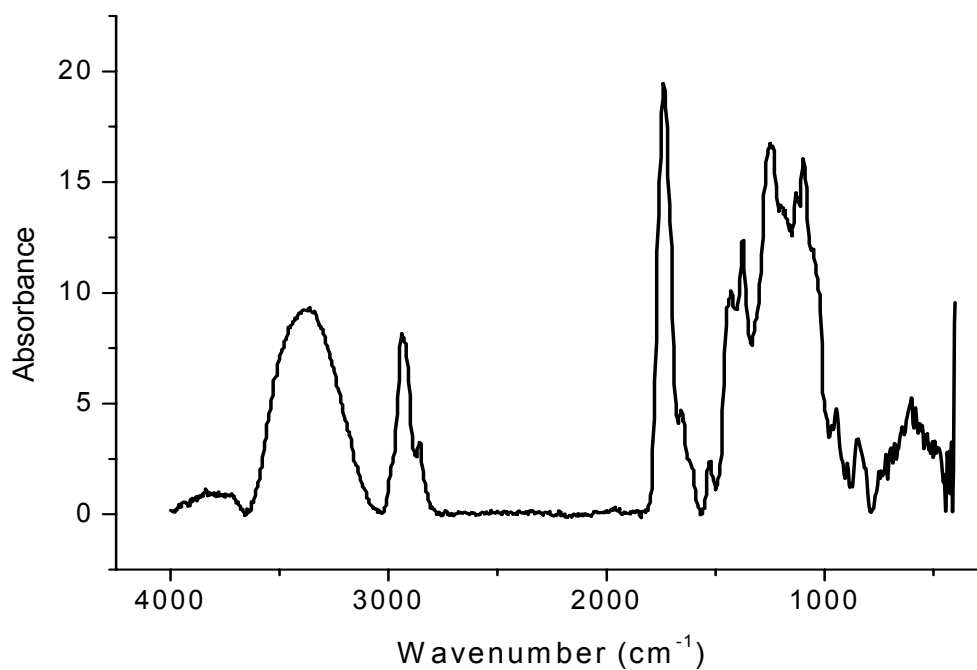


Fig. 9-10 Absorption IR spectra of network type R after 4 weeks of hydrolytical degradation in PBS (pH 7.4) at RT.

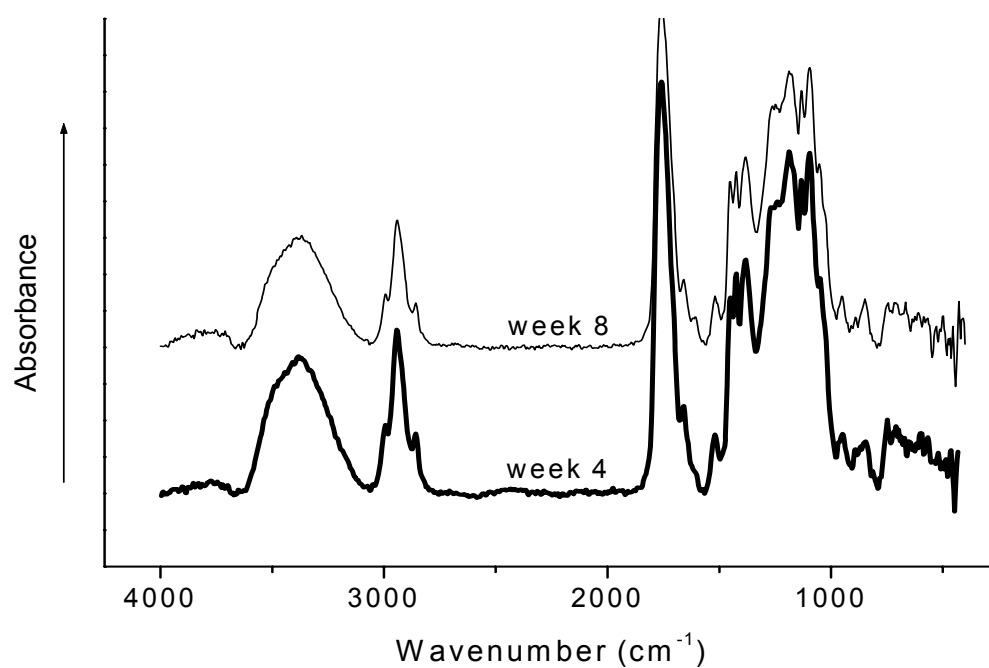


Fig. 9-11 Absorption IR spectra of network type O after 4 and 8 weeks of hydrolytical degradation in PBS (pH 7.4) at RT.

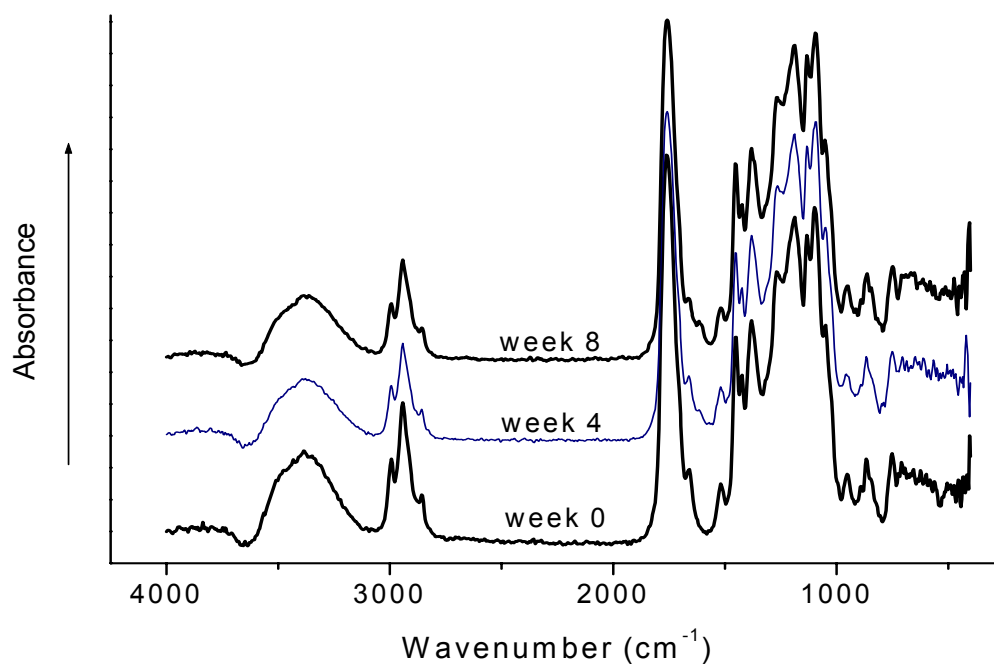


Fig. 9-12 Absorption IR spectra of network type F before and after 4 and 8 weeks of hydrolytical degradation in PBS (pH 7.4) at RT.

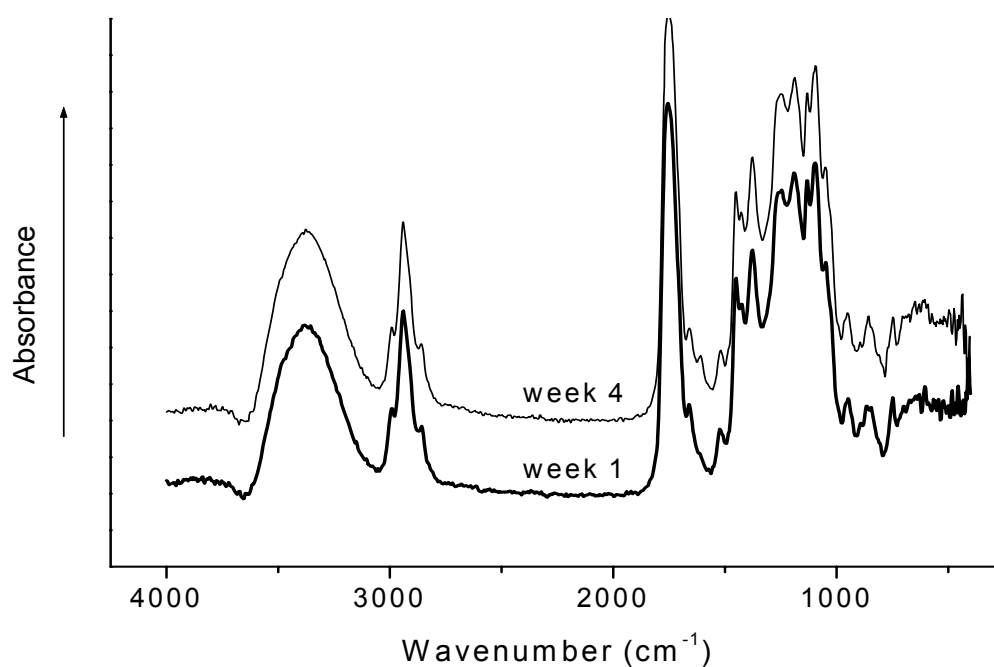


Fig. 9-13 Absorption IR spectra of network type I after 1 and 4 weeks of hydrolytical degradation in PBS (pH 7.4) at RT.

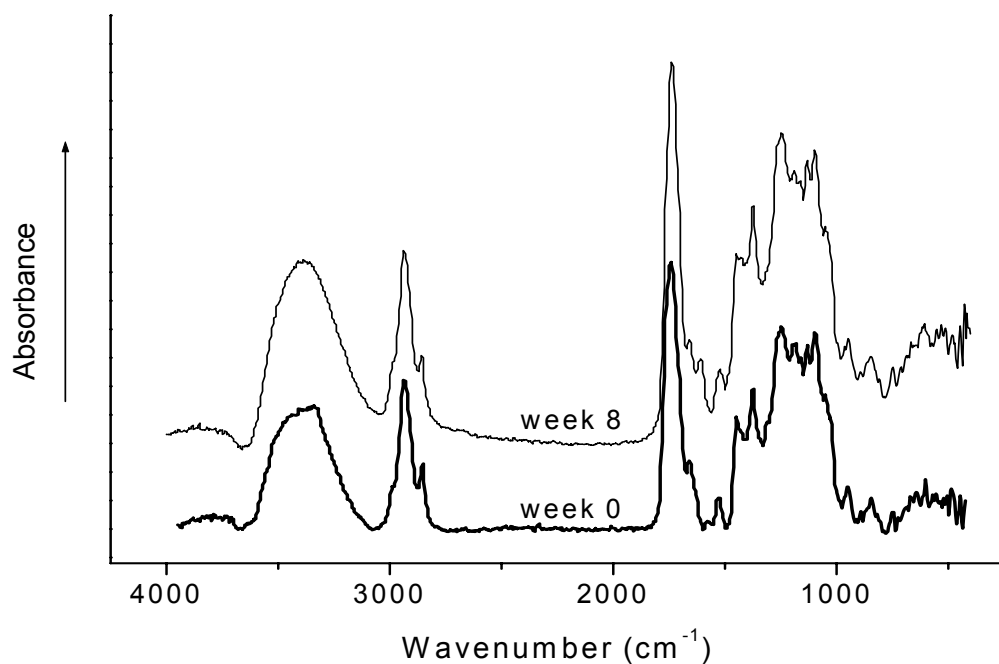


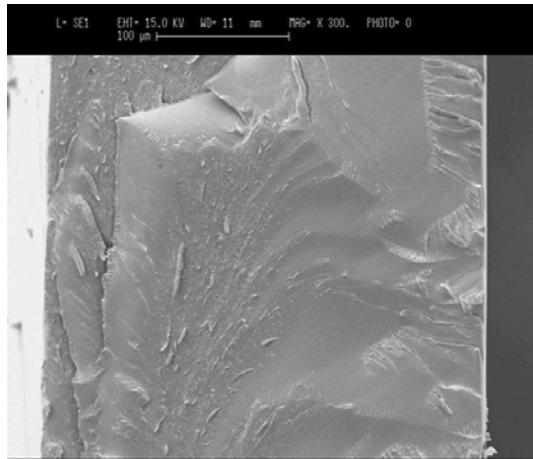
Fig. 9-14 Absorption IR spectra of network type L before and after 8 weeks of hydrolytical degradation in PBS (pH 7.4) at RT.

Tab. 9-2 Young's modulus (E) of hydrogels B, C, E, I, J, L, M, N, P, Q and S (see Tab. 3-1) measured at room temperature at the beginning of hydrolytical degradation.

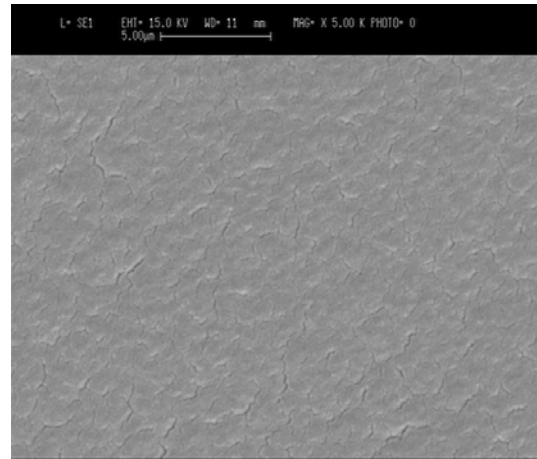
Hydrogel	E / MPa						
	E_1	E_2	E_3	E_4	E_5	MW_E	SD_E
B	4.02	3.37	3.12	3.45	4.51	3.69	0.563
C	1.34	1.39	1.55	1.35		1.41	0.099
E	0.57	0.4	0.45	0.46	0.48	0.47	0.062
F						(103)	
I	19.05	17.84	17.88			18.26	0.687
J	2.68	2.01	4.92	3.80	3.35	3.35	1.280
L	1.00	1.09	0.91	1.10	0.89	1.00	0.098
M	0.06	0.08	0.03	0.07		0.06	0.022
N	0.02	0.03	0.03	0.03	0.04	0.03	0.009
P	1.51	2.53	1.69	2.05	1.95	1.95	0.390
Q	0.85	0.71	0.82	0.75	0.84	0.79	0.061
S	0.01	0.01	0.03	0.01		0.01	0.009

Tab. 9-3 Contact angle obtained by *captive-bubble* method, in water at room temperature. *MW* presents middle values and *SD* presents standard deviation.

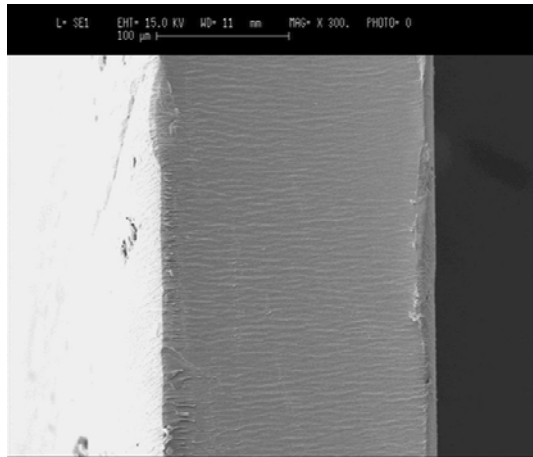
Sample	Contact angle Θ in $^{\circ}$											
	Θ_1	Θ_2	Θ_3	Θ_4	Θ_5	Θ_6	Θ_7	Θ_8	Θ_9	Θ_{10}	MW_{Θ}	SD_{Θ}
A	41	39	45	43	50	45	48	47	46	49	45	3.36
B	40	41	39	41	39	41	39	40	42	41	40	1.39
F	36	37	37	36	38	39	37	35	39	38	37	1.59
J	35	35	33	34	37	34	37	33	36	37	35	1.60
L	28	31	28	32	28	31	29	33	33	27	30	2.26
N	26	27	27	25	27	30	27	30	30	27	28	1.78
O	39	41	40	40	43	42	39	40	41	45	41	1.97
P	35	36	37	35	38	38	37	36	37	37	37	1.18
Q	37	35	37	36	38	38	37	39	38	38	37	1.30



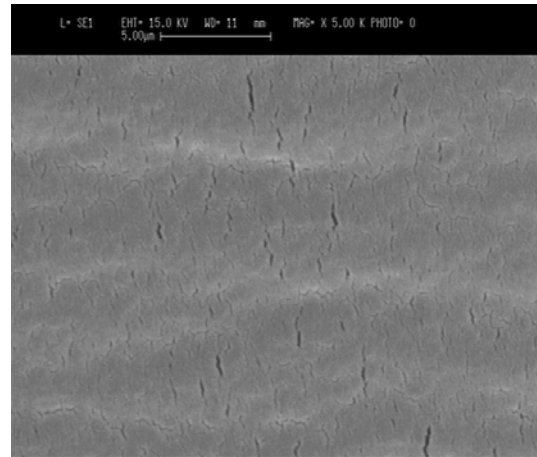
a-1



a-2

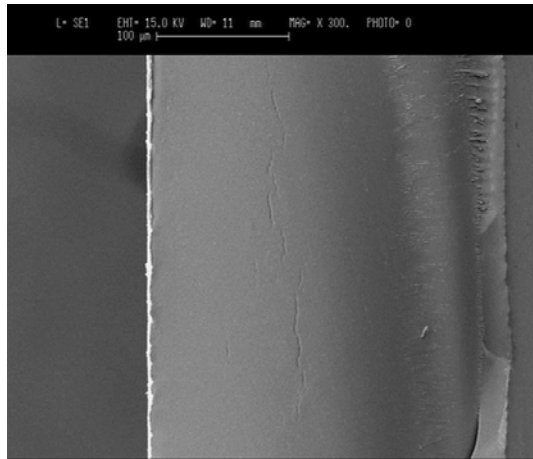


b-1

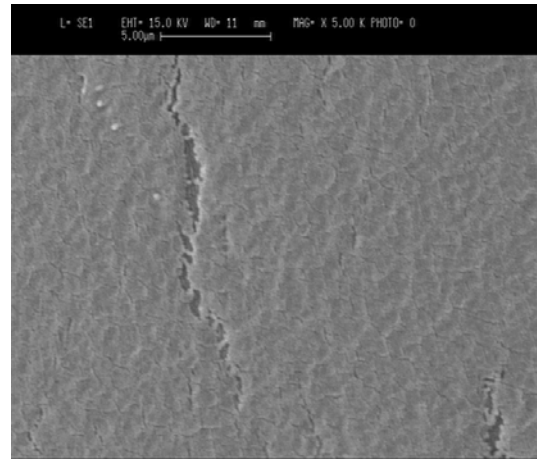


b-2

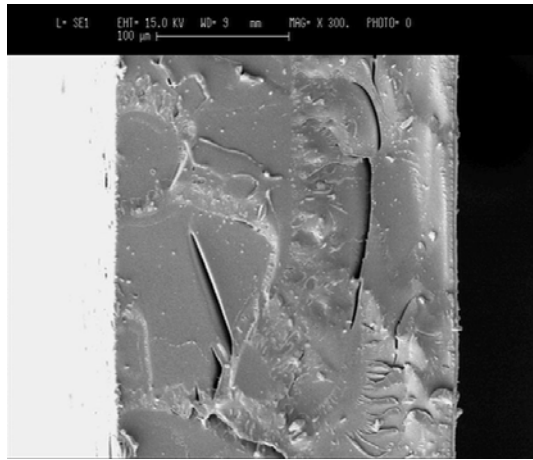
Fig. 9-15 SEM micrographs of network type B
a) before hydrolytical degradation: cross section at MAG x 300 (1) and x 5000 (2)
b) after eight weeks of hydrolytical degradation: cross section at MAG x 300 (1) and x 5000 (2).



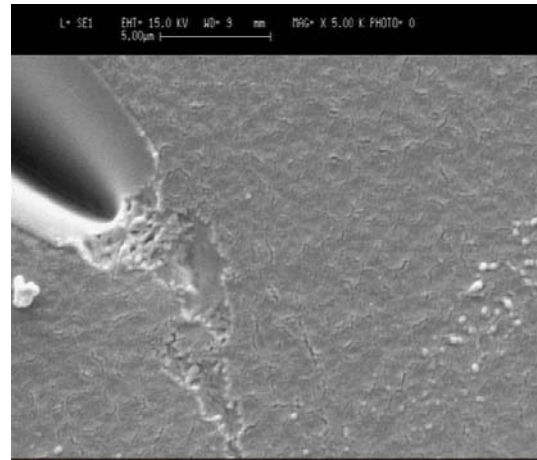
a-1



a-2

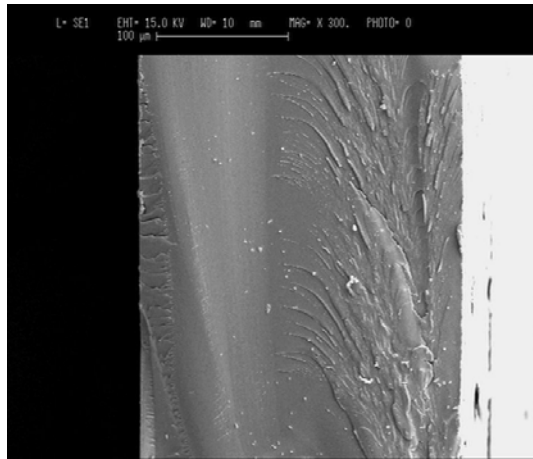


b-1

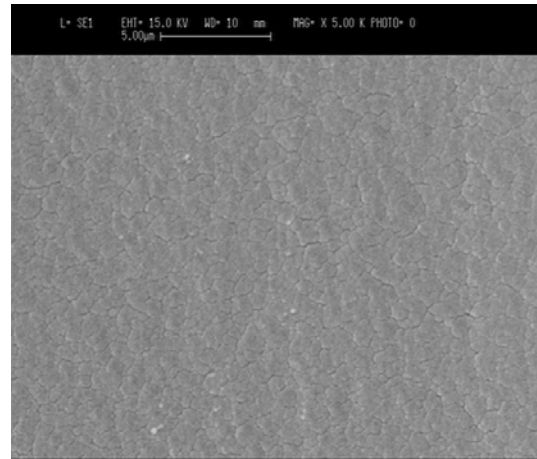


b-2

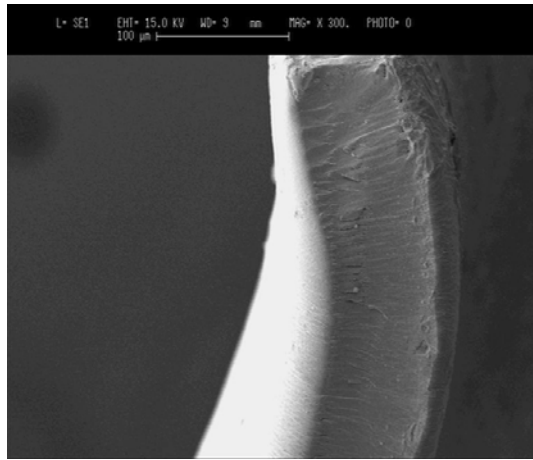
Fig. 9-16 SEM micrographs of network type C
a) before hydrolytical degradation: cross section at MAG x 300 (1) and x 5000 (2)
b) after nine weeks of hydrolytical degradation: cross section at MAG x 300 (1)
and x 5000 (2).



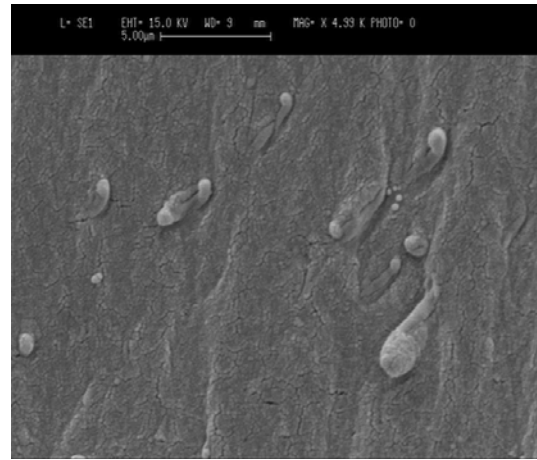
a-1



a-2

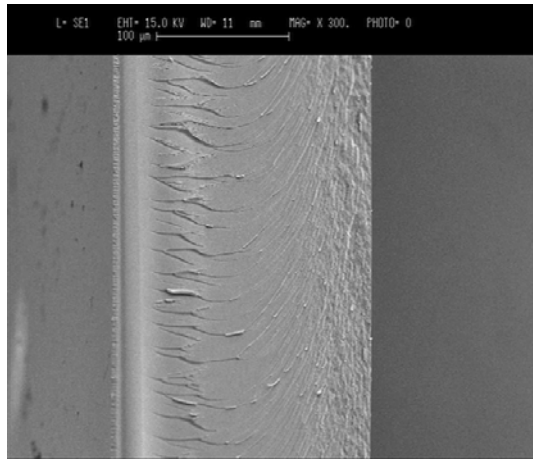


b-1

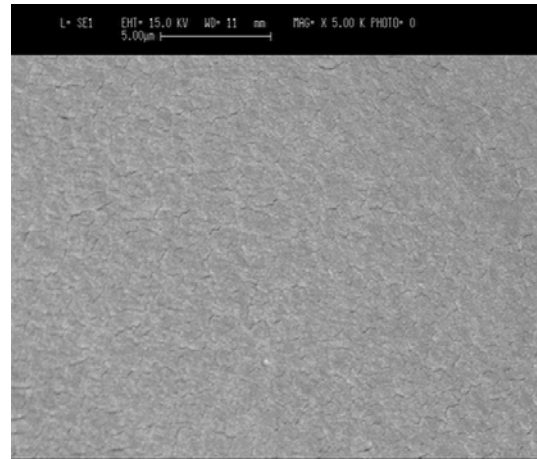


b-2

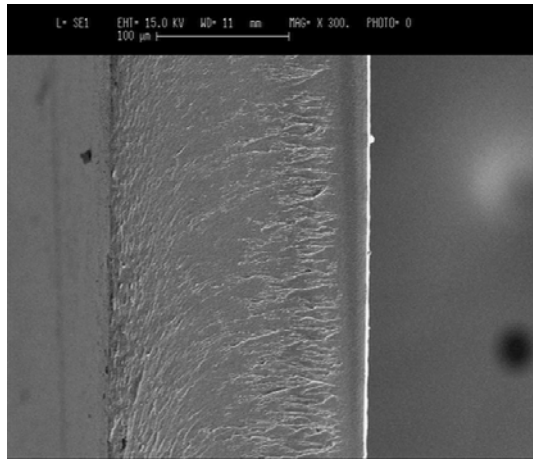
Fig. 9-17 SEM micrographs of network type E
a) before hydrolytical degradation: cross section at MAG x 300 (1) and x 5000 (2)
b) after ten weeks of hydrolytical degradation: cross section at MAG x 300 (1)
and x 5000 (2).



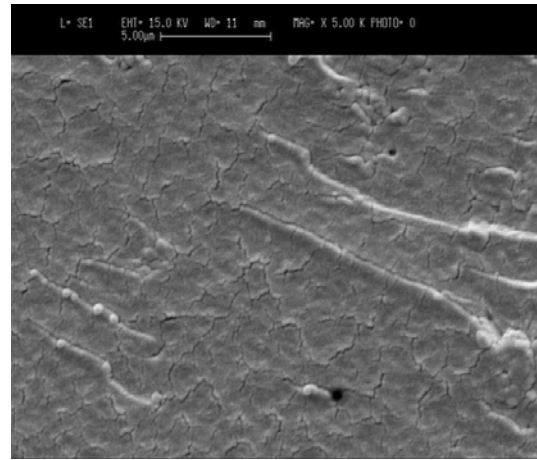
a-1



a-2



b-1



b-2

Fig. 9-18 SEM micrographs of network type F
a) before hydrolytical degradation: cross section at MAG x 300 (1) and x 5000 (2)
b) after eight weeks of hydrolytical degradation: cross section at MAG x 300 (1)
and x 5000 (2).

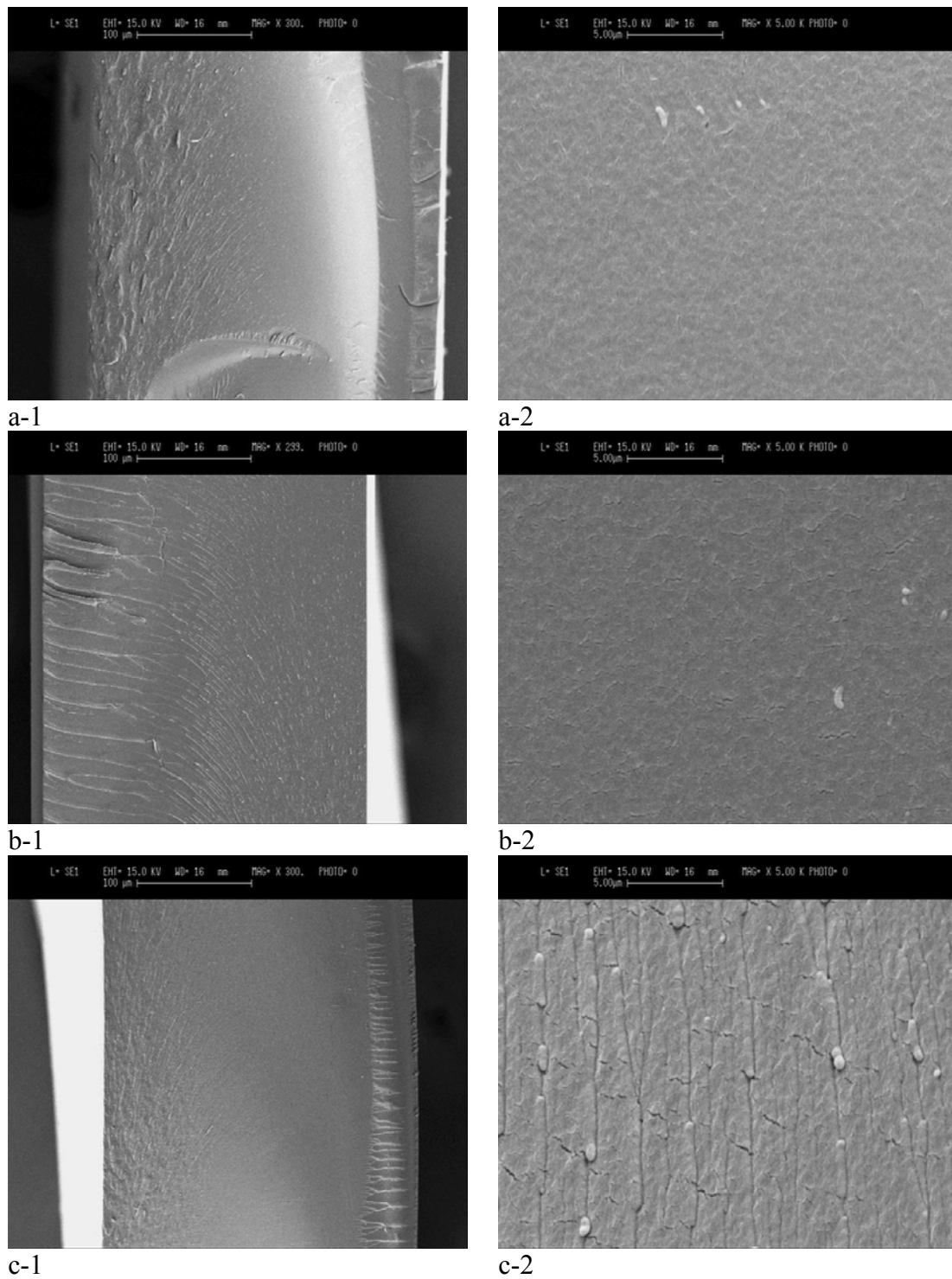
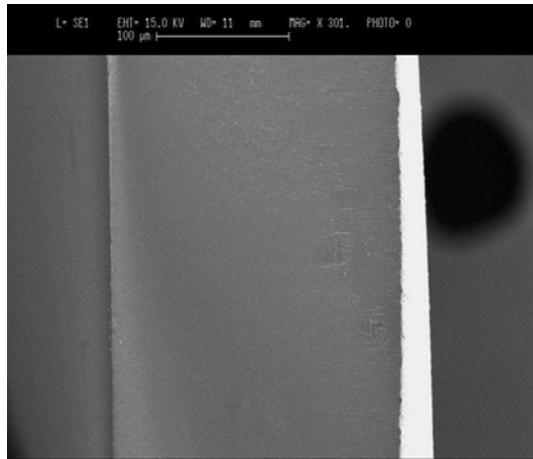
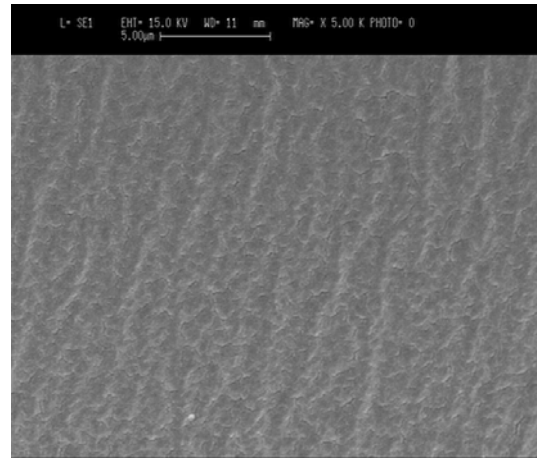


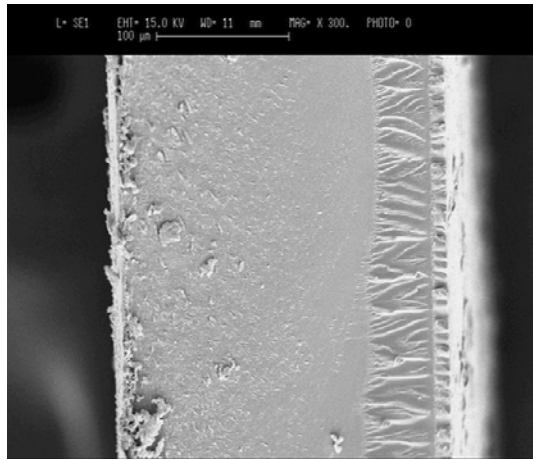
Fig. 9-19 SEM micrographs of network type I
a) before hydrolytical degradation: cross section at MAG x 300 (1) and x 5000 (2)
b) after four weeks of hydrolytical degradation: cross section at MAG x 300 (1) and x 5000 (2)
c) after eight weeks of hydrolytical degradation: cross section at MAG x 300 (1) and x 5000 (2).



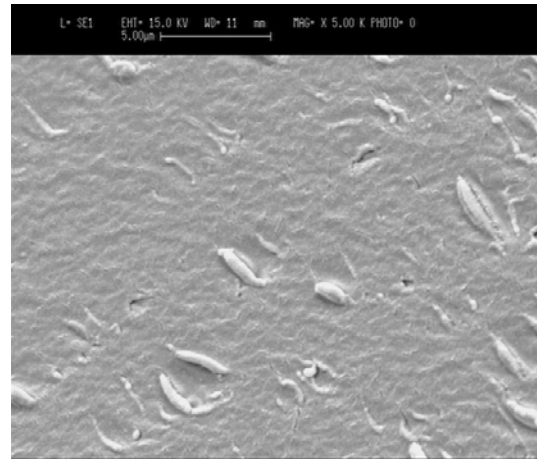
a-1



a-2

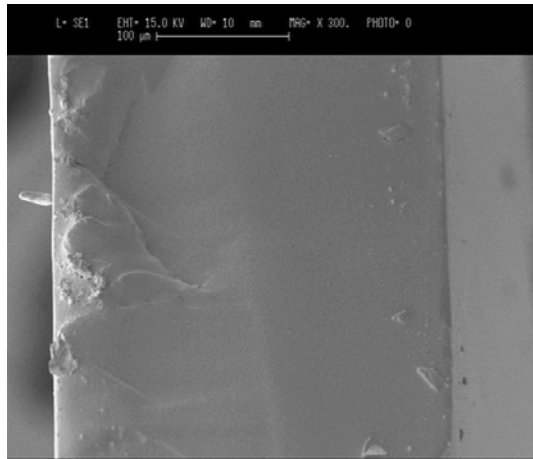


b-1

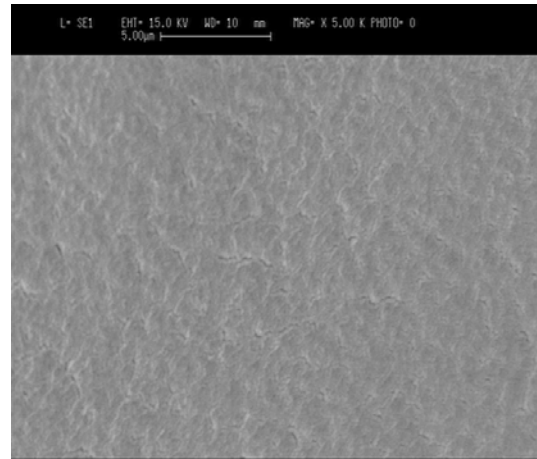


b-2

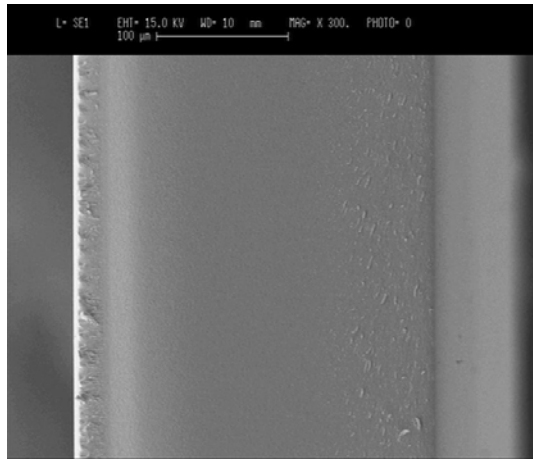
Fig. 9-20 SEM micrographs of network type L
a) before hydrolytical degradation: cross section at MAG x 300 (1) and x 5000 (2)
b) after eight weeks of hydrolytical degradation: cross section at MAG x 300 (1) and x 5000 (2).



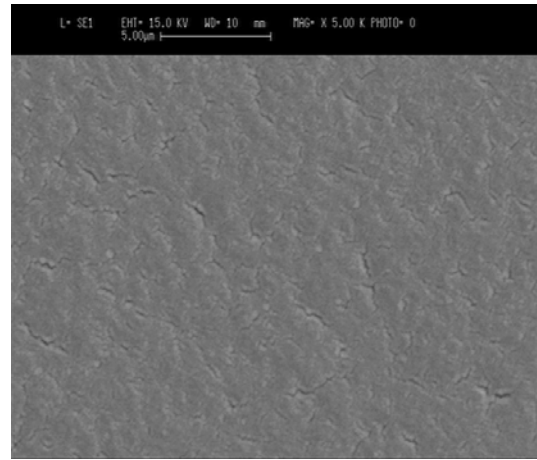
a-1



a-2



b-1



b-2

Fig. 9-21 SEM micrographs of network type O
a) before hydrolytical degradation: cross section at MAG x 300 (1) and x 5000 (2)
b) after eight weeks of hydrolytical degradation: cross section at MAG x 300 (1) and x 5000 (2).

Tab. 9-4 Change of Young's modulus (E) of hydrogels (see Tab. 3-1) measured at room temperature at the beginning of hydrolytical degradation (room temperature. pH 7.4). MW presents middle values and SD presents standard deviation.

Time/ day	E / MPa						
	E_1	E_2	E_3	E_4	E_5	MW_E	SD_E
Hydrogel A							
7	36.89	40.3	38.97	34.82	47.07	39.61	4.660
15	22.90	20.10	32.02	28.20		25.80	5.326
28	20.81	16.10	13.01	19.52		17.36	3.520
42	17.01	14.22	18.23	20.14	13.16	16.55	2.865
56	13.13	14.84	13.13	13.21	19.25	14.71	2.640
133	6.84	8.03	9.39	7.65	8.33	8.048	0.935
Hydrogel B							
7	2.47	2.00	1.34	1.61	2.43	1.97	0.497
14	2.04	1.67	1.66	1.85	2.28	1.90	0.26
28	2.43	2.67	2.79	2.1	2.46	2.49	2.43
42	1.89	1.74	1.58	1.72	1.50	1.69	0.152
56	2.00	1.54	1.65	1.54	1.96	1.74	0.226
126	0.71	0.53	0.71	0.49		0.61	0.119
Hydrogel C							
7	1.12	1.09	1.56	1.16	1.20	1.23	0.191
14	1.43	1.22	1.09	1.09	1.05	1.17	0.156
28	0.92	0.68	0.88	0.91		0.85	0.112
42	0.84	0.69	0.78	0.80	0.79	0.78	0.055
56	0.83	0.70	0.75	0.77	0.77	0.76	0.046
140	0.30	0.37	0.31	0.40		0.34	0.051
225						(0.02)	
Hydrogel D							
7	0.44	0.44	0.51	0.38		0.44	0.053
14	0.41	0.36	0.40	0.40	0.41	0.40	0.024
21	0.54	0.44	0.32	0.45		0.43	0.091
28	0.42	0.34	0.44	0.26		0.36	0.080
42	0.45	0.43	0.35	0.36		0.40	0.049
56	0.36	0.25	0.28			0.30	0.057
70	0.28	0.23	0.26			0.26	0.026
154	0.02	0.01	0.02			0.02	0.005
Hydrogel E							
7	0.49	0.47	0.49	0.45	0.37	0.45	0.049
14	0.44	0.39	0.37	0.33	0.22	0.35	0.081
28	0.43	0.35	0.39	0.31	0.31	0.36	0.053
42	0.35	0.28	0.33	0.27	0.28	0.30	0.034
56	0.26	0.20	0.30	0.22	0.26	0.25	0.042
140	0.04	0.03	0.04			0.04	0.003
220						(0.004)	

Tab. 9-4 cont.

Time/ day	<i>E</i> / MPa						
	<i>E</i> ₁	<i>E</i> ₂	<i>E</i> ₃	<i>E</i> ₄	<i>E</i> ₅	<i>MW_E</i>	<i>SD_E</i>
Hydrogel F							
7	212.90	258.40	172.20	206.90	153.70	200.82	40.428
7	212.90	258.40	172.20	206.90	153.70	200.82	40.428
35	282.20	310.50	191.30	226.30		252.57	53.783
42	244.00	174.80	223.60	238.70		220.27	31.525
56	125.00	160.20	219.10	219.00	179.00	180.46	40.208
Hydrogel I							
7	7.91	8.34	8.89	7.74		8.22	0.513
14	4.21	4.09	4.07	3.37	4.60	4.07	0.4457
28	6.76	7.74	5.57	4.19	4.56	5.76	1.488
42	3.20	3.42	3.79	3.62	3.57	3.52	0.223
56	4.21	3.76	2.21	2.10	2.97	3.05	0.929
Hydrogel J							
7	1.42	1.46	1.41	1.61	1.57	1.49	0.091
14	1.25	1.16	1.27	1.52	1.45	1.33	0.149
28	1.06	1.02	1.13	1.43	1.33	1.19	0.176
42	0.79	0.73	0.91	0.98	0.95	0.87	0.108
56	0.61	0.54	0.61	0.77	0.74	0.65	0.094
Hydrogel K							
7	0.26	0.20	0.27	0.31	0.26	0.26	0.041
14	0.08	0.16	0.11	0.08	0.06	0.10	0.037
28	0.03	0.06	0.04	0.09	0.02	0.05	0.028
42	0.05	0.02	0.01	0.07	0.01	0.03	0.026
56	0.02	0.01	0.01	0.01	0.03	0.01	0.009
Hydrogel L							
7	1.25	1.05	1.35	1.20	1.17	1.20	0.110
14	0.89	0.92	0.77	0.90	0.92	0.88	0.065
28	0.68	0.72	0.76	0.85	0.69	0.74	0.070
42	0.82	0.73	0.65	0.73	0.72	0.73	0.060
56	0.26	0.59	0.49	0.51		0.46	0.142
140	0.03	0.03	0.04	0.02		0.03	0.007
230	0.01	0.01	0.01			(0.01)	0.001
Hydrogel M							
7	0.01	0.05	0.03	0.05	0.12	0.05	0.040
14	0.03	0.04	0.03			0.03	0.006
21	0.03	0.04	0.02			0.02	0.006
28	0.07	0.02	0.09	0.02		0.05	0.035
42	0.09	0.02	0.03	0.01	0.02	0.03	0.029
56	0.01	0.02	0.02			0.02	0.003

Tab. 9-4 cont.

Time/ day	<i>E</i> / MPa						
	<i>E</i> ₁	<i>E</i> ₂	<i>E</i> ₃	<i>E</i> ₄	<i>E</i> ₅	<i>MW_E</i>	<i>SD_E</i>
Hydrogel N							
7	0.04	0.03	0.01	0.03		0.03	0.013
14	0.02	0.03	0.02	0.02		0.02	0.004
28	0.02	0.02	0.01	0.01	0.01	0.02	0.005
42						(0.01)	
Hydrogel O							
7	32.81	47.47	42.38	39.57		40.56	6.113
14	49.03	49.04	42.85	39.19	42.08	44.44	4.413
28	19.91	18.86	19.40	14.79	18.52	18.30	2.030
42	27.16	31.43	35.54	24.61	23.51	28.45	4.999
56	31.11	24.24	26.76	23.46	23.87	25.89	3.190
133	7.03	8.71	9.30			8.35	1.178
Hydrogel P							
7	2.06	1.96	1.88	2.13	2.01	2.01	0.095
14	1.52	1.52	1.70	1.70	1.65	1.61	0.091
21	1.31	1.36	1.41	1.39	1.42	1.38	0.048
28	1.07	0.97	1.08	1.01	1.03	1.03	0.045
35	0.91	0.61	0.73	0.63	0.82	0.74	0.126
42	0.61	0.66	0.55	0.61		0.61	0.043
49	0.51	0.74	0.67	0.47		0.60	0.127
56						(0.49)	
Hydrogel Q							
7	0.86	0.73	0.30	0.80		0.67	0.254
14	0.07	0.14	0.06	0.06	0.13	0.09	0.040
28	0.70	0.68	0.72	0.75	1.05	0.78	0.153
42	0.05	0.08	0.04	0.05		0.05	0.018
56	0.41	0.31	0.37			0.37	0.052
Hydrogel R							
7	0.02	0.03	0.01	0.03	0.03	0.03	0.010
14	0.03	0.01	0.01	0.02		0.02	0.011
28	0.03	0.02	0.04	0.01	0.03	0.03	0.009
42						(0.003)	0.002

Tab. 9-5 Contact angle θ obtained by the *captive-bubble* method. in water at room temperature. *MW* presents middle values and *SD* presents standard deviation.

Day	Contact angle θ in °											
	θ_1	θ_2	θ_3	θ_4	θ_5	θ_6	θ_7	θ_8	θ_9	θ_{10}	MW_θ	SD_θ
Sample A												
8	35	33	35	36	36	37	35	35	36	35	35	0.99
15	33	32	32	33	31	33	37	35	33	33	33	1.79
29	20	21	19	20	21	20	19	21	21	19	20	1.15
43	23	23	23	24	23	23	22	23	24	22	23	1.02
57	21	21	20	21	20	19	20	19	19	19	20	0.79
Sample B												
8	36	36	35	33	35	35	37	38	36	36	36	1.74
15	31	27	27	27	29	28	27	27	28	27	28	1.62
29	23	23	24	25	24	26	23	23	25	25	24	1.75
43	25	25	25	22	27	24	25	21	23	23	24	1.69
57	23	25	24	25	23	24	23	24	24	25	24	0.94
Sample C												
13	27	29	26	28	28	29	27	28	27	28	28	0.95
28	20	19	20	21	23	20	22	21	19	23	21	1.48
42	16	18	16	15	15	16	20	17	18	19	17	1.70
56	20	20	21	19	21	18	16	19	18	18	19	1.56
Sample D												
13	19	23	18	17	23	24	20	17	21	23	21	2.68
27	21	20	18	19	18	17	18	21	18	18	19	1.40
41	19	16	15	15	16	14	16	14	15	17	16	1.49
54	17	20	18	18	18	16	17	16	17	18	18	1.18
Sample E												
8	<20	<20	<20	<20	<20	<20	<20	<20	<20	<20	<20	
13	20	17	17	17	21	20	20	17	20	20	19	1.66
27	16	20	21	18	17	17	15	17	19	15	18	2.01
41	17	15	17	17	20	16	17	17	16	16	17	1.32
54	19	19	19	17	20	21	19	17	18	17	19	1.35
Sample F												
8	33	32	33	33	34	35	33	35	34	35	34	1.23
15	29	29	29	27	29	29	29	29	30	31	29	1.03
36	28	27	26	25	24	25	23	27	27	24	26	1.8
57	18	20	18	18	19	18	20	19	19	19	19	0.93
Sample G												
163	19	14	17	17	16	17	19	19	17	20	18	1.78
300	20	19	18	19	20	19					19	0.75
Sample H												
111	32	16	19	24	31	25	17	16	30	16	23	6.64
147	17	17	16	18	17	18	15	20	19	21	18	1.81
Sample I												
6	23	23	23	23	23	23	24	24	24	24	24	1.37
13	21	21	21	23	22	23	19	22	23	21	21	1.54
27	20	19	21	21	21	23	20	21	21	22	21	1.33
42	19	19	19	19	18	17	18	19	19	17	18	0.80
56	20	21	19	18	19	19	18	19	19	19	19	1.14

Tab. 9-5 cont.

Day	Contact angle Θ in °											
	Θ_1	Θ_2	Θ_3	Θ_4	Θ_5	Θ_6	Θ_7	Θ_8	Θ_9	Θ_{10}	MW_Θ	SD_Θ
Sample J												
7	30	29	30	29	30	30	30	32	31	29	30	0.94
15	27	27	27	28	27	27	27	29	24	26	27	1.29
29	18	18	17	18	18	17	20	19	18	19	18	0.92
57	17	17	19	19	19	23	20	20	18	17	19	1.85
147	23	21	19	21	21	23	21	19	21	21	21	1.17
Sample K												
8	29	26	29	27	25	25	26	27	28	25	27	1.57
22	21	24	26	25	22	24	22	24	24	22	23	1.58
50	20	19	18	21	18	17	21	19	18	20	19	1.37
64	15	15	17	16	15	17	14	17	16	16	16	1.04
144	19	19	19	19	20	19	19	19	20	20	19	0.79
Sample L												
15	22	22	22	22	17	20	21	21	21	19	21	1.64
29	18	17	15	15	18	17	18	16	20	16	17	1.56
43	17	17	20	18	16	16	19	19	18	17	18	1.34
147	20	21	19	19	20	19	19	19	20	20	20	1.23
Sample M												
17	18	19	19	22	19	19	17	20	18	21	19	1.48
31	21	19	18	18	19	22	17	17	19	17	19	1.70
45	16	16	17	15	19	16	17	17	18	15	17	1.26
58	18	20	17	15	17	16	17	18	19	19	18	1.51
Sample N												
8	18	18	20	19	17	17	17	20	20	20	19	1.35
29	20	20	20	19	19	21	19	18	17	19	19	1.14
43	15	14	15	17	15	15	15	16	15	15	15	0.77
57	18	19	19	18	18	17	18	19	19	19	18	0.82
147	19	18	17	17	18	17	18	18	19	19	18	0.81
Sample O												
8	35	35	33	33	34	33	35	35	35	36	34	0.99
15	31	32	33	33	32	30	31	31	31	33	32	1.09
29	19	19	18	18	18	18	19	19	19	19	19	0.69
43	23	23	24	23	23	23	23	25	24	25	24	0.66
57	19	21	18	17	19	17	17	17	18	18	18	1.48

Tab. 9-6 Contact angle θ obtained by *captive-bubble* method in water at room temperature. Hydrogel type P during degradation in water at RT. *MW* presents middle values and *SD* presents standard deviation.

Time /d	Contact angle θ in °											
	θ_1	θ_2	θ_3	θ_4	θ_5	θ_6	θ_7	θ_8	θ_9	θ_{10}	MW_θ	SD_θ
1	35	36	37	35	38	38	37	36	37	37	37	1.18
7	24	23	22	21	23	23	21	21	21	21	22	1.60
14	21	19	19	19	19	20	19	21	19	19	19	0.94
21	21	23	23	17	19	19	21	19	17	17	20	2.27
28	21	19	19	19	19	19	19	17	19	18	19	1.12
35	17	19	20	17	18	18	19	19	19	20	19	1.04
42	17	17	17	16	15	15	15	16	15	16	16	1.23
49	15	15	15	17	15	15	17	16	15	18	16	1.15
56	17	15	14	15	15	15	15	17	16	17	16	1.17

Tab. 9-7 Contact angle θ obtained by *captive-bubble* method in water at room temperature. Hydrogel type P during degradation in water at 37 °C. *MW* presents middle values and *SD* presents standard deviation.

Time /d	Contact angle θ in °											
	θ_1	θ_2	θ_3	θ_4	θ_5	θ_6	θ_7	θ_8	θ_9	θ_{10}	MW_θ	SD_θ
7	31	31	32	32	33	37	37	33	31	33	33	2.38
14	31	29	30	31	32	33	31	33	33		31	1.24
21	27	27	27	28	27	28	25	27	27		27	0.94
28	29	31	27	27	30	29	30	29	29	29	29	1.35
35	21	23	23	23	21	22	22	23	23		22	0.96
42	17	17	17	19	17	19	19	19	21	19	19	1.36
49	17	17	17	16	16	16	15	15	17	17	16	1.11
56	19	19	17	18	19	19	19	17	17	19	18	0.72

Tab. 9-8 Contact angle θ obtained by *captive-bubble* method in water at room temperature. Hydrogel type P during degradation in PBS at 37 °C. *MW* presents middle values and *SD* presents standard deviation.

Time /d	Contact angle θ in °											
	θ_1	θ_2	θ_3	θ_4	θ_5	θ_6	θ_7	θ_8	θ_9	θ_{10}	MW_θ	SD_θ
7	30	28	30	29	29	31	30	29	29	29	29	1.14
14	28	29	29	29	31	29	29	31	29	30	29	1.00
21	21	22	22	21	21	23	23	21	23	21	22	1.04
28	28	29	27	29	29	29	27	29	29	29	28	0.99
35	19	19	19	19	19	18	19	20	20	20	19	0.85
42	17	16	15	14	17	17	16	17	16	16	16	1.02
49	15	15	15	15	15	15	15	15	15	16	15	0.79
56	18	18	17	17	15	16	19	17	18	17	17	1.29

Tab. 9-9 Change of thermal characteristic: glass transition temperature (T_g) and ΔC_p during degradation of hydrogels

Week Sample	4		8		10		24		31	
	$T_g / ^\circ\text{C}$	$\Delta C_p / \text{Jg}^{-1}\text{K}^{-1}$	$T_g / ^\circ\text{C}$	$\Delta C_p / \text{Jg}^{-1}\text{K}^{-1}$	$T_g / ^\circ\text{C}$	$\Delta C_p / \text{Jg}^{-1}\text{K}^{-1}$	$T_g / ^\circ\text{C}$	$\Delta C_p / \text{Jg}^{-1}\text{K}^{-1}$	$T_g / ^\circ\text{C}$	$\Delta C_p / \text{Jg}^{-1}\text{K}^{-1}$
A	60	0.597	61	0.540						
B	65	0.628	68	0.657						
C			73	0.685			72	0.780		
D	72	0.628			72	0.682			70	0.643
E					69	0.673	71	0.567		
O	52	0.614	53	0.641						
P	64	0.660	66	0.698						
Q	74	0.606	76	0.738						
R	73	0.585								
S	71	0.633								

Curriculum Vitae

Name	Elvira Vidović
Date of Birth	29.08.1970
Place of Birth	Mostar (BiH)
Family Status	Single
Nationality	Croatian
Primary Education:	
1977-1985	Elementary school, Mostar
Secondary Education	
1985-1989	Gymnasium, Mostar
Higher Education	
10/1989-10/1995	Faculty of chemical engineering and technology, Zagreb
1996	Language school, Sheffield, England
05/1997-04/2001	M. Sc (Master of Science), Faculty of chemical engineering and technology, Zagreb
04/2001-01/2002	Scientific coworker in the working group of Prof. Dr. Z. Janović at Faculty of chemical engineering and technology, Zagreb
01/2002-01/2005	The PhD work under the supervision of Prof. Dr. H. Höcker at the Department of Textile Chemistry and Macromolecular Chemistry, RWTH Aachen; entitled „The development of bioabsorbable hydrogels on the basis of polyester grafted poly(vinyl alcohol)“.